NATIONAL ADVISORY COMMITTEE FOR AERONAUTICS

TECHNICAL MEMORANDUM

No. 1217

LECTURE SERIES "BOUNDARY LAYER THEORY"

PART I - LAMINAR FLOWS

By H. Schlichting

Translation of "Vortragsreihe" W.S. 1941/42, Luftfahrtforschungsanstalt Hermann Göring, Braunschweig

Washington

April 1949

TABLE OF CONTENTS

NATIONAL ADVISORY COMMITTEE FOR AERONAUTICS

TECHNICAL MEMORANDUM NO. 1217

LECTURE SERIES "BOUNDARY LAYER THEORY"

Part I – Laminar Flows*

By H. Schlichting

First lecture (Dec. 1, 1941)

INTRODUCTION

Gentlemen: In the lecture series starting today I want to give you a survey of a field of aerodynamics which has for a number of years been attracting an ever growing interest. The subject is the theory of flows with friction, and, within that field, particularly the theory of friction layers, or boundary layers.

As you know, a great many considerations of aerodynamics are based on the so-called ideal fluid, that is, the frictionless incompressible fluid. By neglect of compressibility and friction the extensive mathematical theory of the ideal fluid (potential theory) has been made possible.

Actual liquids and gases satisfy the condition of incompressibility rather well if the velocities are not extremely high or, more accurately, if they are small in comparison with sonic velocity. For air, for instance, the change in volume due to compressibility amounts to about 1 percent for a velocity of 60 meters per second.

The hypothesis of absence of friction is not satisfied by any actual fluid; however, it is true that most technically important fluids, for instance air and water, have a very small friction coefficient and therefore behave in many cases almost like the ideal frictionless fluid. Many flow phenomena, in particular most cases of lift, can be treated satisfactorily, – that is, the calculations are in good agreement with the test results, – under the assumption of frictionless fluid. However, the calculations with frictionless flow show a very serious deficiency; namely, the fact, known as d'Alembert's paradox, that in frictionless flow each body has zero drag whereas in actual flow each body experiences a drag of greater or smaller magnitude. For a long time the theory has been unable to bridge this gap between the theory of frictionless flow and the experimental findings about actual flow. The cause of this fundamental discrepancy is the viscosity which is neglected in the theory

*"Vortragsreihe 'Grenzschichttheorie.' Teil A: Laminare Strömungen." Zentrale für wissenschaftliches Berichtswesen der Luftfahrtforshung des Generalluftzeugmeisters (ZWB) Berlin-Adlershof, pp. 1–153. Given in the Winter Semester 1941/42 at the Luftfahrtforschungsanstalt Hermann Göring, Braunschweig. The original language version of this report is divided into two main parts, Teil A and Teil B, which have been translated as separate NACA Technical Memorandums, Nos. 1217 and 1218, designated part I and part II, respectively.

of the ideal fluid; however, in spite of its extraordinary smallness it is decisive for the course of the flow phenomenon. As a matter of fact the problem of drag can not be treated at all without taking the viscosity into account.

Although this fact had been known for a long time, no proper approach to the theoretical treatment of the drag problem could be found until the beginning of the present century. The main reason was that unsurmountable mathematical difficulties stood in the way of theoretical treatment of the flow phenomena of the viscous fluid. It is Professor Prandtl's great merit to have shown a way to numerical treatment of viscosity, particularly of the technically important flows under consideration and thereby to have opened up new vistas on many important perceptions about the drag problem and related questions. Prandtl was able to show that in the case of most of the technically important flows one may treat the flow, as a whole, as frictionless and utilize the simplifications for the calculation thus made possible, but that in the immediate neighborhood of the solid walls one always had to take the friction into consideration. Thus Prandtl subdivides, for the purpose of calculation, the flow surrounding a body into two domains: a layer subject to friction in the neighborhood of the body, and a frictionless region outside of this layer. The theory of this so-called "Prandtl's friction or boundary layer" has proved to be very fruitful in modern flow theory; the present lecture will center around it.

At this point I want to indicate a few applications of the boundary-layer theory. A first important application is the calculation of the frictional surface drag of bodies immersed in a flow, for instance, the drag of a flat plate in longitudinal flow, the frictional drag of a ship, a wing profile, and an airplane fuselage. A special property of the boundary layer is the fact that under certain circumstances reverse flow occurs in the immediate proximity of the surface. Then, in connection with this reverse flow, a separation of the boundary layer takes place, together with a more or less strong formation of vortices in the flow behind the body. Thus a considerable change in pressure distribution, compared with frictionless flow, results, which gives rise to the form drag of the body immersed in the flow: The boundary-layer theory therefore offers an approach to the calculation of this form drag. Separation occurs not only in the flow around a body but also in the flow through a divergent tunnel.

Thus flow phenomena in a diffuser, as, for instance, in the bucket grid of a turbine, may be included in boundary-layer theory. Furthermore, the phenomena connected with the maximum lift of a wing, where flow separation is concerned, can be understood only with the aid of boundary-layer theory. The problems of heat transfer also can be explained only by boundary-layer theory.

As will be shown in detail later, one must distinguish between the two states of boundary-layer flow - laminar and turbulent; their flow laws are very different. Accordingly, the lecture will be divided into three main parts: 1. Laminar flows, 2. Turbulent flows, 3. Laminar-turbulent transition. Although the boundary layer will be our main consideration, it will still be necessary as preparation to discuss to some extent the

general theory of the viscous fluid. This will be done in the first chapter.

CHAPTER I. VISCOSITY

Every fluid offers a resistance to a form variation taking place in finite time interval, which is of different magnitude according to the type of fluid. It is, for instance, very large for syrup or oil, but only small for the technically important fluids (water, air).

The concept of viscosity can be best made clear by means of a test according to figure 1:

Let fluid be between two parallel plates lying at a distance h from each other. Let the lower plate be fixed, while the upper plate is moved with the velocity u_o uniformly and parallel to the lower one. For moving the upper plate a tangential force P must be expended which is

$$P = \mu F \frac{u_o}{h} \tag{1.1}$$

according to experiment, where F is the area of the upper plate and μ is a constant of proportionality. (End effects are not included). The quantity μ is called the viscosity coefficient or the dynamic viscosity.

Since the phenomenon in question is a parallel gliding, the transverse velocity component in the y-direction, denoted by v, equals zero. The fluid adheres to the upper and lower surface, respectively, a linear velocity distribution between the plates is set up, the magnitude of which depends solely on y.

$$u(y) = u_o \frac{y}{h} \quad \text{or:} \quad \frac{du}{dy} = \frac{u_o}{h}$$

Since for $y = 0$: $u = 0$, for $y = h$: $u = u_o$. If one designates P/F, the tangential force per unit area, as the frictional shearing stress τ, there follows:

$$\tau = \mu \frac{du}{dy} \text{ kg/m}^2 \tag{1.2}$$

The dimensions of μ are accordingly kg sec/m^2. A flow as represented in figure 1, where no transverse velocity occurs and the shearing stress at all points of the flow is therefore given by equation (1.2), is called simple shear flow. In the special case described, the shearing stress is everywhere of equal magnitude, and equal to that at the surface. Besides the dynamic viscosity μ the concept of kinematic viscosity ν is required, which for the density $\rho \left[\text{kg sec}^2\text{m}^{-4}\right]$ is defined as

$$\nu = \frac{\mu}{\rho} \left[\text{m}^2/\text{s}\right]$$

For 20° C, ν is, for instance, for water:

$$\nu = 1.01 \times 10^{-6} \text{ m}^2/\text{s}$$

for air:

$$\nu = 14.9 \times 10^{-6} \text{ m}^2/\text{s} \sim \frac{1}{7} 10^{-4} \text{ m}^2/\text{s}$$

if the air pressure has the standard value p_o = 760 mm hg.

CHAPTER II. POISEUILLE FLOW THROUGH A PIPE

The elementary empirical friction law of the simple shear flow derived above permits the immediate determination of the flow and the resistance in a smooth pipe of circular cross section and of constant diameter, d = 2r. At a very large distance from the beginning of the pipe one cuts off a piece of pipe of length l (fig. 2) and examines the cylinder of diameter 2y, the axis of which is identical with the pipe axis. According to what has been said so far, the velocity probably will be again a function of y. A pressure difference $p_1 - p_2$ is required for forcing the fluid through the cylinder. According to practical experience, the static pressure across every cross section may be regarded as constant. The flow is assumed to be steady and not dependent on the distance from the beginning of the pipe. Equilibrium

must then exist between the pressure and the frictional shearing stress which attempts to retard the motion. Thus for the cylinder of radius y the following equation is valid: pressure force difference acting at the cross sections = frictional force acting along the cylinder wall, or

$$\left(p_1 - p_2\right)\pi y^2 = 2\pi y l \tau \tag{2.1}$$

or

$$\tau = \frac{p_1 - p_2}{l}\frac{y}{2} \tag{2.1a}$$

Since flow parallel to the axis is to be expected, one takes from the previous paragraph, $\tau = -\mu\frac{du}{dy}$ (the minus sign indicates that the velocity diminishes with increasing distance from the axis; thus du/dy is negative, the shearing stresses under consideration, however, are positive), and, after separation of the variables, du becomes:

$$du = -\frac{p_1 - p_2}{\mu l}\frac{y}{2}\,dy \tag{2.2}$$

and, on integration:

$$u(y) = \frac{p_1 - p_2}{\mu l}\left(C - \frac{y^2}{4}\right)$$

From the fact that for $y = r$ the velocity is supposed to be $u(y) = 0$ follows that the constant of integration C has to be $C = r^2/4$. Thus:

$$u(y) = \frac{p_1 - p_2}{4\mu l}\left(r^2 - y^2\right) \tag{2.3}$$

This equation (2.3) is Poiseuille's law for pipe flow. It states that the velocity $u(y)$ is distributed parabolically over the pipe cross section. The apex of the parabola lies on the pipe axis; here the velocity is greatest, namely:

$$u_{max} = \frac{p_1 - p_2}{4\mu l} r^2 \tag{2.4}$$

Therewith one may write (2.3):

$$u(y) = u_{max} \left(1 - \frac{y^2}{r^2}\right) \tag{2.3a}$$

By Poiseuille's law (equation (2.3)) the drag of the developed laminar flow (which is proportional to $p_1 - p_2$) is directly proportional to the first power of the velocity.

This statement is characteristic of all kinds of laminar flow whereas, as will be seen later, the drag in turbulent flow is almost proportional to the second power of the velocity.

The flow volume for the present case remains to be given. With dF designating an area element, Q is $Q = \int u(y)\, d\,F$ = volume of the velocity paraboloid, therefore

$$Q = \frac{1}{2} \pi r^2 u_{max} = \frac{\pi r^4}{8\mu l} (p_1 - p_2) \tag{2.5}$$

This flow law is often used for determination of the viscosity, by measuring the quantity flowing subjected to a pressure gradient (usually produced by gravity in a vertical capillary tube). Of course, the starting losses must be taken into consideration which due to the mixing zone (vortex formation) at the pipe end are not recovered to their full extent.

A drag coefficient λ will now be defined. Since turbulent flows are more important than laminar ones and since the drag in turbulent flow increases about as the square of the velocity, λ will also be referred to u^2.

For flow problems, let λ thus be defined as: ratio of the pressure drop along a test section of a specified characteristic length to the dynamic

pressure $q = \rho\bar{u}^2/2$, with $\bar{u} = \frac{Q}{\pi r^2}$ = the mean velocity (average taken across the cross section). Then:

$$\lambda = \frac{dp}{dx} \frac{d}{\rho \frac{\bar{u}^2}{2}} \tag{2.6}$$

with d = characteristic length, thus, for the present case, the pipe diameter, and with λ = dimensionless quantity. For the present developed laminar pipe flow, according to equation (2.5)

$$\frac{dp}{dx} = \frac{p_1 - p_2}{l} = \frac{8\mu Q}{\pi r^4}$$

Thus:

$$\lambda = \frac{2d}{\rho\bar{u}^2} \frac{8\mu Q}{\pi r^4} = \frac{2d8\mu}{\rho\bar{u}r^2} \underbrace{\frac{Q}{\pi r^2 \bar{u}}}_{=1} = \frac{16d\mu}{\rho\bar{u}\left(\frac{d}{2}\right)^2} = \frac{64\mu/\rho}{\bar{u}d}$$

or

$$\lambda = \frac{64}{Re} \tag{2.7}$$

with the dimensionless quantity $Re = \frac{\bar{u}d}{\nu}$ signifying the Reynolds number of the circular pipe. Since the pressure drop which is only linearily dependent on the velocity was referred to $\bar{u}^2$, then, for laminar flow: $\lambda \sim \frac{1}{\bar{u}}$. A logarithmic plot of $\lambda = f(Re)$ or $\lambda = f(\bar{u})$ therefore results in a straight line inclined 45° toward the Re-axis (compare fig. 82 Part II).

After this short analysis of the one-dimensional case of viscous fluid we will now consider the three-dimensional case.

CHAPTER III. EQUATIONS OF MOTION OF THE VISCOUS FLUID

a. State of Stress

For this purpose one must know first of all the general state of stress in a moving viscous fluid and must then connect this state of stress with the state of deformation. For the deformation of solid bodies the resistance to the deformation is put proportional to the magnitude of the deformation (assuming the validity of Hooke's law).

For flowing fluids, on the other hand, the resistance to deformation will depend on the deformation velocity, that is, on the variation of velocity in the neighborhood of the point under consideration. (Solid bodies: displacement gradient = displacement per second. Fluid: velocity gradient).

One starts from the basic law of mechanics according to which: mass x acceleration = sum of the acting, or resultant force. For the mass-per-unit volume, that is, the density ρ, one may write the law

$$\rho \frac{*\underline{Dw}}{Dt} = \underline{K} + \underline{R} + \underline{F} \tag{3.1}$$

$\frac{\underline{Dw}}{Dt}$ = substantial acceleration

$\underline{K}$ = mass forces

$\underline{R}$ = surface forces, composed of pressure forces normal to the surface and frictional forces in the direction of the surface

$\underline{F}$ = negligible extraneous forces

In order to formulate the surface forces, one imagines a small rectangular element of volume $dV = dx\,dy\,dz$ cut out of the flow (fig. 3) the left front corner of which lies at the point (x, y, z). The element is to be very small so that only the linear variations of a Taylor development need to be taken into consideration; on its surfaces $dy\,dz$ act the resultant stresses (vectors):

$$\underline{p}_x \quad \text{or} \quad \underline{p}_x + \frac{\partial \underline{p}_x}{\partial x} dx, \text{ respectively} \tag{3.2}$$

---

* Throughout the text, underscored letters are used in place of corresponding German script letters used in the original text.

(The index x signifies that the stress tensor acts on a surface element normal to the x-direction).

Analogous terms result for the surfaces dz dx normal to the y-axis and dx dy normal to the z-axis, if x in equation (3.2) is replaced everywhere by y or z, respectively. From this there results as components of the resultant force:

Force on the surface element normal to the x-direction: $\frac{\partial \underline{p}_x}{\partial x} dx\, dy\, dz$

Force on the surface element normal to the y-direction: $\frac{\partial \underline{p}_y}{\partial y} dy\, dz\, dx$

Force on the surface element normal to the z-direction: $\frac{\partial \underline{p}_z}{\partial z} dz\, dx\, dy$

The total resultant surface force $\underline{R}$ per unit volume caused by the state of stress is therefore:

$$\underline{R} = \frac{\partial \underline{p}_x}{\partial x} + \frac{\partial \underline{p}_y}{\partial y} + \frac{\partial \underline{p}_z}{\partial z} \tag{3.3}$$

$\underline{p}_x$, $\underline{p}_y$ and $\underline{p}_z$ are vectors which can be further decomposed into components. In this decomposition the components normal to every surface element, that is, the normal stresses, are designated by σ (indicating by the index the direction of this normal stress); the other components (tangential stresses) are denoted by τ (with double index: the first indicates to which axis the surface element is perpendicular, the second, the axial direction of the stress τ). With these symbols there is:

$$\left\{\begin{aligned} \underline{p}_x &= i\sigma_x + j\tau_{xy} + k\tau_{xz} \\ \underline{p}_y &= i\tau_{yx} + j\sigma_y + k\tau_{yz} \\ \underline{p}_z &= i\tau_{zx} + j\tau_{zy} + k\sigma_z \end{aligned}\right\} \tag{3.4}$$

This state of stress represents a tensor with nine vector components, which can be characterized by the stress matrix (stress tensor):

$$\begin{pmatrix} \sigma_x & \tau_{xy} & \tau_{xz} \\ \tau_{yx} & \sigma_y & \tau_{yz} \\ \tau_{zx} & \tau_{zy} & \sigma_z \end{pmatrix} \tag{3.5}$$

It can readily be shown that those of the six tangential stresses which have the same indices, although in interchanged sequence, must be equal. This follows for a homogeneous state of stress from the equilibrium of the small cube dx dy dz with respect to rotation:

Since τ_{xy} dy dx is the force attempting to rotate the cube counter-clockwise about the z-axis, (seen from above in fig. 3), with the lever arm dx, and since, correspondingly, the force $-\tau_{yx}$ dx dz attempts to rotate the cube clockwise about the z-axis, with the lever arm dy the balance of moments requires:

$$\tau_{xy} \text{ dy dz dx} - \tau_{xy} \text{ dx dz dy} = 0, \text{ thus } \tau_{xy} = \tau_{yx}.$$

Correspondingly, because of freedom from rotation about the x-axis $\tau_{yz} = \tau_{zy}$, and because of freedom from rotation about the y-axis $\tau_{zx} = \tau_{xz}$, the nine components of the stress tensor are reduced to six and the stress matrix (equation (3.5)) is converted into the stress matrix symmetrical with respect to the principal diagonal:

$$\begin{pmatrix} \sigma_x & \tau_{xy} & \tau_{xz} \\ \tau_{xy} & \sigma_y & \tau_{yz} \\ \tau_{xz} & \tau_{yz} & \sigma_z \end{pmatrix} \quad \text{(stress matrix)} \tag{3.6}$$

For the frictional force one obtains according to equation (3.3) by insertion of the components from equation (3.4) and by reduction to the six remaining terms according to equation (3.6):

$$\underline{R} = i\left(\frac{\partial \sigma_x}{\partial x} + \frac{\partial \tau_{xy}}{\partial y} + \frac{\partial \tau_{xz}}{\partial z}\right) + j\left(\frac{\partial \tau_{xy}}{\partial x} + \frac{\partial \sigma_y}{\partial y} + \frac{\partial \tau_{yz}}{\partial z}\right)$$

$$= \text{x-component} + \text{y-component} + \underline{k}\left(\frac{\partial \tau_{xz}}{\partial x} + \frac{\partial \tau_{yz}}{\partial y} + \frac{\partial \sigma_z}{\partial z}\right) \tag{3.7}$$

$$+ \text{z-component.}$$

For the case of the <u>frictionless (ideal) fluid</u> all shearing stresses disappear

$$\tau_{xy} = \tau_{yz} = \tau_{zx} = 0 \tag{3.8}$$

and only the normal stresses remain, which in this case are all equal. Since the normal stresses from within toward the outside are denoted as positive, the normal stresses equal the negative fluid pressure:

$$\sigma_x = \sigma_y = \sigma_z = -p \tag{3.9}$$

The static pressure equals the negative arithmetic mean of the normal stresses:

$$-p = \frac{1}{3}\left(\sigma_x + \sigma_y + \sigma_z\right)$$

b. State of Deformation

The state of stress treated so far is, alone, not very useful. Therefore we will now consider the state of deformation (that is the field of velocity variations) and then set up the relations between state of stress and state of deformation.

Let the velocity $\underline{w}_A$ with the components u_A, v_A, w_A in the directions of the axes exist at the point A the coordinates of which are x_A, y_A, z_A.

If one limits oneself to the points x, y, z in the immediate neighborhood of A with the velocity $\underline{w} = iu + jv + \underline{k}w$, and if one limits oneself – as also in setting up the state of deformation – to linear terms only, one obtains for the deformation the relative change in position between the points x, y, z and x_A, y_A, z_A per unit time, that is, the difference of the velocities at the points x, y, z and x_A, y_A, z_A:

$$\left.\begin{aligned} u - u_A &= (x - x_A)\left(\frac{\partial u}{\partial x}\right)_A + (y - y_A)\left(\frac{\partial u}{\partial y}\right)_A + (z - z_A)\left(\frac{\partial u}{\partial z}\right)_A = du \\ v - v_A &= (x - x_A)\left(\frac{\partial v}{\partial x}\right)_A + (y - y_A)\left(\frac{\partial v}{\partial y}\right)_A + (z - z_A)\left(\frac{\partial v}{\partial z}\right)_A = dv \\ w - w_A &= (x - x_A)\left(\frac{\partial w}{\partial x}\right)_A + (y - y_A)\left(\frac{\partial w}{\partial y}\right)_A + (z - z_A)\left(\frac{\partial w}{\partial z}\right)_A = dw \end{aligned}\right\} \quad (3.11)$$

$d\underline{w} = i\,du + j\,dv + \underline{k}\,dw$ = distortion of the fluid region in the neighborhood of the point A.

Omitting the index A one obtains therefore:

$$d\underline{w} = \frac{\partial \underline{w}}{\partial x}dx + \frac{\partial \underline{w}}{\partial y}dy + \frac{\partial \underline{w}}{\partial z}dz = i\left(\frac{\partial u}{\partial x}dx + \frac{\partial u}{\partial y}dy + \frac{\partial u}{\partial z}dz\right)$$

$$+ j\left(\frac{\partial v}{\partial x}dx + \frac{\partial v}{\partial y}dy + \frac{\partial v}{\partial z}dz\right) + \underline{k}\left(\frac{\partial w}{\partial x}dx + \frac{\partial w}{\partial y}dy + \frac{\partial w}{\partial z}dz\right) \quad (3.11a)$$

Thus the velocity variation (and hence, on integration, the velocity itself) in the neighborhood of the point A is known if the nine partial derivatives of the velocity components with respect to the space coordinates are known. Corresponding to the stress matrix, one may form a deformation matrix:

$$\begin{pmatrix} \frac{\partial u}{\partial x} & \frac{\partial u}{\partial y} & \frac{\partial u}{\partial z} \\ \frac{\partial v}{\partial x} & \frac{\partial v}{\partial y} & \frac{\partial v}{\partial z} \\ \frac{\partial w}{\partial x} & \frac{\partial w}{\partial y} & \frac{\partial w}{\partial z} \end{pmatrix} \quad \text{deformation matrix} \qquad (3.12)$$

The friction forces of the viscous fluid are given by a relation (which will have to be determined) between these two matrices. First, the deformation matrix is to be somewhat clarified.

1. Case of pure elongation.

One assumes $u - u_a = a(x - x_A)$, with $a = \frac{\partial u}{\partial x} = \text{constant}$. Let all other terms of the matrix disappear; the matrix will then appear as follows:

$$\begin{pmatrix} a & 0 & 0 \\ 0 & 0 & 0 \\ 0 & 0 & 0 \end{pmatrix}$$

Then the velocity variation is simply $du = a\,dx$, and $u = ax$. All points of the y-axis remain at rest, the points to the right and left of it are elongated or compressed, according to whether $a > 0$ or $a < 0$ (fig. 5). The equation $u = ax$ therefore represents an elongation or expansion parallel to the x-axis. Corresponding relations apply for the other terms of the principal diagonal of the matrix.

2. Case of pure translation

All terms disappear; the matrix then reads:

$$\begin{pmatrix} 0 & 0 & 0 \\ 0 & 0 & 0 \\ 0 & 0 & 0 \end{pmatrix}.$$

In this case, which, as a matter of fact, should have been mentioned first, $u - u_a = 0$, $du = 0$; u = constant. The velocity component parallel to the x-axis is uniform (correspondingly for the other axes).

3. Case of angular deformation.

One assumes $u - u_a = e(y - y_a)$, with $e = \frac{\partial u}{\partial y}$ = constant. All other terms equal zero, and the matrix reads:

$$\begin{pmatrix} 0 & e & 0 \\ 0 & 0 & 0 \\ 0 & 0 & 0 \end{pmatrix}$$

$du = e\,dy$ and $u = ey$; that is, all points of the x-axis retain their position; all points of the y-axis shift to the right (left), when $e > 0$ ($e < 0$); for $e > 0$ the y-axis is rotated clockwise by the angle ϵ (because of the linearity). The y-axis is simultaneously elongated. The phenomenon in question is therefore a shearing (fig. 6), with $\tan \epsilon = e$.

Correspondingly there results for $v - v_a = f\,(x - x_A)$ and

$$M = \begin{pmatrix} 0 & 0 & 0 \\ f & 0 & 0 \\ 0 & 0 & 0 \end{pmatrix}$$

$$dv = f\,dx; \quad v = fx$$

All points of the y-axis retain their position; the points of the x-axis are rotated by the angle δ; $\tan \delta = f$ (fig.7). Terms outside of the principal diagonal of the matrix result therefore in a deformation of the right angle with axis-elongation (shearing). The right angle between the x- and y-axes is, therefore, for $e > 0$ and $f > 0$ deformed by

$$\epsilon + \delta = \frac{\partial v}{\partial x} + \frac{\partial u}{\partial y} = \gamma_{xy} = \text{Deformation about the z-axis}$$

Correspondingly: $\gamma_{zx} = \frac{\partial u}{\partial z} + \frac{\partial w}{\partial x}$ = deformation about the y-axis

$\gamma_{yz} = \frac{\partial w}{\partial y} + \frac{\partial v}{\partial z}$ = deformation about the x-axis

(The deformation angles are herein regarded as small so that the tangent may be replaced by the argument).

c. Navier-Stokes Formulation for the Stress Tensor

One now proceeds to relate the stress matrix (equation (3.6)) with the deformation matrix (equation (3.12)). The former is symmetrical with respect to the principal diagonal, but not the latter. However, one obtains a symmetrical deformation matrix by adding to equation (3.12) its reflection in the principal diagonal. Furthermore, one first splits off the pressure p (contribution of the ideal fluid) from the stress matrix and sets the remaining stress matrix, according to Stokes, proportional to the deformation matrix made symmetrical:

$$\begin{vmatrix} \sigma_x & \tau_{xy} & \tau_{xz} \\ \tau_{xy} & \sigma_y & \tau_{yz} \\ \tau_{xz} & \tau_{yz} & \sigma_z \end{vmatrix} = - \begin{vmatrix} p & 0 & 0 \\ 0 & p & 0 \\ 0 & 0 & p \end{vmatrix} + \mu \begin{vmatrix} \frac{\partial u}{\partial x} & \frac{\partial u}{\partial y} & \frac{\partial u}{\partial z} \\ \frac{\partial v}{\partial x} & \frac{\partial v}{\partial y} & \frac{\partial v}{\partial z} \\ \frac{\partial w}{\partial x} & \frac{\partial w}{\partial y} & \frac{\partial w}{\partial z} \end{vmatrix} + \mu \begin{vmatrix} \frac{\partial u}{\partial x} & \frac{\partial v}{\partial x} & \frac{\partial w}{\partial x} \\ \frac{\partial u}{\partial y} & \frac{\partial v}{\partial y} & \frac{\partial w}{\partial y} \\ \frac{\partial u}{\partial z} & \frac{\partial v}{\partial z} & \frac{\partial w}{\partial z} \end{vmatrix} \qquad (3.13)$$

From equation (3.13) each stress component may be given immediately by coordinating the homologous parts of the matrices to each other. For instance:

$\sigma_x = - p + 2 \mu \frac{\partial u}{\partial x}$ = static pressure + pressure due to velocity variation, or:

$$\sigma_x = -p + 2\mu\frac{\partial u}{\partial x}; \quad \sigma_y = -p + 2\mu\frac{\partial v}{\partial y}; \quad \sigma_z = -p + 2\mu\frac{\partial w}{\partial z}$$

$$\tau_{xy} = \tau_{yx} = \mu\left(\frac{\partial v}{\partial x} + \frac{\partial u}{\partial y}\right)$$

$$\tau_{yz} = \tau_{zy} = \mu\left(\frac{\partial w}{\partial y} + \frac{\partial v}{\partial z}\right)$$

$$\tau_{xz} = \tau_{zx} = \mu\left(\frac{\partial u}{\partial z} + \frac{\partial w}{\partial x}\right)$$

$$\left[\text{Thus for one-dimensional flow} \quad \tau_{xy} = \tau_{yx} = \mu\frac{du}{dy}\right]$$

Furthermore, there follows from equation (3.13):

$$\frac{1}{3}\left(\sigma_x + \sigma_y + \sigma_z\right) = -p + \frac{2}{3}\mu\left(\frac{\partial u}{\partial x} + \frac{\partial v}{\partial y} + \frac{\partial w}{\partial z}\right)$$

or

$$\frac{1}{3}\left(\sigma_x + \sigma_y + \sigma_z\right) = -p \tag{3.14}$$

because

$$\frac{\partial u}{\partial x} + \frac{\partial v}{\partial y} + \frac{\partial w}{\partial z} = \operatorname{div} \underline{w} = 0$$

for the incompressible flows free of sources and sinks under consideration.* Thus for the viscous incompressible flow, as for the ideal fluid the pressure equals the arithmetic mean of the normal stresses.

With these results the components of the friction force may be expressed according to equation (3.7) as follows:

---

* The compressibility manifests itself as normal stress, since it can be interpreted as a pressure disturbance, for instance due to variation in density, which attempts to spread in all directions — considered infinitesimally.

$$R_x = \frac{\partial \sigma_x}{\partial x} + \frac{\partial \tau_{xy}}{\partial y} + \frac{\partial \tau_{xz}}{\partial z} = -\frac{\partial p}{\partial x} + \mu\left(\frac{\partial^2 u}{\partial x^2} + \frac{\partial^2 u}{\partial y^2} + \frac{\partial^2 u}{\partial z^2}\right)$$

$$+ \mu\left(\frac{\partial^2 u}{\partial x^2} + \frac{\partial^2 v}{\partial x \partial y} + \frac{\partial^2 w}{\partial x \partial z}\right)$$

or, since $\operatorname{div} \underline{w} = 0$,

$$\left.\begin{aligned} R_x &= -\frac{\partial p}{\partial x} + \mu \Delta u \\ R_y &= -\frac{\partial p}{\partial y} + \mu \Delta v \\ R_z &= -\frac{\partial p}{\partial z} + \mu \Delta w \end{aligned}\right\} \qquad (3.15)$$

in which $\Delta u = \frac{\partial^2 u}{\partial x^2} + \frac{\partial^2 u}{\partial y^2} + \frac{\partial^2 u}{\partial z^2}$

If one finally designates the mass forces by $\underline{K} = \rho(iX + jY + kZ)$, and assumes the decomposition of the substantial derivative into a local and convective part as known from Euler's equation, one obtains for the components of the equation of motion of the non-stationary, incompressible, and viscous fluid from equation (3.1):

$$\left.\begin{aligned} \rho\left(\frac{\partial u}{\partial t} + u\frac{\partial u}{\partial x} + v\frac{\partial u}{\partial y} + w\frac{\partial u}{\partial z}\right) &= \rho X - \frac{\partial p}{\partial x} + \mu \Delta u \\ \rho\left(\frac{\partial v}{\partial t} + u\frac{\partial v}{\partial x} + v\frac{\partial v}{\partial y} + w\frac{\partial v}{\partial z}\right) &= \rho Y - \frac{\partial p}{\partial y} + \mu \Delta v \\ \rho\left(\frac{\partial w}{\partial t} + u\frac{\partial w}{\partial x} + v\frac{\partial w}{\partial y} + w\frac{\partial w}{\partial z}\right) &= \rho Z - \frac{\partial p}{\partial z} + \mu \Delta w \end{aligned}\right\} \qquad (3.16)$$

In addition, the continuity equation

$$\frac{\partial u}{\partial x} + \frac{\partial v}{\partial y} + \frac{\partial w}{\partial z} = 0 \qquad (3.17)$$

is used. Written in vector form, the Navier–Stokes differential equation and the equation of continuity read

$$\frac{D\underline{w}}{Dt} = \underline{K} - \frac{1}{\rho} \operatorname{grad} p + \nu \Delta \underline{w} \tag{3.18}$$

$$\operatorname{div} \underline{w} = 0 \tag{3.19}$$

Due to the friction terms, therefore, terms of the second order enter the differential equation.

Boundary conditions are attached to these equations. If all friction terms on the right side are cancelled, that is $\nu = 0$, the differential equations become equations of the first order and one boundary condition is sufficient, namely the boundary condition of the potential flow: $v_n = 0$ on the bounding walls.

This means that the normal component v_n of the velocity at the bounding surface must disappear on the surface itself whereas the fluid still can glide parallel to the boundary (tangential velocity v_t parallel to the surface $\neq 0$).

For viscous flow where the differential equation is of the second order, two boundary conditions are required, namely:

$$\underline{v_n = 0} \quad \text{and} \quad \underline{v_t = 0} \quad \text{(condition of no slip)} \tag{3.20}$$

that is, the fluid must in addition adhere to the surface.

Second lecture (Dec. 8, 1941)

CHAPTER IV. GENERAL PROPERTIES OF NAVIER–STOKES EQUATIONS

These Navier–Stokes differential equations represent together with the equation of continuity a system of four equations for the four unknown quantities u, v, w, p. On the left side of the Navier–Stokes differential equations are the inertia terms, on the right side the mass forces, the pressure forces, and the friction forces.

Since Stokes' formulation is, of course, at first purely arbitrary, it is not a priori certain whether the Navier–Stokes differential equations describe the motion of a fluid correctly. They therefore require verification, which is possible only by way of experimentation.

Unfortunately, due to unsurmountable mathematical difficulties, a general solution of the differential equation is not yet known, that is, a solution where inertia and friction terms in the entire flow region are of the same order of magnitude. However, known special solutions (for instance, the pipe flow with predominant viscosity or cases with large inertia effect) agree so well with the experimental findings, that the general validity of Navier–Stokes differential equation hardly seems questionable.

The plane problem:

By far the greatest part of the application of Navier–Stokes differential equations concern "plane" cases, that is, the cases where no fluid flows in one direction. The velocity vector $\underline{w}$ is then given by

$$\underline{w} = iu\,(x, y, t) + jv\,(x, y, t) \tag{4.1}$$

since $w \equiv 0$. The equation system (equations (3.16) and (3.17)) then is transformed into the 3 equations

$$\begin{aligned}
\rho\left(\frac{\partial u}{\partial t} + u\frac{\partial u}{\partial x} + v\frac{\partial u}{\partial y}\right) &= \rho X - \frac{\partial p}{\partial x} + \mu\left(\frac{\partial^2 u}{\partial x^2} + \frac{\partial^2 u}{\partial y^2}\right) \\
\rho\left(\frac{\partial v}{\partial t} + u\frac{\partial v}{\partial x} + v\frac{\partial v}{\partial y}\right) &= \rho Y - \frac{\partial p}{\partial y} + \mu\left(\frac{\partial^2 v}{\partial x^2} + \frac{\partial^2 v}{\partial y^2}\right) \\
\frac{\partial u}{\partial x} + \frac{\partial v}{\partial y} &= 0
\end{aligned} \tag{4.2}$$

with the three unknown factors u, v, p (X and Y are the components of the mass force $\underline{K}$ per unit volume).

After various minor transformations the equation system may be written as a single equation. To this end one introduces the rotational vector rot $\underline{w}$ which for the plane case has only one component not equalling zero:

$$\frac{1}{2}\,\mathrm{rot}_z \underline{w} = \omega_z = \frac{1}{2}\left(\frac{\partial v}{\partial x} - \frac{\partial u}{\partial y}\right) \tag{4.3}$$

Furthermore, the mass force in equation (4.2) is put equal to zero. This is permissible in all cases where the fluid is homogeneous and no free surfaces are present. In order to introduce ω_z into equation (4.2), the first equation of (4.2) is differentiated with respect to y, and the second with respect to x; then the first is subtracted from the second and one obtains:

$$\rho\left[\frac{\partial}{\partial t}\left(\frac{\partial v}{\partial x}-\frac{\partial u}{\partial y}\right)+u\frac{\partial}{\partial x}\left(\frac{\partial v}{\partial x}-\frac{\partial u}{\partial y}\right)+v\frac{\partial}{\partial y}\left(\frac{\partial v}{\partial x}-\frac{\partial u}{\partial y}\right)\right]$$

$$=\mu\left[\frac{\partial^2}{\partial x^2}\left(\frac{\partial v}{\partial x}-\frac{\partial u}{\partial y}\right)+\frac{\partial^2}{\partial y^2}\left(\frac{\partial v}{\partial x}-\frac{\partial u}{\partial y}\right)\right] \qquad (4.4)$$

or

$$\rho\left(\frac{\partial \omega_z}{\partial t}+u\frac{\partial \omega_z}{\partial x}+v\frac{\partial \omega_z}{\partial y}\right)=\mu\left(\frac{\partial^2 \omega_z}{\partial x^2}+\frac{\partial^2 \omega_z}{\partial y^2}\right)=\mu\Delta\omega_z \qquad (4.5)$$

With this transformation the pressure terms have been eliminated. Equation (4.5) may now, with $\mu/\rho=\nu$, be written:

$$\frac{D\omega}{Dt}=\nu\Delta\omega \quad \text{(vorticity transport equation)} \qquad (4.6)$$

with $\omega=\omega_z$ being denoted as the vorticity.

This equation signifies: The convective (substantial) variation of the vortex strength equals the dissipation of vorticity by friction.

Equation (4.6) forms with the equation of continuity a system of two equations with two unknowns, namely u and v, the derivatives of which define ω.

By introducing a flow function $\psi(x,y)$ one may finally introduce a single equation with the unknown ψ. The flow function represents the integral of the equation of continuity. One sets:

$$\left.\begin{aligned} u&=\frac{\partial \psi}{\partial y}\\ v&=-\frac{\partial \psi}{\partial x}\end{aligned}\right\} \qquad \begin{array}{l}\text{That is, therefore, the}\\ \text{equation of continuity}\\ \text{is identically}\\ \text{satisfied by } \psi.\end{array} \qquad (4.7)$$

Moreover,

$$\omega = \frac{1}{2}\left(\frac{\partial v}{\partial x} - \frac{\partial u}{\partial y}\right) = -\frac{1}{2}\left(\frac{\partial^2 \psi}{\partial x^2} + \frac{\partial^2 \psi}{\partial y^2}\right) = -\frac{1}{2}\Delta\psi \tag{4.8}$$

That is: The Laplacian of the flow function is exactly minus two times as large as the vorticity (angular velocity). With this result equation (4.5) becomes, after division by ρ:

$$\left(\frac{\partial}{\partial t} + u\frac{\partial}{\partial x} + v\frac{\partial}{\partial y}\right)\Delta\psi = \nu\Delta\Delta\psi \tag{4.9}$$

or expressed only in ψ with equation (4.7):

$$\frac{\partial \Delta\psi}{\partial t} + \frac{\partial \psi}{\partial y}\frac{\partial \Delta\psi}{\partial x} - \frac{\partial \psi}{\partial x}\frac{\partial \Delta\psi}{\partial y} = \nu\Delta\Delta\psi \tag{4.10}$$

This one equation with the unknown ψ is the vorticity transport equation, but written in terms of ψ.

The inertia terms are again on the left, the viscosity terms on the right side. Equation (4.10) is a differential equation of the fourth order for the flow function. Again, its general solution is extremely difficult because of the non-linearity. For very slow (creeping) motions the friction terms very strongly predominate. Then one may set:

$$\Delta\Delta\psi = 0 \tag{4.11}$$

This simplification is permissible only because the differential equation remains of the fourth order, so that no boundary condition is lost. However, being linear, this equation is at least solvable. It appears also in the theory of elasticity where it is designated as the bipotential equation. There exists a solution of equation (4.11) by Stokes for moving droplets, which was extended by Cunningham to very small drop diameters (comparable to the mean free path of the molecules).

Herewith we shall conclude the more general considerations and turn to the boundary layer problem proper, limiting ourselves to fluids of very small viscosity ν.

A few preparatory considerations will lead up to the boundary layer problem. One might conceive the notion of simply eliminating all the friction terms of the Navier-Stokes' differential equation in the case of small viscosity. However, this would be fundamentally wrong as will be proved below.

An equation which is completely analogous to equation (4.5) occurs in the theory of heat transfer:

$$c_p\left(\frac{\partial \vartheta}{\partial t} + u\frac{\partial \vartheta}{\partial x} + v\frac{\partial \vartheta}{\partial y}\right) = \lambda\left(\frac{\partial^2 \vartheta}{\partial x^2} + \frac{\partial^2 \vartheta}{\partial y^2}\right) \tag{4.12}$$

where the velocity components are retained whereas the rotation ω replaces the temperature ϑ, the density ρ the specific heat c_p per unit volume, and the viscosity μ the thermal conductivity λ. On the left of equation (4.12) stands the temperature change due to convection, on the right the change due to heat transfer.

The temperature distribution around a heated body immersed in a flow with the free stream velocity u_o (for instance fig. 8) is determined by the differential equation (4.12). One perceives intuitively that for small u_o the temperature increase starting from the body extends toward the front and all sides far into the flow (solid contour) whereas for large u_o this influence is mainly limited to a thin layer and a narrow wake (dashed contour).

The analogy of equations (4.12) and (4.5) indicates that the friction-rotation distribution in question must be similar: For small free stream velocity the rotation is noticeable at large distance from the body, whereas for large u_o the rotation is limited to the immediate neighborhood of the body.

Thus for rapid motions, that is, large Reynolds numbers (compare next section), one expects the following solution of Navier-Stokes' differential equations:

1. In the region outside of a thin boundary layer $\omega = 0$, that is, potential flow

2. Inside this thin boundary layer $\omega \neq 0$, thus no potential flow.

Therefore, one must not set $\omega = 0$ in this boundary layer, even for small viscosity.

It is true that the potential flow is also a solution of Navier-Stokes' differential equations, but it does not satisfy the boundary layer condition $v_t = 0$.

Proof: The potential flow may be derived from potential $\Phi(x,y,z)$ as:

$$\underline{w} = \text{grad } \Phi, \text{ with } \Delta\Phi = \frac{\partial^2 \Phi}{\partial x^2} + \frac{\partial^2 \Phi}{\partial y^2} + \frac{\partial^2 \Phi}{\partial z^2} = 0 \tag{4.13}$$

However, if $\Delta\Phi = 0$, then also $\text{grad}\,\Delta\Phi = \Delta\,\text{grad}\Phi = 0$, that is, $\Delta\underline{w} = 0$ for potential flow. According to equation (3.18) this fact signifies that in the Navier–Stokes differential equations the friction terms vanish identically, and hence that the potential flow actually satisfies the Navier–Stokes differential equations. However, it satisfies only the one boundary condition $v_n = 0$.

Thus, for the limiting case of small viscosity, one obtains useful solutions for the limiting process $\nu \longrightarrow 0$ not by cancelling the friction terms in the differential equation, since this reduces its order (the differential equation of the fourth order for the flow function would turn into an equation of the second order; the Navier–Stokes differential equations would change from the second to the first order), so that one can satisfy only correspondingly fewer boundary conditions.

Thus the limiting process $\nu \longrightarrow 0$ must not be performed in the differential equation itself, but only in its solution.

This can be clearly demonstrated on an example (referred to for comparison by Prandtl) of the solution of an ordinary differential equation. Consider the damped oscillation of a mass point. The differential equation

$$m\frac{d^2x}{dt^2} + k\frac{dx}{dt} + cx = 0 \qquad (4.14)$$

applies in which m represents the oscillating mass, k the damping constant and c the spring constant. (x = elongation, t = time).

Let for instance the two initial conditions be:

$$t = 0; \quad x = 0; \quad dx/dt = 1$$

In analogy to the case in question one considers here the limiting case of a very small mass m, since then the term of the highest order tends toward zero. If one would simply put $m = 0$, one would treat nothing but the differential equation

$$k\frac{dx}{dt} + cx = 0 \qquad (4.15)$$

which by assuming the solution to be of the form $x = A\,e^{\lambda t}$ is transformed into $k\lambda + c = 0$, whence $\lambda = -c/k$. That is, the solution reads:

$$x = A\, e^{-\frac{c}{k}t} \tag{4.16}$$

However, the two initial conditions $x = 0$ and $dx/dt = 1$ at the time $t = 0$ cannot be satisfied with this solution. But if one treats the complete differential equation (4.14) in the same manner there results:

$$m\lambda^2 + k\lambda + c = 0$$

and hence:

$$\lambda_{1,2} = \frac{-k \pm k\sqrt{1 - \frac{4cm}{k^2}}}{2m}$$

or the square root might be developed into a series and (since now the limiting process $m \longrightarrow 0$ is to be performed) broken off after the second term:

$$\lambda_{1,2} = \frac{-k \pm k\left(1 - \frac{2cm}{k^2}\right)}{2m} \quad \text{thus } \lambda_1 = -\frac{c}{k};\quad \lambda_2 = -\frac{k}{m} + \frac{c}{k}$$

Thus λ_1 corresponds to the previous solution of the first order differential equation, where, however, λ_2 had been lost. For very small m, $\lambda_2 \approx -k/m$; therewith the general solution becomes, by combination of the particular solutions,

$$x = A_1\, e^{\lambda_1 t} + A_2\, e^{\lambda_2 t} = A_1\, e^{-\frac{c}{k}t} + A_2\, e^{-\frac{k}{m}t} \tag{4.17}$$

Since for $t = 0$, x is also supposed to equal zero, there follows: $A_2 = -A_1$, thus:

$$x = A_1\left(e^{-\frac{c}{k}t} - e^{-\frac{k}{m}t}\right) \tag{4.18}$$

This equation is plotted schematically in figure 9. The first term of equation (4.18), which alone cannot satisfy the boundary conditions,

starts from the value A_1 at the time $t = 0$ and decreases exponentially. The second term is important only for small t-values and plays no role for large t. It is very rapidly variable and assures that the total solution (solid line) satisfies the boundary conditions. The slowly variable solution (in λ_1) corresponds to the potential flow, the second, rapidly variable particular solution (in λ_2) indicates, as it were, the narrow region of the boundary layer; the smaller m, the narrower this region.

Herewith we shall conclude the general remarks and turn to the law of similarity.

CHAPTER V. REYNOLDS' LAW of SIMILARITY

So far no general methods for the solution of the Navier-Stokes differential equations are known. Solutions that are valid for all values of the viscosity are so far known only for a very few special cases (for instance, Poiseuille's pipe flow). Meanwhile the problem of flow in a viscous fluid has been tackled by starting from the limits, that is, one has treated on the one hand flows of very great viscosity, on the other hand flows of very small viscosity, since one obtains in this manner certain mathematical simplifications. However, starting from these limiting cases one cannot possibly interpolate for flows of average viscosity.

The theoretical treatment of the limiting cases of very great and very small viscosity is mathematically still very difficult. Thus research on viscous fluids was undertaken largely from the experimental side. The Navier-Stokes differential equations offer very useful indications, which permit a considerable reduction of the volume of experimental investigation. The rules in question are the so-called laws of similarity.

The problem is: Under what conditions are the forms of flows of any liquids or gases around geometrically similarly shaped bodies themselves geometrically similar? Such flows are called mechanically similar.

Consider for instance the flows of two different fluids of different velocities around two spheres of different size (fig. 10). Under what conditions are the flows geometrically similar to each other? Obviously this is the case when at points of similar position in the two flow patterns the forces acting on volume elements at these points have the same ratio. Depending on what kinds of forces are in effect, various laws of similarity will result from this requirement.

Most important for this investigation is the case where all forces except the inertia and friction forces are negligible. Furthermore, no free surfaces are to be present, so that the effect of gravity is compensated by the hydrostatic pressure. In this case the flow around

the two spheres is geometrically similar when the inertia and friction forces have the same ratio at every point.

The expressions for the inertia and viscosity forces acting on the volume element will now be derived: there is as friction force per unit volume $\frac{d\tau}{dy} = \mu \frac{\partial^2 u}{\partial y^2}$, whereas the inertia force per unit volume is $\rho u \frac{\partial u}{\partial x}$. The ratio

$$\frac{\text{inertia force}}{\text{friction force}} = \frac{\rho u \frac{\partial u}{\partial x}}{\mu \frac{\partial^2 u}{\partial y^2}} \tag{5.1}$$

must, therefore, be the same at all points of the flow. One now inquires as to the variation of these forces with variation in the quantities characteristic of the phenomenon: free stream velocity V, diameter d, density ρ, and viscosity μ. For variation of V and d the individual quantities in equation (5.1) at similarly located points vary as follows:

$$u \sim V; \quad \frac{\partial u}{\partial x} \sim \frac{V}{d}; \quad \frac{\partial^2 u}{\partial y^2} \sim \frac{V}{d^2}$$

Therewith equation (5.1) becomes:

$$\frac{\text{inertia force}}{\text{friction force}} = \frac{\rho \frac{V^2}{d}}{\mu \frac{V}{d^2}} = \frac{\rho V d}{\mu} = \boxed{\frac{Vd}{\nu} = Re} \tag{5.2}$$

The law of mechanical similarity is therefore: The flows around geometrically similar bodies similarly located and alined with respect to the flow have, for equal $\rho V d/\mu$, geometrically similar stream lines as well. If the flows in question are, for instance, two flows of the same fluid of equal temperature and density (μ and ρ equal) around two spheres, one of which has a diameter twice that of the other, the flows are geometrically similar provided that the free stream velocity for the larger sphere has half the magnitude of that for the smaller sphere.

The quantity $\rho V d/\mu$ is, as a quotient of two forces, a dimensionless number. This fact is immediately recognized by substituting for the quantities their dimensions:

$$\rho\left[\text{kg sec}^2\ \text{m}^{-4}\right];\quad V\left[\frac{\text{m}}{\text{sec}}\right];\quad d\left[\text{m}\right];\quad \mu\left[\frac{\text{kg sec}}{\text{m}^2}\right]$$

$$\frac{\rho V d}{\mu} = \frac{\text{kg sec}^2}{\text{m}^{-4}}\frac{\text{m}}{\text{sec}}\,\text{m}\,\frac{\text{m}^2}{\text{kg sec}} = 1$$

This law of similarity was discovered by Osborne Reynolds in his studies of fluid flows in a pipe. The dimensionless quantity is called after him:

$$\rho V\ d/\mu = V\ d/\nu = \text{Re} = \text{Reynolds' number}$$

The introduction of this dimensionless quantity helped greatly in advancing the development of modern hydrodynamics.

Connection between Similarity and Dimensional Considerations

As is known, all physical laws can be expressed in a form free of the units of measure. Thus the similarity consideration may be replaced by a dimensional analysis. The following quantities appearing in the Navier–Stokes differential equations are essential for the stream line pattern: V, d, ρ, μ. The question is whether there is a combination

$$V^{\alpha}\ d^{\beta}\ \rho^{\gamma}\ \mu^{\delta}$$

which is a Reynolds number and therefore has the dimension 1. This amounts to determining α, β, γ, δ in such a manner that

$$V^{\alpha}\ d^{\beta}\ \rho^{\gamma}\ \mu^{0} = K^{0}\ L^{0}\ T^{0} = 1 \qquad (5.3)$$

with K, L, T representing the symbols for force, length, and time, respectively. Without limiting the generality α may be set equal to unity ($\alpha = 1$) since any power of a dimensionless quantity is still a pure number. With $\alpha = 1$ there results from equation (5.3)

$$\left[Vd^{\beta}\ \rho^{\gamma}\ \mu^{\delta}\right] = \frac{L}{T} L^{\beta} \left(\frac{KT^2}{L^4}\right)^{\gamma} \left(\frac{KT}{L^2}\right)^{\delta} = K^{o}\ L^{o}\ T^{o} \tag{5.4}$$

By equating the exponents of L, T, K on the left and right sides one obtains the three equations:

$$\left.\begin{array}{lrl} K: & & \gamma + \delta = 0 \\ L: & 1 + \beta & -4\gamma - 2\delta = 0 \\ T: & & 2\gamma + \delta = 1 \end{array}\right\} \tag{5.5}$$

The solution gives:

$$\beta = 1; \quad \gamma = 1; \quad \delta = -1 \tag{5.6}$$

Accordingly the only possible dimensionless combination of V, d, ρ, μ is the quotient

$$\frac{Vd\rho}{\mu} = Re \tag{5.7}$$

This dimensional analysis lacks the pictorial quality of the similarity consideration; however, it offers the advantage of applicability even when knowledge of the exact equation of motion is still missing, if there is only known what physical quantities determine the phenomenon.

CHAPTER VI. EXACT SOLUTIONS OF THE NAVIER–STOKES EQUATIONS

In general, the problem of finding exact solutions of the Navier–Stokes differential equations encounters insurmountable difficulties, particularly because of the non–linearity of these equations which prohibits application of the principle of superposition. Nevertheless one can give exact solutions for a few special cases, mostly, when the second power terms vanish automatically. A few of these exact solutions will be treated here.

One investigates first layer flows in general, that is, flows where only one velocity component exists which, moreover, is not dependent on the analagous position coordinate, whereas the two other velocity components vanish identically; thus for instance:

$$A = \sqrt{\nu\, a}; \quad \alpha = \sqrt{\frac{a}{\nu}} \tag{6.27a}$$

the differential equation for $\varphi(\xi)$ with $\xi = \sqrt{\frac{a}{\nu}}\, y$ reads:

$$\varphi''' + \varphi\, \varphi'' = \varphi'^2 + 1 = 0 \tag{6.28}$$

with the boundary conditions

$$\xi = 0: \quad \varphi = \varphi' = 0$$

$$\xi = \infty: \quad \varphi' = 1$$

The solution found by series development can be found in the thesis of Hiemenz (reference 10), compare table 1*. The velocity component parallel to the surface is

$$\frac{u}{U} = \frac{1}{a} f'(y) = \varphi'(\xi) \tag{6.29}$$

It is indicated in figure 16. The curve $\varphi'(\xi)$ increases linearly at $\xi = 0$ and approaches one asymptotically. For about $\xi = 2.6$, $\varphi' \approx 0.99$; thus within about one percent of the final value. If one again designates the corresponding distance from the surface $y = \delta$ as the boundary layer thickness (friction layer thickness), then

$$\delta = \frac{1}{\alpha}\, \xi_\delta = 2.6\sqrt{\frac{\nu}{a}} \tag{6.30}$$

Thus in this flow, as in the former ones,

$$\delta \sim \sqrt{\nu}$$

It is also remarkable that the dimensionless velocity distribution according to equation (6.29) and the boundary layer thickness according to equation (6.30) are independent of x, thus do not vary along the wall.

---

*The tables appear in appendix, chapter XII.

For later applications the characteristics important for the friction layer, displacement thickness δ^* and momentum thickness ϑ, are introduced here; they are defined by

$$U\delta^* = \int_{y=0}^{\infty} (U - u)\, dy \tag{6.31}$$

$$U^2\vartheta = \int_{y=0}^{\infty} u(U - u)\, dy \tag{6.32}$$

The displacement thickness gives the deflection of the stream lines of the potential flow from the surface by the friction layer; the momentum thickness is a measure of the momentum loss in the friction layer. By insertion of equation (6.29) in (6.31) and (6.32) and calculation of the definite integral one finds

$$\delta^* = \sqrt{\frac{\nu}{a}} \int_{\xi=0}^{\infty} (1 - \varphi')\, d\xi = 0.6482 \sqrt{\frac{\nu}{a}} \tag{6.33}$$

$$\vartheta = \sqrt{\frac{\nu}{a}} \int_{\xi=0}^{\infty} \varphi' (1 - \varphi')\, d\xi = 0.2923 \sqrt{\frac{\nu}{a}} \tag{6.34}$$

and hence

$$\frac{\delta^*}{\vartheta} = 2.218 \tag{6.35}$$

The quantity δ^* is indicated in figure 16. For comparison with a later approximate solution one also notes the numerical value of the dimensionless quantity $\frac{\delta^{*2}}{\nu} \frac{dU}{dx}$. One finds from equations (6.17) and (6.33)

$$\frac{\delta^{*2}}{\nu} \frac{dU}{dx} = 0.4202 \tag{6.36}$$

The exact solution of the Navier–Stokes differential equations found here gives, therefore, for large Reynolds numbers a friction layer thickness decreasing with $\sqrt{\frac{\nu}{a}}$ and a transverse pressure gradient

decreasing with $\rho a \sqrt{\nu a}$. Both confirm the boundary layer assumptions* to be discussed later.

d. Convergent and Divergent Channel

A further class of exact solutions of the Navier–Stokes differential equations exists for the convergent and divergent channel with plane walls (fig. 17), as given by G. Hamel (reference 11).

Without entering into the details of the rather complicated calculations the character of the solutions will be briefly sketched:

The velocity distributions for convergent channels, plotted against distance along the surface for various included angles α and for various Re–numbers appear as indicated in figure 18. At the tunnel center the velocity is almost constant, and at the surfaces it suddenly declines to zero.

In the case of divergent tunnels one obtains greatly differing forms for the velocity profiles, depending on the included angle and the Re–number. Here all velocity profiles have two inflection points. For small Re–numbers and small included angles the velocity is positive over the entire cross section (solid curve in fig. 19); for larger angles and larger Re–numbers, on the other hand, the velocity profiles have reverse flow at the surface (dashed curve in fig. 19). The reverse flow is the initial phase of a vortex formation and therefore of the separation of the flow from the surface. Generally, the separation does not occur symmetrically on both surfaces; the flow separates from one side and adheres to the other surface (fig. 20).

These examples also confirm the theory that exact solutions have the same character as approximate solutions of boundary layer theory; in particular, they confirm that for the convergent channel a very thin layer with considerable friction effect is present near the surface (here also the calculation shows that the layer thickness $\sim \sqrt{\nu}$) and that for the divergent channel reverse flow and separation occur.

We here conclude the chapter on the exact solutions of the Navier–Stokes differential equations and turn to the approximate solutions. By exact solutions have been understood those where in the Navier–Stokes differential equations all terms are taken into consideration that, in the various cases, are not identically zero. By approximate solutions of the Navier–Stokes differential equations will be understood, in contrast, solutions where terms of small magnitude are neglected in the differential equations themselves. However, by no means are all the friction terms to be neglected simultaneously, since this would represent the case of potential flow.

---

*The rotationally–symmetrical stagnation–point flow has been calculated by Homann (reference 17). Instead of equation (6.28) one obtains the differential equation $\varphi''' + 2\varphi\varphi'' - \varphi'^2 + 1 = 0$.

CHAPTER VII. VERY SLOW MOTION (STOKES, OSEEN)

The exact solutions of the Navier–Stokes differential equations discussed in the previous chapter are of a very special kind. Most of them dealt with flows along a plane surface, where the stream lines are rectilinear. Most flows existing in practice, as for instance flows around arbitrary bodies, cannot be calculated exactly from the Navier–Stokes differential equations, but must be treated by approximate methods. Two kinds of such approximations are possible:

1. For predominant viscosity, completely neglecting the inertia terms suggests itself (very small Re–number; $Re < 1$).

2. For very small viscosity and therefore predominant inertia one takes the viscosity into consideration only in a very thin layer in the neighborhood of the solid wall; for the rest, the flow is regarded as frictionless. Here the Re–number is very large (Prandtl's boundary layer theory).

The first limiting case with very small Re–number will be discussed in this chapter. A small Re–number indicates small velocities, small body dimensions, and large viscosity. Since the inertia terms depend on the square of the velocity whereas the friction terms are linear, all inertia terms in the Navier–Stokes differential equations are, for very small Re–numbers, negligible. It is to be expected that an approximation will thereby be obtained for very slow (creeping) motion, as for instance the falling of a minute fog particle*) or the slow motion of a body in a very viscid oil.

Neglecting all inertia terms one obtains from the Navier–Stokes differential equations (3.16) the following:

$$\left.\begin{aligned} \frac{\partial p}{\partial x} &= \mu \Delta u \\ \frac{\partial p}{\partial y} &= \mu \Delta v \\ \frac{\partial p}{\partial z} &= \mu \Delta w \end{aligned}\right\} \tag{7.1}$$

$$\frac{\partial u}{\partial x} + \frac{\partial v}{\partial y} + \frac{\partial w}{\partial z} = 0 \tag{7.2}$$

*For a sphere falling in air ($\nu = 14 \times 10^{-6}$ m^2/sec) for instance: $Re = V\, d/\nu = 1$, for $d \doteq 1$ mm; $V = 1.40$ cm/sec.

The same boundary conditions apply to this system of equations as apply to the complete Navier–Stokes differential equations, namely vanishing of the normal component $v_n = 0$ and the tangential component $v_t = 0$ at the bounding surfaces.

The neglect of all inertia terms in Navier–Stokes differential equations does not represent as serious an inaccuracy as the neglect of all friction terms when transforming the Navier–Stokes differential equations into Euler's differential equations of the frictionless flow. That is, by neglecting the inertia terms, the order of the differential equations is not lowered so that in the simplified differential equations the same boundary conditions as in the Navier–Stokes complete differential equations can still be satisfied.

Furthermore one obtains from the equations (7.1), taking into account the continuity, by differentiating the first with respect to x, the second with respect to y, the third with respect to z, the following equation for the pressure p

$$\frac{\partial^2 p}{\partial x^2} + \frac{\partial^2 p}{\partial y^2} + \frac{\partial^2 p}{\partial z^2} = \Delta p = 0 \tag{7.3}$$

that is, for creeping motions the pressure function $p(x, y, z)$ is a potential function.

The details of the calculation will not be discussed more thoroughly, particularly since the creeping motion is technically not very important. However, at least Stokes' famous solution for the sphere will be discussed briefly (fig. 21). The drag of a sphere for creeping motion consists of the contributions of the pressure drag (form drag) and the surface friction drag. The latter is obtained by integration of the wall shearing stress over the entire sphere surface. Stokes performed the integration of the equation systems (7.1) and (7.2) for a sphere in a uniform flow of velocity U_o. There results, according to Stokes, for the entire drag of the sphere of radius R:

$$W = W_{Dr} + W_R = 6\,\pi\mu R\,U_o \tag{7.4}$$

The drag is, therefore, proportional to the first power of the velocity. If one introduces for the sphere a drag coefficient c_w which, in the customary manner, is referred to the frontal area and the dynamic pressure of the free stream velocity

$$W = c_w \pi R^2 \frac{\rho}{2} U_o^2 \tag{7.5}$$

there results for the drag coefficient according to Stokes' formula:

$$c_w = \frac{24}{Re}; \quad Re = \frac{U_o D}{\nu} \tag{7.6}$$

One can state immediately that the stream line pattern of this creeping motion must be the same ahead of and behind the sphere since for reversal of the initial flow (sign reversal of the velocity components) the equation system (equation (7.1)) goes over into itself. The stream-line pattern for the viscous sphere flow, as it presents itself to an observer who is at rest relative to the flow at infinity, is shown in figure 22. The fluid particles are pushed aside by the sphere in front and come together again behind it.

As shown by a comparison of Stokes' drag formula equation (7.6) with test results (reference 33), this formula is valid only for the region $Re < 1$.

Correction by Oseen

In Oseen's later improvement of Stokes' solution for the sphere the inertia terms in the differential equations are partly taken into consideration. Oseen formulates the velocity components u, v, w:

$$u = U_o + u'; \quad v = v'; \quad w = w' \tag{7.7}$$

where u', v', w' may be considered as disturbance velocities which in general are small compared with the free stream velocity U_o. This assumption is not actually correct for the immediate proximity of the sphere surface. With the formulation (equation (7.7)) the inertia terms in equation (3.16) are divided into two groups, for instance:

$$U_o \frac{\partial u'}{\partial x}, \; U_o \frac{\partial v'}{\partial x}, \; \ldots \quad \text{and} \quad u' \frac{\partial u'}{\partial x}, \; u' \frac{\partial v'}{\partial x}, \; \ldots$$

The second group of second order, as compared with the first group, is neglected. Therewith one then obtains from the Navier-Stokes equations of motion (3.16) the following equations of motion, which are taken as a basis by Oseen.

$$\left.\begin{aligned} \rho U_o \frac{\partial u'}{\partial x} + \frac{\partial p}{\partial x} &= \mu \Delta u' \\ \rho U_o \frac{\partial v'}{\partial x} + \frac{\partial p}{\partial y} &= \mu \Delta v' \\ \rho U_o \frac{\partial w'}{\partial x} + \frac{\partial p}{\partial z} &= \mu \Delta w' \end{aligned}\right\} \tag{7.8}$$

In addition, one uses the continuity equation:

$$\frac{\partial u'}{\partial x} + \frac{\partial v'}{\partial y} + \frac{\partial w'}{\partial z} = 0 \tag{7.9}$$

and the same boundary conditions as in the Navier–Stokes differential equations. One calls the contributions of the convective terms in these equations that were taken into consideration, for instance $U_o \frac{\partial u'}{\partial x}$, the semi–quadratic terms. These differential equations of Oseen and Stokes' differential equations are both linear. The stream line pattern, as it results for this sphere flow according to Oseen, is given in figure 23. Here again the observer is at rest relative to the fluid at large distance from the sphere. Thus the sphere is dragged past the observer with the velocity U_o. The stream line pattern ahead of and behind the sphere are now not the same, as was the case in Stokes' solution. Ahead of the sphere exists almost the same displacement flow as in Stokes' pattern; behind the sphere, however, the stream lines are closer together, that is the velocity is greater here than in Stokes' case. A wake is present behind the sphere similar to that from test results for large Reynolds numbers.

For the sphere drag calculated by Stokes there results with the drag coefficient c_w introduced in equation (7.5) the formula:

$$c_w = \frac{24}{Re}\left(1 + \frac{3}{16} Re\right); Re = \frac{U_o D}{\nu} \tag{7.10}$$

The test results (reference 33) show that Oseen's formula is fairly accurate up to about $Re = 5$.

With these brief remarks we conclude the limiting case of small Reynolds numbers and turn to the case which is of foremost interest in practice: the case of very large Reynolds number.

CHAPTER VIII. PRANDTL'S BOUNDARY LAYER EQUATIONS

The other extreme case of very small viscosity or of very large Reynolds number will now be treated. In this case the inertia effects are predominant within the main body of the fluid whereas the viscosity effects there are almost negligible.

A significant advance in the treatment of motion of fluids for large Reynolds numbers, that is, in general, of fluids of very small viscosity, was attained by L. Prandtl in 1904 (reference 7). Prandtl demonstrated in what way viscosity is essential for large Reynolds numbers and how one can simplify the Navier–Stokes differential equations in order to obtain at least approximate solutions.

Let us consider the motion of fluid of very small viscosity, for instance of air or water surrounding a cylindrical streamline body (fig. 24). Up to very near the surface the velocities are of the order of magnitude of the free stream velocity U_0. The stream line pattern as well as the velocity distribution agree to a large extent with those of the frictionless fluid (potential flow). More thorough investigations show, however, that the fluid by no means glides along the surface (as in potential flow) but adheres to it. The transition from zero velocity at the surface to the fully developed velocity as it exists at some distance from the body, is effected in a very thin layer. Thus one must distinguish between two regions which, it is true, cannot be rigorously separated:

1. A thin layer in the immediate proximity of the body where the velocity gradient normal to the surface $\frac{\partial w}{\partial n}$ is very large (boundary layer). Here the viscosity μ, though very small, plays an essential role inasmuch as the frictional shearing stress $\tau = \mu \frac{\partial w}{\partial n}$ can assume considerable values.

2. In the remaining region outside of this layer velocity gradients of such magnitude do not occur, so that there the effect of viscosity becomes insignificant. Here frictionless potential flow prevails.

In general one may say that the boundary layer is thinner, the smaller the viscosity or, more generally, the larger the Re–number. It was shown before on the basis of exact solutions of the Navier–Stokes differential equations that the boundary layer thickness is

$$\delta \sim \sqrt{\nu}$$

The approximations to the Navier–Stokes differential equations to be made below are more valid the thinner the boundary layer. Thus the solutions of the boundary layer equations have an asymptotic character for infinitely increasing Reynolds numbers.

Let us now make the simplifications of the Navier–Stokes differential equations for the boundary layer. To this end the order of magnitude of the separate terms of the Navier–Stokes differential equations must be estimated. One considers the flow around a cylindrical body according to figure 24. One imagines the Navier–Stokes differential equations written non–dimensionally, by referring all velocities to the free stream velocity U_o and the lengths to a body length l. The pressure will be made dimensionless with ρU_o^2, the time with l/U_o. Furthermore $Re = \frac{U_o l}{\nu}$ represents the Reynolds number. Accordingly, the Navier–Stokes differential equations become – omitting the mass forces according to equation (4.2), by writing the same letters for the dimensionless quantities as for the dimensional ones –

$$\left.\begin{array}{l} \dfrac{\partial u}{\partial t} + u\dfrac{\partial u}{\partial x} + v\dfrac{\partial u}{\partial y} = -\dfrac{\partial p}{\partial x} + \dfrac{1}{R}\dfrac{\partial^2 u}{\partial x^2} + \dfrac{\partial^2 u}{\partial y^2} \\ \quad 1 \quad\; 1\;1 \quad\; \delta \quad \dfrac{1}{\delta} \qquad\qquad \delta^2 \quad 1 \quad\; 1/\delta^2 \\[2ex] \dfrac{\partial v}{\partial t} + u\dfrac{\partial v}{\partial x} + v\dfrac{\partial v}{\partial y} = -\dfrac{\partial p}{\partial y} + \dfrac{1}{R}\dfrac{\partial^2 v}{\partial x^2} + \dfrac{\partial^2 v}{\partial y^2} \\ \quad \delta \quad\; 1\;\delta \quad\; \delta \quad 1 \qquad\qquad \delta^2 \quad \delta \quad\; \dfrac{1}{\delta} \\[2ex] \dfrac{\partial u}{\partial x} + \dfrac{\partial v}{\partial y} = 0 \\ \quad 1 \quad\; 1 \end{array}\right\} \qquad (8.1)$$

The estimation gives: Longitidinal velocity u is of the order of magnitude 1. Dimensionless boundary layer thickness $\delta/l \ll 1$. Therefrom follows:

$$\frac{\partial u}{\partial y} \sim \frac{1}{\delta};\quad \frac{\partial^2 u}{\partial y^2} \sim \frac{1}{\delta^2}$$

whereas the derivatives with respect to x are of normal order of magnitude, thus

$$\frac{\partial u}{\partial x} \sim 1;\quad \frac{\partial^2 u}{\partial x^2} \sim 1$$

From the continuity equation follows therefore:

$$\frac{\partial v}{\partial y} \sim 1: \quad v = \int_0^{\delta} \frac{\partial v}{\partial y} \sim \delta$$

The transverse velocity v in the boundary layer is therefore, to the first order, small in comparison with the longitudinal velocity. Further there follows:

$$\frac{\partial v}{\partial x} \sim \delta; \quad \frac{\partial^2 v}{\partial x^2} \sim \delta; \quad \frac{\partial^2 v}{\partial y^2} \sim \frac{1}{\delta}$$

Thus there result for the single terms of Navier–Stokes differential equations the orders of magnitude noted in equation (8.1): On the right side in the first equation

$$\frac{\partial^2 u}{\partial x^2} \ll \frac{\partial^2 u}{\partial y^2}$$

so that it can be neglected

One now obtains within the boundary layer friction terms which are of the same order of magnitude as the inertia terms, if $1/R$ is of the order of magnitude δ^2, or, if the dimensional quantities are again written,

$$\frac{\delta}{l} \sim \frac{1}{\sqrt{R}} = \sqrt{\frac{\nu}{l U_o}} \tag{8.2}$$

In the second equation of motion all terms then are of the order of magnitude δ, including the transverse pressure gradient $\frac{\partial p}{\partial y}$. In the boundary layer, as long as it is thin, the dependence of the pressure on y may therefore be neglected. Thus approximately the same pressure prevails within the boundary layer as at its edge, that is, the pressure of the potential flow. The pressure within the boundary layer is therefore, as it were, impressed by the potential flow.

The second equation of motion is therewith exhausted and does not have to be considered further. Using again the dimensional quantities

one now makes the Navier–Stokes differential equations assume the following simplified form:

$$\left.\begin{aligned} \frac{\partial u}{\partial t} + u\frac{\partial u}{\partial x} + v\frac{\partial u}{\partial y} &= -\frac{1}{\rho}\frac{\partial p}{\partial x} + \nu\frac{\partial^2 u}{\partial y^2} \\ \frac{\partial u}{\partial x} + \frac{\partial v}{\partial y} &= 0 \end{aligned}\right\} \qquad (8.3)$$

Boundary conditions: $y = 0$: $u = v = 0$
$y = \infty$: $u = U$

The pressure in the boundary layer, which is dependent only on x, is determined from the potential flow $U(x, t)$, assumed to be known according to Bernoulli's equation.

$$\left.\begin{aligned} p + \frac{\rho}{2}U^2 &= p_o + \frac{\rho}{2}U_o^2 \quad \text{for stationary flow} \\ \text{or} \\ -\frac{1}{\rho}\frac{\partial p}{\partial x} &= U\frac{\partial U}{\partial x} + \frac{\partial U}{\partial t} \quad \text{for nonstationary flow} \end{aligned}\right\} \qquad (8.4)$$

With the potential flow known, the equation system (8.3) represents a system of two equations with the two unknowns u and v.

Numerical example: In order to help clarify the concepts a numerical example is given for the thickness of the boundary layer. The problem is: What is the boundary layer thickness, for instance, in the case of the plate in longitudinal flow at the distance $l = 100$ centimeters from the leading edge? Let the velocity be $u_o = 30$ meters per second and the kinematic viscosity for air $\nu = 0.14 \times 10^{-4}$ meters square per second; then the Reynolds number is $R = U_o \frac{l}{\nu} = 2.1 \times 10^6$ and $\sqrt{R} = 1.45 \times 10^3$. A numerical factor is still missing in the formula (8.2) for the boundary layer thickness. For the plate in longitudinal flow it is, as later calculations will show, five, provided one understands by the boundary thickness δ that distance from the surface where the velocity has the value $0.99\, u_o$. Thus a calculation by the formula

$$\frac{\delta}{l} = \frac{5.0}{\sqrt{R}}$$

results for the present case in a boundary layer thickness $\delta = 3.45$ mm. It should be added that the Reynolds number is already so large that the boundary layer at the end of the plate would be turbulent. The transition from laminar to turbulent lies further upstream, and at this point the boundary layer thickness would then be somewhat smaller than the value determined above.

Fourth lecture on December 22, 1942

Physical Summary and Conclusions

The physical content of the considerations so far can be summed up in the following sentences:

1. In a very thin layer on the body, the boundary layer, the velocity passes from the value zero at the surface to the value which the potential flow would have in the neighborhood of the surface.

2. The pressure in the boundary layer is practically independent of the coordinate normal to the surface and equals the pressure of the potential flow along the surface.

3. In the boundary layer the only friction force to be taken into consideration is the shearing stress $\tau = \mu \frac{\partial u}{\partial y}$.

4. (without proof) The curvature of the surface may be neglected in the boundary layer as long as the radius of curvature is large compared with the boundary layer thickness (Boltz, Thesis, (reference 9)).

5. All these considerations are valid only as long as no separation of the flow from the surface occurs.

Without integration of the boundary layer equations one can draw from these sentences important physical conclusions as to the flow pattern: In particular separation occurs if a transport of boundary layer material into the interior of the fluid takes place. If a region with pressure increase exists along the body contour, the retarded fluid in the boundary layer is in general, because of its small kinetic energy, not able to penetrate too far into the region of higher pressure. It then withdraws laterally from the region of higher pressure, separating from the body, and is deflected into the interior (fig. 25). As the point of separation one defines the boundary between forward flow and reverse flow of the layer nearest the surface, thus

$$\text{point of separation:} \quad \left(\frac{\partial u}{\partial y}\right)_{y=o} = 0^* \tag{8.5}$$

Determining when and where separation occurs requires for each case the integration of the boundary layer equations.

One can readily understand that for the velocity profile $u(y)$ at the separation point and for all velocity profiles in the decelerating flow $\left(\frac{\partial p}{\partial x} > 0\right)$ an inflection point** must be present. From equation (8.3) namely, for the surface $y = 0$ there follows immediately the relation

$$\mu \left(\frac{\partial^2 u}{\partial y^2}\right)_{y=o} = \frac{dp}{dx} \tag{8.6}$$

The curvature of the velocity profile at the surface therefore exchanges signs with the pressure gradient. Thus for flow with pressure decrease $\left(\text{accelerated flow } -\frac{dp}{dx} < 0\right)$, $\left(\frac{\partial^2 u}{\partial y^2}\right)_{\text{surface}} < 0$ is valid and therefore also $\frac{\partial^2 u}{\partial y^2} < 0$ in the entire boundary layer (fig. 26). For the region of the pressure increase $\left(\text{decelerating flow, } \frac{dp}{dx} > 0\right)$ $\left(\frac{\partial^2 u}{\partial y^2}\right)_{\text{surface}} > 0$.

However, since in any case at larger distances from the surface $\frac{\partial^2 u}{\partial y^2} < 0$, there must exist, for decelerating flow, within the boundary layer a point where $\frac{\partial^2 u}{\partial y^2} = 0$ (inflection point) (fig. 27). For decelerating potential flow the boundary layer profile has, therefore, an inflection point. Since the separation profile with vanishing surface tangent must necessarily have an inflection point, it follows that separation can occur only when the potential flow is decelerating $\left(\frac{dp}{dx} > 0\right)$.

---

* The velocity profile at the point of separation therefore starts with a vanishing tangent (fig. 25). Velocity profiles behind the point of separation have reverse flow in the neighborhood of the surface (fig. 25).

** The presence of an inflection point is significant for the stability of the velocity profile (transition from laminar to turbulent, compare chapter XXI Part II.)

If separation is present, the potential flow can no longer envelop the body closely everywhere. Thus the pressure distribution sometimes deviates considerably from that given by the potential theory. In such cases the pressure variation impressed on the boundary layer can in most cases be determined only empirically, because the frictionless outer flow itself depends on the complicated phenomena connected with the separation.

Thus the boundary layer theory explains also the fact that in addition to the frictional drag a pure pressure drag, called "form drag," appears.

In regard to later calculations the following explanation shall be given: If equation (8.3) is differentiated with respect to y, there results for stationary flow

$$u\frac{\partial^2 u}{\partial x \partial y} + \frac{\partial u}{\partial y}\frac{\partial u}{\partial x} + v\frac{\partial^2 u}{\partial y^2} + \frac{\partial v}{\partial y}\frac{\partial u}{\partial y} = -\frac{1}{\rho}\frac{\partial^2 p}{\partial x \partial y} + \nu\frac{\partial^3 u}{\partial y^3} \tag{8.7}$$

Due to $\frac{\partial p}{\partial y} = 0$ and to the boundary conditions $u = v = 0$ one obtains from equation (8.7) for the surface $y = 0$ the relation

$$\left(\frac{\partial^3 u}{\partial y^3}\right)_{\text{surface}} = 0 \tag{8.8}$$

which is valid for all stationary boundary layer profiles (pressure increase and pressure decrease).

Frictional Drag

As a result of the integration of the boundary layer equation one obtains the velocity distribution and the separation point and can therefrom calculate the particularly interesting surface friction drag in the following manner. The friction drag W_R results from the integration of the surface shearing stress over the surface of the body. For the plane case one obtains, with the symbols according to figure 28, for the friction drag

$$W_R = 2b\int_{s=0}^{l'} \tau_o \cos\varphi \, ds \tag{8.9}$$

The integration has to be extended over both sides of the surface from the stagnation point to the separation point ($s = l'$), b signifies the height of the cylindrical body. Because $\cos \varphi \, ds = dx$ and $\tau_o = \mu \left(\frac{\partial u}{\partial y}\right)_o$ one obtains for the friction drag

$$W_R = 2b\mu \int_{x=o}^{l} \left(\frac{\partial u}{\partial y}\right)_o dx \tag{8.10}$$

This integration also has to be extended along both sides of the body. For calculation of the friction drag one needs, therefore, the velocity gradient at the surface. The latter can only be obtained by integration of the boundary-layer differential equations. If the separation point appears ahead of the trailing edge, the formula has to be applied only up to the separation point or, sometimes, up to the point of laminar-to-turbulent transition which is located further upstream. Behind this transition point exists turbulent surface friction drag. In order to obtain the total drag, the form drag has to be added to this friction drag; however, the form drag cannot be obtained from the boundary layer calculation in a simple manner.

CHAPTER IX. EXACT SOLUTIONS OF THE BOUNDARY LAYER EQUATIONS FOR THE PLANE PROBLEM

a. The Flat Plate in Longitudinal Flow

One of the simplest examples for the application of the boundary layer equations (8.3) is the flow along a flat plate. Let the plate begin at $x = 0$, extend parallel to the x-axis, and be infinitely long (fig. 29). Let the stationary flow of the free stream velocity U_o be treated. The calculations for it were made by H. Blasius (reference 8) in his Göttingen thesis. In this case the velocity of the potential flow is constant, thus $dp/dx \equiv 0$. The boundary layer equations (8.3) become therefore

$$\left.\begin{aligned} u \frac{\partial u}{\partial x} + v \frac{\partial u}{\partial y} &= \nu \frac{\partial^2 u}{\partial y^2} \\ \frac{\partial u}{\partial x} + \frac{\partial v}{\partial y} &= 0 \end{aligned}\right\} \tag{9.1}$$

with the boundary conditions

$$\begin{aligned} y = 0: &\quad u = v = 0 \\ y = \infty: &\quad u = U_o \end{aligned} \tag{9.1a}$$

Since the entire system has no characteristic length, the assumption suggests itself that the velocity profiles at various distances x are affine to each other, so that one may write $u/U_o = \varphi\,(y/\delta)$. Let therein $\delta = \delta(x)$ represent a measure of the boundary layer thickness, increasing with the length of run. One arrives at an estimate of the boundary layer thickness in the following manner:

According to the former exact solutions of Navier–Stokes equations (chapter VI), for instance for the non-stationary problem of the surface suddenly set in motion,

$$\delta \sim \sqrt{\nu t}$$

with t denoting the time since the beginning of the motion. Applied to the present stationary problem one may substitute for the time t the time required by a fluid particle to travel from the leading edge of the plate to the point x. This time $t = \frac{x}{U_o}$ and one has, therefore, for the present case

$$\delta \sim \sqrt{\frac{\nu x}{U_o}} \tag{9.2}$$

Thus it is useful to introduce for the distance from the surface y the new dimensionless coordinate $\eta = y/\delta$ or according to equation (9.2)

$$\eta = y \sqrt{\frac{U_o}{\nu x}} \tag{9.3}$$

For further calculations one observes that

$$\frac{\partial \eta}{\partial x} = -\frac{1}{2}\frac{\eta}{x}; \quad \frac{\partial \eta}{\partial y} = \sqrt{\frac{U_o}{\nu x}}$$

The continuity equation is again integrated by introduction of the stream function ψ; for the latter one assumes

$$\psi = \sqrt{\nu x\, U_o}\, f(\eta) \tag{9.4}$$

Accordingly $f(\eta)$ is a dimensionless stream function; for the velocity components one obtains from equation (9.4)

$$u = \frac{\partial \psi}{\partial y} = \frac{d\psi}{d\eta}\frac{\partial \eta}{\partial y} = U_o\, f'(\eta) \tag{9.5}$$

$$\left.\begin{aligned} v &= -\frac{\partial \psi}{\partial x} = -\sqrt{\nu x\, U_o}\, f'(\eta)\, \frac{\partial \eta}{\partial x} - \frac{1}{2}\sqrt{\frac{\nu\, U_o}{x}}\, f(\eta) \\ v &= \frac{1}{2}\sqrt{\frac{\nu\, U_o}{x}}\, (\eta f' - f) \end{aligned}\right\} \tag{9.6}$$

Furthermore one obtains

$$\frac{\partial u}{\partial x} = -\frac{1}{2}\frac{U_o}{x}\,\eta f''; \quad \frac{\partial u}{\partial y} = U_o\sqrt{\frac{U_o}{\nu x}}\, f''; \quad \frac{\partial^2 u}{\partial y^2} = \frac{U_o^2}{\nu x}\, f''' \tag{9.7}$$

By insertion of these values in equation (9.1) there results

$$-\frac{U_o^2}{2x}\,\eta f' f'' + \frac{U_o^2}{2x}\,(\eta f' - f)\, f'' = \nu \frac{U_o}{x\nu}\, f'''$$

or, after simplifying, the following differential equation for the stream function $f(\eta)$

$$f\, f'' + 2\, f''' = 0 \tag{9.8}$$

Because of equation (9.1a) and of equations (9.5) and (9.6) the boundary conditions are

$$\eta = 0: \quad f = f' = 0; \quad \eta = \infty: \quad f' = 1 \tag{9.9}$$

For the present case therefore, there results from the two partial differential equations (9.1), by the similarity transformation (equation (9.3)), an ordinary non-linear differential equation of the third order.

The three boundary conditions according to equation (9.9) are sufficient for a unique determination of the function $f(\eta)$ from this equation

A particular solution of the differential equation (9.8) is the solution

$$f = \eta + \text{constant}$$

This solution corresponds to the potential flow; we shall revert to it presently.

The general solution of the differential equation (9.8) cannot be given in closed form. Therefore one must calculate it either by numerical methods or by series developments. Blasius obtained the solution by a power series development near $\eta = 0$ and an asymptotic development near $\eta = \infty$, which are combined at an appropriate point. Since the method of calculation is characteristic of the solution of the boundary layer differential equations it will be described in more detail. The power series around $\eta = 0$ is formulated in the form

$$\left.\begin{aligned} f(\eta) &= A_o + A_1\eta + \frac{A_2}{2!}\eta^2 + \frac{A_3}{3!}\eta^3 + \cdots \\ f''(\eta) &= A_2 + A_3\eta + \frac{A_4}{2!}\eta^2 + \frac{A_5}{3!}\eta^3 + \cdots \\ f'''(\eta) &= A_3 + A_4\eta + \frac{A_5}{2!}\eta^2 + \frac{A_6}{3!}\eta^3 + \cdots \end{aligned}\right\} \qquad (9.10)$$

Because of the boundary conditions for $\eta = 0$ one has immediately

$$A_o = A_1 = 0$$

By insertion of the equations (9.10) into the differential equation (9.8) one obtains

$$2A_3 + \eta\, 2A_4 + \frac{\eta^2}{2!}\left(A_2^2 + 2A_5\right) + \frac{\eta^3}{3!}\left(4A_2 A_3 + 2A_6\right) + \cdots = 0$$

In order to make the equation (9.10) represent a solution of the differential equation it is required that in the last equation all coefficients of the single powers of η vanish. First, one has immediately $A_3 = A_4 = 0$* and further

*This also follows at once from equations (8.6) and (8.8).

$$A_5 = -\frac{1}{2} A_2^2; \quad A_6 = 0; \quad A_7 = 0$$

$$A_8 = -\frac{11}{2} A_2 A_5 = \frac{11}{4} A_2^3$$

. . . .

Thus only the coefficients A_2, A_5, A_8. . . . are different from zero. The coefficient A_2 remains at first undetermined since the third boundary condition for $\eta = \infty$ was not yet satisfied. The remaining coefficients A_5, A_8, A_{11}. . . can all be expressed in terms of A_2. One therefore sets up, with $A_2 = \alpha$, a series for $f(\eta)$ which progresses by powers of η^3, in the following form:

$$f = \sum_{n=0}^{\infty} \left(-\frac{1}{2}\right)^n \frac{C_n \alpha^{n+1}}{(3n+2)!} \eta^{3n+2} \tag{9.11}$$

The results for the first coefficients are:

$$C_0 = 1; \quad C_1 = 1; \quad C_2 = 11;$$

$$C_3 = 375; \quad C_4 = 27897; \quad C_5 = 3\ 817137$$

The asymptotic development near $\eta = \infty$ is formulated in the form

$$f = f_1 + f_2 + \ldots \tag{9.12}$$

where the higher approximations are to be small in comparison with the lower approximations, for instance $f_2 \ll f_1$. The first asymptotic approximation to correspond to the potential flow is, as was mentioned above,

$$f_1 = \eta - \beta \tag{9.13}$$

For this approximation $f_1'' = 0$, and one obtains therefore by replacing the quantity ff'' in the differential equation (9.8) by $f_1 f_2''$ the following equation for the second asymptotic approximation:

$$(\eta - \beta)\, f_2'' + 2f_2'' = 0$$

or

$$\frac{f_2''}{f_2''} = \frac{1}{2}(\beta - \eta)$$

or

$$\log f_2'' = \frac{1}{2}\beta\eta - \frac{1}{4}\eta^2 + C$$

If one substitutes for the integration constant $C = -\beta^2/4 + \log \gamma$, ($\gamma$ is thus a new integration constant) one obtains

$$f_2'' = \gamma\, e^{-\frac{1}{4}(\eta - \beta)^2}$$

and after integration

$$f_2' = \gamma \int_{\eta=\infty}^{\eta} e^{-\frac{1}{4}(\eta - \beta)^2}\, d\eta \qquad (9.14)$$

Because $f_1'(\infty) = 1$ and $f_2'(\infty) = 0$, the solution $f' = f_1' + f_2'$ satisfies the third boundary condition $f'(\infty) = 1$. Another integration of equation (9.14) gives as second asymptotic solution for $f = f_1 + f_2$

$$f = \eta - \beta + \gamma \int_{\infty}^{\eta} d\eta \int_{\infty}^{\eta} e^{-\frac{1}{4}(\eta - \beta)^2}\, d\eta \qquad (9.15)$$

This solution still contains two integration constants β and γ corresponding to the fact that only one of the three boundary conditions was satisfied. The asymptotic solution can, in the same manner, be improved still farther by equating $f = f_1 + f_2 + f_3$. The differential equation for f_3 was solved by Blasius; a more detailed discussion is unnecessary.

These two solutions, the power series near $\eta = 0$ according to equation (9.11) and the asymptotic solution near $\eta = \infty$ according to equation (9.15), now have to be joined together and the three integration

constants α, β and γ have thereby to be determined. This is effected in the following way: At a point $\eta = \eta_1$, where both solutions are serviceable, f, f' and f" from the power series and the asymptotic solution are brought to agreement. Because of the differential equation (9.8) the higher derivatives will then automatically agree. In this manner one obtains three equations for the three unknown integration constants. The numerical calculation gives

$$\alpha = 0.332; \quad \beta = 1.73; \quad \gamma = 0.231$$

A table for f, f', f" taken from a treatise by L. Howarth (reference 18) is given in table 2*. The velocity distribution in the boundary layer $u/U_o = f'(\eta)$ according to equation (9.5) is represented in figure 30. In comparison with the stagnation point profile (fig. 16) it is striking that the velocity profile of the plate flow near the surface has a very slight curvature. At the surface itself it has an inflection point, that is, for $y = 0$: $\frac{\partial^2 u}{\partial y^2} = 0$.

The transverse component of the velocity in the boundary layer given by equation (9.6) is plotted in figure 31. It is noteworthy that outside of the friction layer, for $\eta \to \infty$

$$v = v_\infty = 0.865\, U_o \sqrt{\frac{\nu U_o}{x}}$$

The fact that on the outer edge of the boundary layer the transverse component $v \neq 0$ is caused by the deflection of the potential flow from the body due to the boundary layer thickness increasing downstream. For very large distances from the wall (far in the potential flow) the boundary layer solution does not go over exactly into the undistrubed potential flow $u = U_o$; $v = 0$. This has to be tolerated as a (very slight) deficiency of the boundary layer solution.

For the present case a separation of the boundary layer does not exist since the pressure gradient equals zero.

Friction Drag

From the solution given above the surface friction drag of the plate in longitudinal flow is to be calculated. According to equation (8.9) the friction drag for one side of the plate is

---

* See appendix, chapter XII.

$$W = b\int_{x=o}^{l} \tau_o \, dx = b\mu \int_{x=o}^{l} \left(\frac{\partial u}{\partial y}\right)_{y=o} dx \tag{9.16}$$

with b denoting the width, l the length of the plate. According to equations (9.7) and (9.11)

$$\left(\frac{\partial u}{\partial y}\right)_o = U_o\sqrt{\frac{U_o}{\nu x}}\, f''(o) = \alpha U_o\sqrt{\frac{U_o}{\nu x}}$$

Therewith the local surface shearing stress is

$$\tau_o = \alpha\mu\, U_o\sqrt{\frac{U_o}{\nu x}} = 0.332\mu\, U_o\sqrt{\frac{U_o}{\nu x}} \tag{9.17}$$

The friction drag according to equation (9.16) is therewith

$$W = \alpha\mu b\, U_o\sqrt{\frac{U_o}{\nu}} \int_{x=o}^{l} \frac{dx}{\sqrt{x}} = 2\alpha\, b\, U_o\sqrt{\mu\rho l U_o}$$

and therefore the drag of the plate wetted on both sides is

$$\left.\begin{aligned} 2W &= 4\alpha\, b\, \sqrt{U_o^{\,3}\, \mu\rho\, l} \\ &= 1.328\, b\sqrt{U_o^{\,3}\, \mu\rho\, l} \end{aligned}\right\} \tag{9.18}$$

If one introduces in the customary manner a dimensionless drag coefficient by the equation

$$c_w = \frac{2W}{F\,\frac{\rho}{2}\,U_o^{\,2}} \qquad (F = 2\,b\,l = \text{wetted area})$$

one obtains for the drag coefficient the formula

$$c_w = \frac{1.328}{\sqrt{Re}} \qquad \left(Re = \frac{U_o l}{\nu}\right) \tag{9.19}$$

Displacement Thickness of the Boundary Layer

By the development of the boundary layer on the plate, which increases downstream with $\sqrt{x}$, the potential flow is deflected outward from the surface by an amount δ^*, which is called the displacement thickness of the boundary layer. It can be easily calculated from the velocity distribution in the boundary layer, as follows: Let y_1 denote a point outside the boundary layer; then according to the definition for δ^*

$$\int_{y=o}^{y_1} u\,dy = U_o\left(y_1 - \delta^*\right)$$

or

$$\delta^* = \int_{y=o}^{y_1} \left(1 - \frac{u}{U_o}\right)dy \tag{9.20}$$

According to equation (9.5)

$$\int_{y=o}^{y_1} \left(1 - \frac{u}{U_o}\right)dy = \sqrt{\frac{\nu x}{U_o}} \int_{\eta=o}^{\eta_1} \left[1 - f'(\eta)\right]d\eta$$

$$= \sqrt{\frac{\nu x}{U_o}} \left[\eta_1 - f(\eta_1)\right]$$

Since the point $\eta = \eta_1$ lies outside of the boundary layer, one can put for $f(\eta)$ the first approximation of the asymptotic solution according to equation (9.13), thus

$$f(\eta_1) = \eta_1 - \beta = \eta_1 - 1.73$$

Thus one finds for the displacement thickness of the boundary layer

$$\delta^* = 1.73\sqrt{\frac{\nu x}{U_o}} \tag{9.21}$$

The distance from the surface $y = \delta^*$ is also shown in figure 30. Thus the stream lines of the potential flow are, because of the friction effect, deflected outward by this amount.

The actual boundary layer thickness δ cannot be given accurately since the friction effect in the boundary layer thickness decreases asymptotically toward the outside. The component of velocity parallel to the surface u is asymptotically converted into the velocity U_o of the potential flow (the function $f'(\eta)$ asymptotically approaches the value 1). If one wants to define the boundary layer thickness as the point where the velocity $u = 0.99\ U_o$ (full value), one obtains for it according to table 2, $\eta = 5.0$. Therewith one has for the thus defined boundary layer thickness

$$\delta = 5.0\sqrt{\frac{\nu x}{U_o}} \tag{9.21a}$$

The thus defined boundary layer thickness equals about three times the displacement thickness of the boundary layer.

Let here also be introduced the value for the momentum thickness ϑ, needed later. This latter is a measure for the momentum loss due to friction in the boundary layer and is, as indicated before in equation (6.32), defined by the equation

$$\vartheta = \int_{y=o}^{\infty} \frac{u}{U_o}\left(1 - \frac{u}{U_o}\right) dy$$

The calculation results, because of equation (9.5), in

$$\vartheta = \int_{\eta=o}^{\infty} f'(1 - f')d\eta \sqrt{\frac{\nu x}{U_o}} = 0.664\sqrt{\frac{\nu x}{U_o}} \tag{9.21b}$$

Finally the form parameter becomes therewith

$$\frac{\delta^*}{\vartheta} = 2.605 \qquad (9.21c)$$

Experimental investigations of the laminar boundary layer on the flat plate were performed by B. G. van der Hegge Zynen (reference 19) and M. Hansen (reference 20). In all essential points the theoretical results were well confirmed. The measurements showed that the laminar boundary layer exists to about the Reynolds number $(U_o\, x/\nu)_{crit} = 3.5$ to 5×10^5, if x denotes the length of run of the boundary layer. For larger Reynolds numbers transition to the turbulent state of flow takes place.

Fifth lecture on January 5, 1942.

b. The Boundary Layer on the Cylinder (symmetrical case)

The integration method of Blasius given in the previous section was used by Hiemenz (thesis Göttingen 1911) for calculating the boundary layer on the circular cylinder. The same method was later further extended by Howarth (reference 15) to the general case of a cylindrical body of arbitrary cross section. This method will be briefly presented for the symmetrical case. One considers (fig. 32) a cylindrical body with symmetrical cross section in a flow approaching in the direction of the symmetry axis with the velocity U_o. Let x be the arc length along the contour, measured from the front stagnation point, y the vertical distance from the surface. Let the potential flow $U(x)$ be given by its power series development in x. At the stagnation point $(x = 0)$, $U(x) = 0$, and for the symmetrical case only the odd terms of the power series are different from zero. Therefore:

$$U(x) = u_1 x + u_3 x^3 + u_5 x^5 + \ldots \qquad (9.22)$$

The coefficients u_1, u_3, . . . depend solely on the shape of the body and are therefore quantities known from the potential flow.

The stationary boundary layer equations according to equation (8.3) are also valid for this case with a curved surface and therefore read:

$$\left.\begin{aligned} u\frac{\partial u}{\partial x} + v\frac{\partial u}{\partial y} &= U\frac{dU}{dx} + \nu\frac{\partial^2 u}{\partial y^2} \\ \frac{\partial u}{\partial x} + \frac{\partial v}{\partial y} &= 0 \end{aligned}\right\} \qquad (9.23)$$

From equation (9.22) one obtains for the pressure term:

$$U\frac{dU}{dx} = u_1\left[u_1 x + 4u_3 x^3 + \left(6u_5 + \frac{3u_3^2}{u_1}\right)x^5 + \ldots\right] \qquad (9.24)$$

The continuity equation is again integrated by the stream function:

$$u = \frac{\partial\psi}{\partial y}; \quad v = -\frac{\partial\psi}{\partial x} \qquad (9.25)$$

It is now necessary to find a suitable formulation for the velocity distribution $u(x, y)$, $v(x, y)$ and therewith for the stream function $\psi(x, y)$. In analogy to equation (9.22) a power series in x suggests itself for $u(x, y)$ as well, with coefficients, however, which are dependent on y. It is important to find a form where the coefficients (or functions) dependent on y have a universal character, that is, need not be calculated anew for each shape of body, but may be calculated once for all. Howarth (reference 15) succeeded in finding such a formulation.

For the distance from the surface one introduces the dimensionless variable:

$$\eta = y\sqrt{\frac{u_1}{\nu}} \qquad *(9.26)$$

The expression (9.24) for the pressure term suggests that the following equation be selected for ψ

$$\psi = \sqrt{\frac{\nu}{u_1}}\left\{u_1 x f_1(\eta) + 4u_3 x^3 f_3(\eta) + 6x^5\left[u_5 g_5(\eta) + \frac{u_3^2}{u_1}h_5(\eta)\right] + \ldots\right\} \qquad (9.27)$$

This yields: ($'$ = differentiation with respect to η):

$$u = u_1 x f_1' + 4u_3 x^3 f_3' + 6x^5\left[u_5 g_5' + \frac{u_3^2}{u_1}h_5'\right] + \ldots \qquad (9.28)$$

---

*One obtains this equation from that of Blasius according to equation (9.3) by substituting for U_o the first term of the series equation (9.22).

$$\frac{\partial u}{\partial x} = u_1 f_1' + 12u_3 x^2 f_3' + 30x^4 \left[u_5 g_5' + \frac{u_3^2}{u_1} h_5' \right] + \cdots \tag{9.29}$$

$$\frac{\partial u}{\partial y} = \sqrt{\frac{u_1}{\nu}} \left\{ u_1 x f_1'' + 4u_3 x^3 f_3'' + 6x^5 \left[u_5 g_5'' + \frac{u_3^2}{u_1} h_5'' \right] + \cdots \right\} \tag{9.30}$$

$$\frac{\partial^2 u}{\partial y^2} = \frac{u_1}{\nu} \left\{ u_1 x f_1''' + 4u_3 x^3 f_3''' + 6x^5 \left[u_5 g_5''' + \frac{u_3^2}{u_1} h_5''' \right] + \cdots \right\} \tag{9.31}$$

$$v = -\sqrt{\frac{\nu}{u_1}} \left\{ u_1 f_1 + 12u_3 x^2 f_3 + 30x^4 \left[u_5 g_5 + \frac{u_3^2}{u_1} h_5 \right] + \cdots \right\} \tag{9.32}$$

After insertion of the expressions (9.24) and (9.28) to (9.32) into the first equation (9.23) one obtains by comparison of the coefficients a system of ordinary differential equations for the unknown functions f_1, f_3, g_5, h_5, ... , which appears as follows:

terms with	gives the differential equation
$u_1 x$	$f_1^2 - f_1 f_1'' = 1 + f_1'''$
$4u_1 u_3 x^3$	$4f_1' f_3' - 3f_1'' f_3 - f_1 f_3'' = 1 + f_3'''$
$6u_1 u_5 x^5$	$6f_1' g_5' - 5f_1'' g_5 - f_1 g_5'' = 1 + g_5'''$
$6u_3^2 x^5$	$6f_1' h_5' - 5f_1'' h_5 - f_1 h_5'' = \frac{1}{2} + h_5''' - 8(f_3'^2 - f_3 f_3'')$

(9.33)

Formulation of the flow function according to equation (9.27) has thus accomplished the elimination of the coefficients depending on body

shape (u_1, u_3, . . .) from the differential equations for the functions f_1, f_3, . . . which thus now have a universal character.

The boundary conditions for the functions f_1, f_3, . . . follow from

$$y = 0: \quad u = v = 0$$

$$y = \infty: \quad u = U$$

by comparison of equation (9.28) with equation (9.22); they are

$$\begin{aligned} \eta = 0: \quad & f_1 = f_1' = 0; \quad f_3 = f_3' = 0; \quad g_5 = g_5' = 0 \\ & h_5 = h_5' = 0; \ . \ . \ . \\ \eta = \infty: \quad & f_1' = 1; \quad f_3' = \tfrac{1}{4}; \quad g_5' = \tfrac{1}{6}; \quad h_5' = 0; \ . \ . \ . \end{aligned} \tag{9.34}$$

The differential equations (9.33) are all of the third order, and equation (9.34) gives three boundary conditions for each. The differential equation for $f_1(\eta)$ is non-linear and is identical with the differential equation (6.28) obtained in chapter VI for the stagnation point flow: $f_1 \equiv \varphi$; $\eta \equiv \xi$, as follows by comparison of equation (6.26a) with equation (6.26). All the remaining differential equations in equation (9.33) are linear, with the coefficients determined by the functions of the preceding approximations.

The solutions of the differential equations (9.33) are best obtained by numerical integration. The functions f_1 and f_3 were already calculated by Hiemenz (reference 10). Howarth (reference 15) improved the tables for f_3 and recently Nils Frössling (reference 16) calculated g_5 and h_5 as well. The f_1' which is identical with φ' according to equation (6.28) was already given in figure 16. The function f_3' can be seen from figure 33, the functions g_5' and h_5' from figure 34. The numerical values are compiled in table 3.

Concerning the applicability of this calculation method it must be mentioned that for slender body shapes the series for $U(x)$ and $u(x,y)$ converge poorly. The reason is, that for these body shapes $U(x)$ has a very steep ascent in the neighborhood of the stagnation point (fig. 35), while showing a rather flat curve further on. Such a function cannot be developed readily into a Taylor series. For such body shapes many more of the functions of the differential-equation system (9.33) would be required

than have been calculated so far. For blunt bodies, as for instance the circular cylinder, the convergence is considerably better so that one proceeds rather far with this calculation although not always up to the point of separation.

Howarth (reference 15) also performed the corresponding calculation for the unsymmetrical case where the even coefficients also appear in the power series for $U(x)$. This is the case for a symmetrical body at an angle of attack and quite generally for any unsymmetrical body.

Frössling (reference 16) made the application to the rotationally symmetrical case.

Circular Cylinder

The boundary layer on the circular cylinder will be treated as an example for the application of this method. Whereas Hiemenz (reference 10) took a pressure distribution measured by him as the basis for this case, we shall here calculate with the potential-theoretical pressure distribution. The velocity distribution of the potential flow reads, with the symbols according to figure 36,

$$U(x) = 2U_o \sin \varphi = 2U_o \sin \frac{x}{R} \tag{9.35}$$

The power series development gives:

$$U(x) = 2\,U_o \left\{ \frac{x}{R} - \frac{1}{3!}\left(\frac{x}{R}\right)^3 + \frac{1}{5!}\left(\frac{x}{R}\right)^5 + \ldots \right\} \tag{9.36}$$

In comparison with equation (9.22):

$$u_1 = 2\,\frac{U_o}{R}; \quad u_3 = -\frac{2}{3!}\,\frac{U_o}{R^3}; \quad u_5 = \frac{2}{5!}\,\frac{U_o}{R^5}; \quad \ldots \tag{9.36a}$$

Therewith follows from equation (9.26):

$$\eta = \frac{y}{R}\sqrt{\frac{2U_oR}{\nu}} = \frac{y}{R}\sqrt{\frac{U_oD}{\nu}} \tag{9.37}$$

It follows that for the velocity distribution from equation (9.28)

$$\frac{1}{2}\frac{u(x,y)}{U_o} = \frac{x}{R} f_1' - \frac{4}{3!}\left(\frac{x}{R}\right)^3 f_3' + \frac{1}{5!}\left(\frac{x}{R}\right)^5 \left(6g_5' + 20h_5'\right) - + \ldots \qquad (9.38)$$

One further calculates the position of the separation point x_A which is, according to equation (8.5) determined by $\left(\frac{\partial u}{\partial y}\right)_{y=0} = 0$. Therewith results from equation (9.36):

$$f_1''(0)\frac{x_A}{R} - \frac{4}{3!} f_3''(0)\left(\frac{x_A}{R}\right)^3 + \ldots = 0 \qquad (9.38a)$$

With the numerical values $f_1'(0) = 1.23264$; $f_3''(0) = 0.7246$ one finds:

$$\frac{x_A}{R} = 1.60; \quad \varphi_A = 92^\circ \ * \qquad (9.39)$$

Hiemenz (reference 10) based his calculation on his experimental pressure distribution; he calculated the separation point to be at $\varphi_A = 82^\circ$, whereas his measurements gave $\varphi_A = 81^\circ$. This result is considerably different from that obtained with the potential-theoretical pressure distribution. The reason is that for a body as blunt as the circular cylinder the experimental and the potential-theoretical pressure distribution in the neighborhood of the separation point differ greatly.

The method described here of calculating the boundary layer by a power-series development starting from the stagnation point has found but little acceptance because of the extensive calculation required. It is, however, indispensable for fundamental considerations, since there exist no other exact solutions of the differential equations of the boundary layer for the flow about a body.

Thus approximation methods came into use for the practical performance of boundary layer calculations; they will be discussed in the following chapter. It is true that their accuracy is sometimes considerably lower than that of the previously discussed exact solutions.

c. Wake behind the Flat Plate in Longitudinal Flow

The application of the boundary layer equations is not absolutely limited to the presence of solid walls. They may also be applied if there is present within the flow a layer in which the friction effect is

*This result varies somewhat if in the series development equation (9.38a), one takes further terms into consideration. However, for this purpose one would have to calculate at least up to the term x^7.

predominant. This is the case for instance when within the flow two layers of different velocities adjoin, as for instance in the wake region behind a body or at the outflow from an opening. In this and the following chapter we shall treat two examples of such flows which we shall later encounter again in the discussion of turbulent flows.

The wake flow behind the flat plate in longitudinal flow is chosen as the first example (fig. 37). At the trailing edge of the plate the two boundary layer profiles grow together and form a "wake profile" the width of which increases with distance while the velocity decrement at its center decreases. The size of the "wake" is directly connected with the drag of the body. Otherwise, however, the form of the velocity distribution in the wake at a large distance from the body is not dependent on the shape of the body, whereas the velocity distribution very close behind the body naturally depends on the boundary layer of the body and on any existing separation.

From the velocity distribution measured in the wake one may calculate the drag by means of the momentum theorem in the following manner. The momentum theorem states: The variation of the momentum with time (= momentum flow through a control area fixed in space) equals the sum of the resultant forces. By resultant forces one has to understand: 1. Pressure forces on the control area, 2. Extraneous forces, which are transferred from solid bodies to the flowing fluid, for instance the shearing stress at the surface which gives the friction drag. For the present case the control area AA_1BB_1 is placed as indicated in figure 38. Let the boundary A_1B_1 which is parallel to the plate be so far distant from it that it lies everywhere in the undisturbed velocity U_o. Furthermore, the rear cross section BB_1 is to lie so far behind the plate that the static pressure there has the same undisturbed value as in front of the plate. Then the pressure is constant on the entire control area, so that the pressure forces make no contribution. In calculating the momentum flow through this control area one has to consider that, due to continuity, fluid must flow out through the boundary A_1B_1, namely the difference between the larger quantity flowing through the cross section AA_1 and the smaller quantity flowing through the cross section BB_1. The cross section AB does not make a contribution to the x-momentum, since for reasons of symmetry the transverse velocity on it equals zero. The momentum balance is given in the table below, with entering momentums counted as positive, outgoing ones as negative.

Cross section	Mass $\left[m^3/sec\right]$	Momentum flow in x-direction = volume × density × velocity
A B	0	0
A A_1	$b\int_0^h U_o \, dy$	$\rho \, b\int_0^h U_o^2 \, dy$
B B_1	$-b\int_0^h u \, dy$	$-\rho \, b\int_0^h u^2 \, dy$
A_1B_1	$-b\int_0^h (U_o - u)dy$	$-\rho \, b \, U_o\int_0^h (U_o - u) \, dy$
$\sum$ = Control area	$\sum$ Mass = 0	$\sum$ Momentum Flow = W

The total momentum loss of the flow for the present case equals the drag W of one side of the plate. Thus one obtains

$$W = b\,\rho\int_0^h u\,(U_o - u)\,dy = b\,\rho\int_0^\infty u\,(U_o - u)\,dy \qquad (9.40)$$

The integration therein may be extended from $y = 0$ to ∞, instead of from $y = 0$ to h, since for $y > h$ the integrand in equation (9.40) vanishes. For the drag of the plate wetted on both sides one obtains therefore:

$$2W = b\rho \int_{-\infty}^{+\infty} u(U_o - u)\, dy \tag{9.41}$$

In equations (9.40) and (9.41) the integrals are to be extended over the wake as indicated at a distance behind the plate where the static pressure has its undisturbed value. However, one may naturally apply equations (9.40) and (9.41) also to the boundary layer on the plate at a certain point x; then they give the drag of the part of the plate from the leading edge to this point. The definite integrals in equations (9.40) and (9.41) represent physically the momentum loss due to the friction effect. As mentioned before, it is customary to introduce for this integral also the momentum loss thickness ϑ by the following equation (compare equation (6.32)).

$$U_o^2 \vartheta = \int_{y=o}^{\infty} u\,(U_o - u)\, dy \tag{9.42}$$

Therewith the formula for the drag may also be written, by comparison with equation (9.40):

$$W = b\,\rho\, U_o^2 \vartheta \tag{9.43}$$

The velocity distribution in the wake, particularly at large distance x behind the plate in longitudinal flow (fig. 37) is to be calculated next. This calculation must be performed in two steps: 1. By a development "from the front", that is, by a calculation which follows the further development of the Blasius-boundary layer profile present at the trailing edge of the plate. 2. By a development "from the rear" that is, by an asymptotic calculation for the wake, under the assumption that the difference velocity

$$u_1(x, y) = U_o - u(x, y) \tag{9.44}$$

is small.

The first calculation was performed by S. Goldstein (reference 21) and is very troublesome; the second was indicated by Tollmien (reference 3) and yields rather simple laws, in particular also an exact solution of the differential boundary layer equation. Since such exact solutions are

comparatively rare and since, moreover, the asymptotic law for the wake applies not only for the flat plate in longitudinal flow but for any arbitrary body shape, this asymptotic solution will be treated here somewhat more thoroughly. The wake velocity $u_1(x, y)$ introduced in equation (9.44) is assumed to be so small in comparison with the free stream velocity U_o that the second-power terms $(u_1/U_o)^2$ are negligible relative to 1. Moreover, the pressure term dp/dx in the boundary layer equation is to be set equal to zero for the first asymptotic approximation. Therewith the differential boundary layer equation (8.3) becomes, for the present case:

$$U_o \frac{\partial u_1}{\partial x} = \nu \frac{\partial^2 u_1}{\partial y^2} \tag{9.45}$$

With the boundary conditions:

$$\begin{aligned} y = 0: \quad & \frac{\partial u_1}{\partial y} = 0 \\ y = \infty: \quad & u_1 = 0 \ (u = U_o) \end{aligned} \tag{9.45a}$$

For the solution of the differential equation (9.45) one introduces as before in the plate flow according to Blasius' equation (9.3) the new variable

$$\eta = y\sqrt{\frac{U_o}{\nu x}} \tag{9.46}$$

Further, one uses for u_1 the equation:

$$u_1 = U_o \, C \left(\frac{x}{l}\right)^{-\frac{1}{2}} g(\eta) \tag{9.47}$$

The distance x from the trailing edge of the plate is thus made dimensionless by dividing by the plate length. The power $-\frac{1}{2}$ for x is given by the fact that the momentum integral which, according to equation (9.41), gives the plate drag must be independent of x. With the second-power terms neglected the drag of the plate wetted on both sides is, according to equation (9.41):

$$2W = b\,\rho\,U_o \int_{y=-\infty}^{+\infty} u_1\,dy \tag{9.48}$$

One finds further:

$$\int_{-\infty}^{+\infty} u_1(x,y)dy = U_o\,C\left(\frac{x}{l}\right)^{-\frac{1}{2}} \sqrt{\frac{\nu x}{U_o}} \int_{\eta=-\infty}^{+\infty} g(\eta)d\eta = U_o\,C\sqrt{\frac{\nu l}{U_o}} \int_{-\infty}^{+\infty} g(\eta)d\eta \tag{9.49}$$

and therewith:

$$2W = b\,\rho\,U_o^{\,2}\,C\sqrt{\frac{\nu l}{U_o}} \int_{-\infty}^{+\infty} g(\eta)\,d\eta \tag{9.50}$$

The calculation of the single terms in equation (9.45) gives:

$$\left.\begin{aligned} \frac{\partial u_1}{\partial x} &= -\,U_o\,\frac{C}{2}\left(\frac{x}{l}\right)^{-\frac{1}{2}}\frac{1}{x}\,(g + \eta g') \\ \frac{\partial u_1}{\partial y} &= U_o\,C\left(\frac{x}{l}\right)^{-\frac{1}{2}}\sqrt{\frac{U_o}{\nu x}}\,g' \\ \nu\,\frac{\partial^2 u_1}{\partial y^2} &= U_o\,C\left(\frac{x}{l}\right)^{-\frac{1}{2}}\frac{1}{x}\,g'' \end{aligned}\right\} \tag{9.51}$$

By insertion into equation (9.45) one obtains after division by $C\,U_o^{\,2}\,(x/l)^{-\frac{1}{2}}\,x^{-1}$ the following differential equation for the velocity distribution $g(\eta)$:

$$g'' + \frac{1}{2}\,\eta g' + \frac{1}{2}\,g = 0 \tag{9.52}$$

with the boundary conditions:

$$\eta = 0: \quad g' = 0; \quad \eta = \infty: \quad g = 0$$

A single integration gives:

$$g' + \frac{1}{2} \eta \, g = K = 0$$

where, because of the boundary condition at $\eta = 0$, the integration constant K must be zero. Repeated integration gives the solution:

$$g = e^{-\frac{\eta^2}{4}} \tag{9.53}$$

where a multiplicative integration constant may be put equal to one without limiting the generality since the velocity distribution u_1 still contains, according to equation (9.47), the multiplicative free constant C. This constant C is determined from the consideration that the plate drag obtained from the momentum loss (equation (9.50)) must be the same as the frictional drag of the plate. First,

$$\int_{-\infty}^{+\infty} g(\eta) \, d\eta = \int_{-\infty}^{+\infty} e^{-\frac{\eta^2}{4}} \, d\eta = 2\sqrt{\pi}$$

and therewith from equation (9.50):

$$2W = \rho \, b \, U_o^2 \, C \sqrt{\frac{\nu l}{U_o}} \, 2\sqrt{\pi}$$

On the other hand, the friction drag of the plate wetted on both sides was according to the solution of Blasius (equation (9.18))

$$2W = 1.328 \, \rho \, U_o^2 \sqrt{\frac{\nu l}{U_o}}$$

Therefrom follows $2C\sqrt{\pi} = 1.328$ and

$$C = \frac{0.664}{\sqrt{\pi}} \qquad (9.54)$$

Thus the final solution for the wake velocity for the flat plate in longitudinal flow becomes:

$$\frac{u_1}{U_o} = \frac{0.664}{\sqrt{\pi}} \left(\frac{x}{l}\right)^{-\frac{1}{2}} e^{-\frac{1}{4}\frac{y^2 U_o}{x\nu}} \qquad (9.55)$$

The velocity distribution of this asymptotic law is represented in figure 39. It is noteworthy that the function for the velocity distribution is identical with Gauss' error function. In keeping with the hypothesis the law according to equation (9.55) is valid only for large distances behind the plate, according to the calculations by Tollmien (reference 3) for $x \geq 3l$.

The development of the wake from the front, performed by Goldstein is valid only for comparatively small x/l. However, for intermediate x/l both solutions can be joined to some extent, so that one then obtains the velocity distribution in the entire wake. Such a figure is given by Tollmien (reference 3).

Sixth Lecture on January 12, 1942.

d. The Plane Jet

A further example of a flow without bounding wall to which the boundary layer theory is applicable is the outflow of a jet from a hole. The problem to be treated is the plane stationary one where the jet goes out from a long narrow slot and mixes with the surrounding fluid at rest. This is one of the rare cases where the differential boundary layer equations may be integrated exactly. The calculations were performed by H. Schlichting (reference 22) and W. Bickley (reference 30) and will be discussed a little more thoroughly.

Due to the friction effect the jet entrains a part of the fluid at rest and sweeps it along. There results a stream-line pattern like the one drawn in figure 40. Let the x-direction coincide with the jet axis and the origin lie in the slot. It then immediately becomes clear that the width of the jet increases with the distance x and the mid-velocity decreases with the distance x. For the calculation the slot is assumed to be infinitely narrow. In order to make the volume of flow, together with its momentum, finite, the velocity in the slot is then infinitely large. Again, as in the previous example concerning the wake flow, the pressure term dp/dx may be neglected since the pressure varies only very little in the x-direction. The smallness of the pressure term can

also be shown subsequently from the finished solution. Thus the differential boundary layer equations for the present case read, according to equation (8.3):

$$\left.\begin{aligned} u\frac{\partial u}{\partial x} + v\frac{\partial u}{\partial y} &= \nu\frac{\partial^2 u}{\partial y^2} \\ \frac{\partial u}{\partial x} + \frac{\partial v}{\partial y} &= 0 \end{aligned}\right\} \tag{9.56}$$

with the boundary conditions:

$$\left.\begin{aligned} y = 0: \quad v = 0; \quad \frac{\partial u}{\partial y} &= 0 \\ y = \infty: \quad u &= 0 \end{aligned}\right\} \tag{9.56a}$$

Since the pressure is constant, the entire momentum flow in the x-direction for control area fixed in space (compare figure 40) must be independent of the distance from the hole x. If one chooses the lateral boundaries of the control area at so large a distance from the axis that there $u = 0$, then

$$J = \rho\int_{-\infty}^{+\infty} u^2 dy = \text{Constant} \tag{9.57}$$

It is to be noted for the integration of the equation of motion equation (9.56) that for this problem, as before for the plate in longitudinal flow, no special length-dimension exists. Thus affinity of the velocity profiles $u(x, y)$ is suggested, that is: with b signifying a suitable width of the jet, the velocity profiles are only functions of y/b. Accordingly one uses the following expression for the stream function ψ:

$$\psi = x^p f\left(\frac{y}{x^q}\right) = x^p f\left(\frac{y}{b}\right) \tag{9.58}$$

The two – at first unknown – exponents p and q are determined from the conditions that

1. the momentum flow for the x-direction is independent of x according to equation (9.57), and that
2. the acceleration terms, for instance $u\frac{\partial u}{\partial x}$, and the inertia term in equation (9.56) are of the same order of magnitude and hence must be of the same degree in x.

This yields the two equations

$$\left.\begin{aligned} 2p - q &= 0 \\ 2p - 2q - 1 &= p - 3q \end{aligned}\right\} \tag{9.59}$$

It follows that

$$p = 1/3; \quad q = 2/3 \tag{9.60}$$

Therewith the final equations, after addition of suitable constant factors, read as follows:

$$\eta = \frac{1}{3\nu^{1/2}} \frac{y}{x^{2/3}} \tag{9.61}$$

$$\psi = \nu^{1/2} x^{1/3} f(\eta) \tag{9.62}$$

Therefrom one obtains, with

$$\frac{\partial \eta}{\partial x} = -\frac{2}{3}\frac{\eta}{x}; \quad \frac{\partial \eta}{\partial y} = \frac{x^{-2/3}}{3\nu^{1/2}}$$

the following expressions for the velocity components and their derivatives:

$$\left.\begin{aligned} u &= \frac{1}{3x^{1/3}}\, f'(\eta) \\ v &= -\frac{1}{3}\,\nu^{1/2}\, x^{-2/3}\,(f-2\eta f') \end{aligned}\right\} \qquad (9.63)$$

$$\frac{\partial u}{\partial x} = -x^{-4/3}\,\frac{1}{9}\,(2\eta f''-f')$$

$$\frac{\partial u}{\partial y} = x^{-1}\,\frac{1}{9}\,\nu^{-1/2}\,f''$$

$$\nu\,\frac{\partial^2 u}{\partial y^2} = x^{-5/3}\,\frac{1}{27}\,f'''$$

By substitution into the differential equation (9.56) there results, after cancelling the factor $\frac{1}{27}\,x^{-5/3}$, the following differential equation for the flow function $f(\eta)$:

$$f'^2 + ff'' + f''' = 0 \qquad (9.64)$$

with the boundary conditions:

$$\begin{aligned} &\eta = 0: \quad f = 0; \quad f'' = 0 \\ &\eta = \infty: \quad f' = 0 \end{aligned} \qquad (9.64a)$$

As for Blasius' plate flow here also an ordinary differential equation (9.64) was obtained from the two partial differential equations (9.56) by means of the similarity transformation equation (9.61). Here also, as in most boundary-layer problems, the differential equation is non-linear and of the third order.

The integration of this differential equation (9.64) is attained in a surprisingly simple manner. First, one obtains by a single integration

$$ff' + f'' = \text{Constant} = 0 \qquad (9.65)$$

The constant of integration therein is zero because of the boundary condition $f''(o) = 0$. The second order differential equation now obtained could be integrated once more if a factor 2 were present in the first term. This factor can be obtained by performing the following further similarity transformation:

One puts:

$$\xi = \alpha \eta \tag{9.66}$$

$$f = 2\alpha \; F(\xi) \tag{9.67}$$

α is a free constant which is determined later. With the equations (9.66) and (9.67) one obtains from equation (9.65), the prime now signifying differentiation with respect to ξ,

$$F''' + 2FF' = 0 \tag{9.68}$$

with the boundary conditions:

$$\xi = 0: \quad F = 0; \quad \xi = \infty: \quad F' = 0 \tag{9.68a}$$

This differential equation can now be integrated again and yields

$$F' + F^2 = K$$

The constant of integration K is obtained from the boundary conditions, equation (9.68a), as $K = 1$, if one stipulates $F'(o) = 1$, which is possible without limiting the generality because α is still present as a free constant in F. One now has for F the first order non-linear differential equation

$$F' + F^2 = 1 \tag{9.69}$$

which is a Riccati differential equation. The integration yields

$$\xi = \int \frac{dF}{1 - F^2} = \frac{1}{2} \log \frac{1 + F}{1 - F} = \operatorname{arc\,tanh} F$$

and therewith for the inverse function

$$F = \tanh \xi = \frac{1 - e^{-2\xi}}{1 + e^{-2\xi}} \tag{9.70}$$

Furthermore, $\frac{dF}{d\xi} = 1 - \tan^2 \xi$. If one inserts the solution found into equation (9.63), one obtains for the velocity distribution

$$u = \frac{2}{3} \alpha^2 x^{-\frac{1}{3}} (1 - \tanh^2 \xi) \tag{9.71}$$

The velocity distribution over the width of the jet calculated from this equation is represented in figure 41. The free constant α remains to be determined. This can be done from the condition (equation (9.57)) according to which the momentum flow in the x-direction is independent of x. From equation (9.71) and (9.57) one obtains

$$J = \frac{8}{3} \rho \alpha^3 \nu^{1/2} \int_0^\infty \left(1 - \tanh^2 \xi\right)^2 d\xi = \frac{16}{9} \rho \alpha^3 \nu^{1/2} \tag{9.72}$$

Let the momentum J for the jet be a prescribed constant which is, for instance, directly related to the excess pressure under which the jet flows from the slot. Then α becomes, according to equation (9.72),

$$\alpha = 0.8255 \left(\frac{J}{\rho \nu^{1/2}}\right)^{1/3} \tag{9.73}$$

and therewith the velocity distribution

$$\left.\begin{aligned} u &= 0.4543 \left(\frac{J^2}{\rho^2 \nu x}\right)^{1/3} \left(1 - \tanh^2 \xi\right) \\ v &= 0.5503 \left(\frac{J\nu}{\rho x^2}\right)^{1/3} \left\{2\xi \left(1 - \tanh^2 \xi\right) - \tanh \xi\right\} \\ \xi &= 0.2752 \left(\frac{J}{\rho \nu^2}\right)^{1/3} \frac{y}{x^{2/3}} \end{aligned}\right\} \tag{9.74}$$

The value of the transverse component of the velocity at the edge of the jet ($y = \infty$) also is noteworthy. From equation (9.74) one finds for this lateral inflow velocity

$$v_\infty = -0.550 \frac{(Jv)^{1/3}}{\rho x^{2/3}} \tag{9.75}$$

One can further calculate the flow volume for a layer of unit height $Q = \rho \int_{-\infty}^{+\infty} u \, dy$. One finds

$$\frac{Q}{\rho} = 3.3019 \left(\frac{Jvx}{\rho}\right)^{1/3} \tag{9.76}$$

The flow volume increases downstream, since fluid at rest is carried along from the side.

The solution indicated here naturally has a singular point at $x = 0$, since an infinitely narrow slot with infinitely large exit velocity was assumed. Actually for a narrow slot of finite width one has immediately behind the slot opening a velocity distribution that is rectangular across the jet cross section but which at some distance is transformed into the bell-shaped distribution found here with width $b \sim x^{2/3}$ and mid-velocity $\sim x^{-1/3}$.

Finally it should be mentioned that the corresponding rotationally-symmetrical problem where the jet goes out from a very small circular hole also can be solved in closed form. (compare H. Schlichting (reference 22)). In this case the width of the jet is proportional to x and the midvelocity proportional to x^{-1}.

e. The Boundary Layer for the Potential Flow $U = u_1 x^m$.

Another class of exact solutions of the boundary layer equations will be discussed briefly which includes the plate in longitudinal flow and the stagnation point flow as special cases. Falkner and Skan (reference 37) have shown that, just as for Blasius' plate flow, the boundary layer differential equations for the potential flow

$$U(x) = u_1 x^m \tag{9.77}$$

can be reduced by a similarity transformation to an ordinary differential equation (u_1 = constant, $m > 0$ accelerated, $m < 0$ retarded flow). For $m > 0$, $x = 0$ is the stagnation point of the flow. For $m = 0$ one obtains $U = u_1 = U_o$, therefore the plate flow; $m = 1$ gives $U = u_1 x$, therefore the stagnation point flow according to equation (6.17).

The differential equations of the boundary layer read

$$u \frac{\partial u}{\partial x} + v \frac{\partial u}{\partial y} = U \frac{dU}{dx} + \nu \frac{\partial^2 u}{\partial y^2}$$

$$\frac{\partial u}{\partial x} + \frac{\partial v}{\partial y} = 0$$

The pressure term becomes

$$U \frac{dU}{dx} = m u_1^2 \, x^{2m-1}$$

As a new independent variable one introduces

$$\xi = \sqrt{\frac{m+1}{2}} \sqrt{\frac{u_1}{\nu}} \, y \, x^{\frac{m-1}{2}} \tag{9.78}$$

and the continuity equation is integrated by introduction of a stream function for which one uses the equation:

$$\psi = \sqrt{\frac{2}{m+1}} \sqrt{\nu u_1} \, x^{\frac{m+1}{2}} \varphi(\xi) \tag{9.79}$$

One has

$$\frac{\partial \xi}{\partial x} = \frac{m-1}{2} \frac{\xi}{x}; \quad \frac{\partial \xi}{\partial y} = \sqrt{\frac{m+1}{2}} \sqrt{\frac{u_1}{\nu}} \, x^{\frac{m-1}{2}}$$

and one obtains

$$u = u_1 x^m \varphi'(\xi) = U\varphi'(\xi) \tag{9.80}$$

$$\frac{\partial u}{\partial y} = \sqrt{\frac{m+1}{2}} \sqrt{\frac{u_1}{\nu}} u_1 x^{\frac{3m-1}{2}} \varphi''(\xi)$$

$$\nu \frac{\partial^2 u}{\partial y^2} = \frac{m+1}{2} u_1^2 x^{\frac{4m-2}{2}} \varphi'''(\xi)$$

$$\frac{\partial u}{\partial x} = u_1 x^{m-1} \left\{ m \varphi' + \frac{m-1}{2} \xi \varphi'' \right\}$$

$$v = - \sqrt{\frac{2}{m+1}} \sqrt{\nu u_1} x^{\frac{m-1}{2}} \left\{ \frac{m+1}{2} \varphi + \frac{m-1}{2} \xi \varphi' \right\} \tag{9.81}$$

After insertion into the first equation of motion and division by $m u_1^2 x^{2m-1}$ one obtains, when

$$\frac{2m}{m+1} = \beta \tag{9.82}$$

the following differential equation for $\varphi(\xi)$:

$$\varphi''' = - \varphi\varphi'' + \beta (\varphi'^2 - 1) \tag{9.83}$$

Boundary conditions:

$$\xi = 0: \quad \varphi = \varphi = 0; \quad \xi = \infty: \quad \varphi' = 1$$

The differential equation (9.83) was solved for different values by Hartree (reference 38). The result is given in figure 41a. The corresponding values of β and m are given in the following table.

m	β
-0.0654	-0.14
0	0
0.111	0.2
0.333	0.5
1	1
4	1.6

For accelerated flow ($m > 0$, $B > 0$) one obtains velocity profiles without inflection points, for retarded flow ($m < 0$, $\beta < 0$) velocity profiles with inflection points. Separation occurs for

$$\beta = -0.199, \text{ that is, } m = -0.091$$

Separation takes place for the potential flow $U(x) = u_1 x^{-0.091}$, thus for very weak retardation. Compare chapter XI a, where almost the same result is obtained from an approximation calculation.

Special cases:

1. Stagnation point flow: It is obtained for

$$m = 1; \quad \beta = 1$$

Then $\xi = \sqrt{\frac{u_1}{\nu}}\, y$; $\psi = \sqrt{\nu\, u_1}\; x\, \varphi(\xi)$. These are the same expressions as for the stagnation point flow, equation (6.26a) and (6.27a), also (6.19) and (6.26b). The differential equation (9.83) also is transformed into the equation of the stagnation point flow (equation (6.28)).

2. Plate in longitudinal flow: This case is obtained for

$$m = 0; \quad \beta = 0$$

Then $\xi = \frac{1}{\sqrt{2}} \sqrt{\frac{u_1}{\nu x}}\, y = \frac{1}{\sqrt{2}} \sqrt{\frac{U_o}{\nu x}}\, y = \frac{\eta}{\sqrt{2}}$ with η signifying Blasius' variable according to equation (9.3). Furthermore, ψ becomes $\psi = \sqrt{2}\, \sqrt{\nu U_o x}\, \varphi(\xi)$; thus $\varphi = \frac{f}{\sqrt{2}}$ compared with the expression for ψ for the plate flow equation (9.4). Because of $\frac{d\varphi}{d\xi} = \frac{df}{d\eta}$, $\varphi''(\xi) = \sqrt{2}\, f''(\eta)$, and $\varphi'''(\xi) = 2f'''(\eta)$, the differential equation (9.83) is for this case transformed into $2f'''(\eta) + ff''(\eta) = 0$. This is identical with equation (9.8).

CHAPTER X. APPROXIMATE SOLUTION OF THE BOUNDARY LAYER EQUATION BY MEANS OF THE MOMENTUM THEOREM (KARMAN-POHLHAUSEN METHOD, PLANE PROBLEM)

a. The Flat Plate in Longitudinal Flow

The examples of exact solutions of the boundary layer equation discussed in the previous chapter give sufficient proof of the rather considerable mathematical difficulties in solving the differential equation. Yet the examples treated were selected as simple as possible. In some other cases the mathematical calculations are still more difficult than in those examples. Particularly the problem of flow about a body of arbitrarily prescribed shape cannot, in general, be solved by exact solution of the differential equations of the boundary layer. Just this problem, however, is of special practical importance, for instance for the calculation of the boundary layers on airplane wings.

There exists therefore a tendency to apply at least approximate methods, even if their accuracy is sometimes not quite satisfactory, for cases where the exact solution cannot be obtained with a reasonable expenditure of calculation time. Such simpler approximate solutions can be attained if one does not attempt to satisfy the differential boundary layer equation for every particle of fluid. Instead one selects a plausible expression for the velocity distribution in the boundary layer and satisfies merely the momentum equation which is obtained by integration from the equation of motion. A method on this basis for the plane problem of flow about an arbitrary body was worked out by von Karman and Pohlhausen (references 23 and 24). We shall try out this method in this chapter at first on the simpler case of the flat plate in longitudinal flow, where no pressure variations exist. For this special case the momentum theorem yields the statement that the momentum loss of the flow through a control area fixed in space according to figure 42 equals the friction drag $W(x)$ of the plate from the leading edge $(x = 0)$ to

the point x. Application of the momentum theorem for this case was discussed in detail in chapter IX; for the drag of the plate wetted on one side according to equation (9.40) it had resulted in the formula:

$$W(x) = b\,\rho \int_{y=0}^{\infty} u\,(U_o - u)\,dy \tag{10.1}$$

On the other hand the friction drag can also be expressed as the integral of the surface shearing stress, namely:

$$W(x) = b \int_{x=0}^{x} \tau_o\,(x)\,dx \tag{10.2}$$

In forming the integral (equation (10.1)) it is to be noted that the integrand outside of the boundary layer, where $u = U_o$, does not make a contribution. By comparison of equations (10.1) and (10.2) it follows that:

$$\tau_o = \rho \frac{d}{dx} \int_{y=0}^{\infty} u\,(U_o - u)\,dy \tag{10.3}$$

If one introduces moreover the momentum loss thickness, as defined in equation (9.42), equation (10.3) can also be written in the form:

$$U_o^2 \frac{d\vartheta}{dx} = \frac{\tau_o}{\rho} \tag{10.4}$$

This is the momentum theorem of the boundary layer for the special case of the flat plate in longitudinal flow. Physically it states that the surface shearing stress equals the momentum loss in the friction layer, since in the present case the pressure gradient makes no contribution. The next chapter will acquaint us with the extension of equation (10.4) to include the more general case of a boundary layer with pressure difference.

Equations (10.4) and (10.3), respectively, will now be used for approximate calculation of the friction layer on the flat plate in longitudinal flow. A comparison of the results of this approximate

calculation with the exact solution according to chapter IXa will give information about the usefulness of the approximation method. For the approximate calculation one selects a suitable expression for the velocity distribution in the boundary layer in the form:

$$u = U_o \, f\left(\frac{y}{\delta}\right) = U_o \, f(\eta) \tag{10.5}$$

with

$$\eta = \frac{y}{\delta}; \quad \delta = \delta(x) \tag{10.6}$$

δ represents the boundary layer thickness, undetermined at first. For the flat plate it may, moreover, be assumed again that the velocity profiles at various distances from the leading edge of the plate are affine to each other. This assumption is contained in equation (10.5). if $f(\eta)$ there stands for a function which no longer contains any free parameters. Furthermore, $f(\eta)$ must, for large values η, assume the constant value 1.

The velocity distribution being given by equation (10.5), the momentum integral in equation (10.3) may be evaluated. It yields:

$$\int_o^\infty u \, (U_o - u) \, dy = U_o^2 \, \delta \int_{\eta=o}^1 f \, (1 - f) \, d\eta \tag{10.7}$$

The definite integral in equation (10.7) can be calculated immediately if a definite formulation is given for $f(\eta)$. Thus one puts

$$\alpha = \int_{\eta=o}^1 f(1 - f) \, d\eta \tag{10.8}$$

Hence

$$U_o^2 \, \vartheta = \int_{y=o}^\infty u(U_o - u) \, dy = \alpha \, \delta \, U_o^2 \tag{10.9}$$

or:

$$\vartheta = \alpha \, \delta \tag{10.10}$$

Furthermore, the displacement thickness of the boundary layer δ^* becomes, according to equation (9.20):

$$\delta^* = \delta \int_0^1 (1 - f)\, dn = \alpha_1 \delta \tag{10.10a}$$

On the other hand, the shearing stress τ_o at the surface is:

$$\frac{\tau_o}{\rho} = \nu \left(\frac{\partial u}{\partial y}\right)_{y=0} = \frac{\nu U_o}{\delta} f'(0) = \beta \frac{\nu U_o}{\delta} \tag{10.11}$$

if one introduces the further simplification

$$\beta = f'(0) \tag{10.12}$$

By introduction of these expressions into the momentum equation (10.4) there results:

$$\beta \frac{\nu U_o}{\delta} = U_o^2 \alpha \frac{d\delta}{dx} \tag{10.13}$$

or

$$\delta \frac{d\delta}{dx} = \frac{\beta}{\alpha} \frac{\nu}{U_o} \tag{10.14}$$

The integration with the initial value $\delta = 0$ for $x = 0$ yields, as first result of the calculation:

$$\delta = \sqrt{\frac{2\beta}{\alpha}} \sqrt{\frac{\nu x}{U_o}} \tag{10.15}$$

Hence the shearing stress becomes, according to equation (10.11):

$$\tau_o = \sqrt{\frac{\alpha\beta}{2}}\, \mu U_o \sqrt{\frac{U_o}{\nu x}} \tag{10.16}$$

and furthermore

$$\int_0^l \tau_o \, dx = \sqrt{2\alpha\beta} \sqrt{\mu\rho U_o^3 l}$$

and hence, finally, the total drag of the plate wetted on both sides according to equation (10.2):

$$2W = 2b \sqrt{2\alpha\beta} \sqrt{\mu\rho U_o^3 l} \tag{10.17}$$

A comparison of the results for boundary layer thickness, surface shearing stress, and total drag, which were thus found, with the corresponding formulas for the exact solution according to equation (9. . .) shows that the approximate calculation according to the momentum theorem reproduces the characteristics of the formulas with perfect correctness in all cases, that is, the dependence of the boundary layer quantities on the length of run x, the free stream velocity U_o, and the viscosity coefficient ν. The numbers α, β, unknown at first, can be determined only after making special assumptions for the velocity distribution, that is, explicitly prescribing the function $f(\eta)$ in equation (10.5).

Numerical examples

The usefulness of the method of approximation will be investigated by a few numerical examples. The accuracy of the results will depend to a great extent on a suitable choice of the expression for the velocity distribution according to equation (10.5). At any rate the function $f(\eta)$ must equal zero for $\eta = 0$ and have the constant value 1 for large η. As first example we select the very rough assumption that the velocity distribution in the boundary layer is represented by a linear function according to figure 43a. Thus:

$$\begin{aligned} 0 \leq \eta \leq 1: \quad & f(\eta) = \eta \\ \eta \geq 1: \quad & f(\eta) = 1 \end{aligned} \tag{10.18}$$

Hence the results for the numbers α, β according to equation (10.8) and (10.12) are:

$$\alpha = \frac{1}{6}; \quad \beta = 1 \tag{10.19}$$

The formulas (10.15), (10.16) and (10.17) can now be evaluated immediately. One obtains the results:

$$\delta = 2\sqrt{3}\sqrt{\frac{\nu x}{U_o}} = 3.464\sqrt{\frac{\nu x}{U_o}} \tag{10.20}$$

$$\tau_o = \frac{1}{2\sqrt{3}}\mu U_o\sqrt{\frac{U_o}{\nu x}} = 0.289\ \mu U_o\sqrt{\frac{U_o}{\nu x}} \tag{10.21}$$

$$2W = \frac{2}{\sqrt{3}}\, b\sqrt{\mu\rho U_o{}^3 x} = 1.155\, b\sqrt{\mu\rho U_o{}^3 x} \tag{10.22}$$

A velocity distribution in the form of a cubic parabola according to figure 43b is selected as second numerical example in the following manner:

$$\begin{aligned} 0 \leq \eta \leq 1: \quad & f(\eta) = \frac{3}{2}\eta - \frac{1}{2}\eta^3 \\ \eta \geq 1: \quad & f(\eta) = 1 \end{aligned} \tag{10.23}$$

This satisfies the conditions:

$$\eta = 0: \quad f = 0; \quad \eta = 1: \quad f = 1; \quad f' = 0;$$

that is, the boundary layer profile joins the velocity of the potential flow with a continuous tangent. The calculation of the numerical factors according to equations (10.8) and (10.12) gives:

$$\alpha = \frac{39}{280}; \quad \beta = \frac{3}{2} \tag{10.24}$$

and hence for the characteristic parameters of the boundary layer:

$$\delta = 4.64\sqrt{\frac{\nu x}{U_o}} \tag{10.25a}$$

$$\tau_o = 0.323\ \mu U_o\sqrt{\frac{U_o}{\nu x}} \tag{10.25b}$$

$$2W = 1.29\, b\sqrt{\mu\rho U_o^3 l} \qquad (10.25c)$$

The exact value for the drag is, according to equation (9.18), $2W = 1.328\, b\sqrt{U_o^3 \mu\rho l}$. The simple assumption of a linear velocity distribution therefore gives a drag too small by thirteen percent, the cubic velocity distribution a drag too small by three percent.

The calculation of the displacement thicknesses of the boundary layers according to equation (10.10a) results, for the linear velocity distribution, in $\delta^* = \frac{1}{2}\delta$, and for the cubic velocity distribution in $\delta^* = \frac{3}{8}\delta$. This gives, because of equations (10.15) and (10.25a):

$$\left.\begin{aligned} \delta^* &= 1.732\sqrt{\frac{\nu x}{U_o}} \quad \text{(linear velocity distribution)} \\ \delta^* &= 1.740\sqrt{\frac{\nu x}{U_o}} \quad \text{(cubic velocity distribution)} \end{aligned}\right\} \qquad (10.26)$$

The agreement with the exact value $\delta^* = 1.728\sqrt{\frac{\nu x}{U_o}}$ according to equation (9.21) is surprisingly good; this is, however, more or less accidental.

The essential characteristics of the boundary layer according to the approximate calculation described above are once more compiled with the exact solution in the table below.

Characteristics of the Boundary Layer on the Flat Plate;

Comparison of Approximate Calculation and Exact Solution

Kind of calculation	$\delta^*\sqrt{\frac{U_o}{\nu x}}$	$\vartheta\sqrt{\frac{U_o}{\nu x}}$	$\frac{\delta^*}{\vartheta}$	$\frac{\tau_o}{\mu U_o}\sqrt{\frac{\nu x}{U_o}}$	$c_w\left(\frac{U_o l}{\nu}\right)^{1/2}$
Linear approximation (fig. 43a)	1.732	0.578	3.00	0.289	1.155
Cubic approximation (fig. 43b)	1.740	0.645	2.70	0.323	1.29
Exact solution (Blasius)	1.729	0.664	2.61	0.332	1.328

As one can see from this table, the agreement, particularly of the cubic approximation and the exact solution, is rather good. On the whole, the results of this calculation with the aid of the momentum theorem may be regarded as very satisfactory, especially in view of the simplicity, as compared to the exact calculation.

Seventh Lecture (January 19, 1942)

b. The Momentum Theorem for the Boundary Layer with Pressure Drop (Plane Problem)

Last time the boundary layer on the flat plate in longitudinal flow was calculated by means of the momentum theorem. Today the general case of the boundary layer with a pressure difference in the flow direction will be treated. One considers the flow along a curved surface, and measures the coordinate x as arc length along the surface; let y be the perpendicular distance from the surface, $U(x)$ the given potential flow (fig. 44). The fundamental equation may be obtained by a momentum consideration as in chapter IXc; now, however, the pressure difference has to be taken into consideration. The same result is obtained by integration of the equation of motion of the boundary layer with respect to y from $y = 0$ (surface) to $y = h$, the layer $y = h$ lying everywhere outside of the friction layer (fig. 44).

The differential equations of the boundary layer for the steady case read, according to equation (8.3),

$$\left.\begin{aligned} u\frac{\partial u}{\partial x} + v\frac{\partial u}{\partial y} &= -\frac{1}{\rho}\frac{\partial p}{\partial x} + \nu\frac{\partial^2 u}{\partial y^2} \\ \frac{\partial u}{\partial x} + \frac{\partial v}{\partial y} &= 0 \end{aligned}\right\} \qquad (10.27)$$

with the boundary conditions: $y = 0$: $u = v = 0$; $y = \infty$: $u = U$. The integration from $y = 0$ to h gives:

$$\frac{1}{2}\frac{d}{dx}\int_{y=0}^{h} u^2\,dy + \int_{0}^{h} v\frac{\partial u}{\partial y}\,dy = -h\frac{1}{\rho}\frac{dp}{dx} + \nu\left[\frac{\partial u}{\partial y}\right]_0^h \qquad (10.28)$$

In the first term the differentiation with respect to x and the integration with respect to y may be interchanged, since the upper limit h is independent of x. On the left side the second term is transformed by integration by parts:

$$\int_0^h v \frac{\partial u}{\partial y} dy = \left[u\, v\right]_0^h - \int_0^h \frac{\partial v}{\partial y} u\, dy = U\, v_h - \int_0^h \frac{\partial v}{\partial y} u\, dy$$

v_h representing the transverse velocity outside of the boundary layer. By continuity, $\frac{\partial v}{\partial y} = -\frac{\partial u}{\partial x}$ and

$$v_h = -\int_0^h \frac{\partial u}{\partial x} dy \tag{10.29}$$

and hence:

$$\int_0^h v \frac{\partial u}{\partial y} dy = -U \int_0^h \frac{\partial u}{\partial x} dy + \int_0^h \frac{\partial u}{\partial x} dy$$

Insertion in equation (10.28) gives, because of:

$$\nu \left[\frac{\partial u}{\partial y}\right]_0^h = -\frac{\tau_o}{\rho} \tag{10.30}$$

the relation:

$$\frac{d}{dx}\int_0^h u^2\, dy - U\int_0^h \frac{\partial u}{\partial x} dy = -\frac{h}{\rho}\frac{dp}{dx} - \frac{\tau_o}{\rho} \tag{10.31}$$

This is the so-called Karman integral-condition, first given by v. Kármán (reference 23).

For the pressure term one now introduces the potential velocity $U(x)$; furthermore, equation (10.31) is to be transformed so that the displacement thickness δ^* and the momentum thickness ϑ appear in it as defined by equation (6.31) and (6.32), namely:

$$U\,\delta^* = \int_0^h (U - u)\,dy \tag{10.32}$$

$$U^2\vartheta = \int_0^h u\,(U - u)\,dy \tag{10.33}$$

According to Bernoulli's equation:

$$\frac{1}{\rho}\frac{dp}{dx} = -U\frac{dU}{dx} = -\frac{dU^2}{dx} + U\frac{dU}{dx}$$

which can also be written:

$$\frac{h}{\rho}\frac{dp}{dx} = -\frac{d}{dx}\int_0^h U^2\,dy + U\frac{d}{dx}\int_0^h U\,dy \tag{10.34}$$

By substitution of equation (10.34) into equation (10.31) there results:

$$\frac{\tau_o}{\rho} = \frac{d}{dx}\int_0^h (U^2 - u^2)\,dy - U\frac{d}{dx}\int_0^h (U - u)\,dy$$

$$= \frac{d}{dx}\int_0^h (U - u)\,u\,dy + \frac{d}{dx}\left\{U\int_0^h (U - u)\,dy\right\} - U\frac{d}{dx}\int_0^h (U - u)\,dy$$

and after differentiation of the second term:

$$\frac{\tau_o}{\rho} = \frac{d}{dx}\int_0^h (U - u)\,u\,dy + \frac{dU}{dx}\int_0^h (U - u)\,dy \tag{10.35}$$

The displacement thickness and the momentum thickness can now be introduced directly and one obtains:

$$\frac{\tau_o}{\rho} = \frac{d}{dx}(U^2\vartheta) + \frac{dU}{dx}\delta^* U$$

or

$$\boxed{\frac{\tau_o}{\rho} = U^2\frac{d\vartheta}{dx} + (2\vartheta + \delta^*)\,U\frac{dU}{dx}} \qquad (10.36)$$

This is the form of the momentum equation for the boundary layer with pressure drop that will be used as a basis for further considerations. Since in it τ_o is quite generally the surface shearing stress, equation (10.36) must apply in the same way to turbulent flow, too. We shall come back to that later. For the special case of vanishing pressure drop $\frac{dU}{dx} = 0$, equation (10.36) is transformed into equation (10.4) found before for the flat plate in longitudinal flow.

The further calculation of the boundary layer on the basis of equation (10.36) is performed for the laminar case according to the method of Pohlhausen (reference 24) and for the turbulent case according to the method of Gruschwitz (reference 34) (chapter XVIII).

c. Calculation of the Boundary Layer According to the Method of Karman–Pohlhausen–Holstein

For further calculation it is of importance to find a suitable expression for the velocity distribution in the boundary layer $u(x, y)$. According to our understanding of the exact solutions of the differential equations of the boundary layer this expression must at least satisfy the conditions that for $y = 0$: $u = 0$, and for $y = \infty$: $u = U$. Furthermore the derivative $\partial u/\partial y$ must vanish for large y. Moreover, velocity profiles with and without inflection points must be possible, as they occur in the pressure decrease and pressure increase region, respectively. Finally, a profile with $\left(\frac{\partial u}{\partial y}\right)_{y=o} = 0$ must be possible in order to have a separation point result from the approximate calculation.

One chooses for the velocity distribution an expression of the form $u\,(x, y) = Uf(y/\delta_p)$, and sets, according to Pohlhausen,

for $f(y/\delta_p)$ a polynomial of the fourth order, hence:

$$\frac{u}{U} = a\,\eta + b\,\eta^2 + c\,\eta^3 + d\,\eta^4; \quad \eta = \frac{y}{\delta_p(x)} \tag{10.37}$$

valid for $0 \leq y \leq \delta_p$: $0 \leq \eta \leq 1$. $\delta_p(x)$ stands for the boundary layer thickness, the dependence of which on x has yet to be calculated. The boundary layer thickness of the approximate calculation δ_p is here provided with the index P (= Pohlhausen) in order to avoid confusion with the boundary layer thickness δ used before. Whereas for the exact solutions the velocity in the boundary layer asymptotically approaches the velocity of the potential flow, ($u \rightarrow U$ for $y \rightarrow \infty$); the value $u = U$ is to be attained in the approximation at a finite distance from the surface $y = \delta_p$, for reasons of calculation. This modification of the actual relation is physically insignificant.

For the determination of the free constants a, b, c, d in equation (10.37) the following boundary conditions are prescribed, all of which follow from the differential equation of the boundary layer (equation (8.3)):

$$\left.\begin{aligned} y = \delta_p: \quad & u = U; \quad \frac{\partial u}{\partial y} = 0; \quad \frac{\partial^2 u}{\partial y^2} = 0 \\ y = 0: \quad & u = 0; \quad \nu \frac{\partial^2 u}{\partial y^2} = -U \frac{dU}{dx} \end{aligned}\right\} \tag{10.38}$$

Since the condition of no slip $u = 0$ for $y = 0$ is automatically satisfied by expression (10.37), the four free constants a, b, c, d are sufficient to satisfy the remaining four conditions. The last of the five conditions follows immediately from the exact differential equation of the boundary layer if one puts $y = 0$ and takes the boundary conditions into consideration. This condition is particularly important since it determines the curvature of the velocity profiles near the surface and assures that boundary layer profiles do not acquire an inflection point in the region of pressure decrease and do acquire one in the region of pressure increase, as required by the exact solution according to chapter VIII. From equation (10.38) follows for the coefficients a, b, c, d the equation system:

$$\left.\begin{aligned} a + b + c + d &= 1 \\ a + 2b + 3c + 4d &= 0 \\ 2b + 6c + 12d &= 0 \\ \frac{2\nu U b}{\delta_P^2} &= -U U' \end{aligned}\right\} \qquad (10.39)$$

From the last equation follows immediately:

$$b = -\frac{1}{2}\frac{\delta_P^2}{\nu} U' = -\frac{\lambda}{2} \qquad (10.40)$$

if one introduces the simplification:

$$\lambda = \frac{\delta_P^2}{\nu}\frac{dU}{dx} \qquad (10.41)$$

The dimensionless quantity λ plays the role of a form parameter of the velocity profiles as will become clear presently. For the remaining coefficients one obtains from equation (10.39):

$$a = 2 + \frac{\lambda}{6}; \quad c = -2 + \frac{\lambda}{2}; \quad d = 1 - \frac{\lambda}{6} \qquad (10.40b)$$

Hence the expression for the velocity distribution, which satisfies all boundary conditions according to equation (10.37), reads:

$$\frac{u}{U} = (2\eta - 2\eta^3 + \eta^4) + \frac{\lambda}{6}(\eta - 3\eta^2 + 3\eta^3 - \eta^4)$$

$$\frac{u}{U} = F(\eta) + \lambda\, G(\eta) \qquad (10.42)$$

in which

$$\left.\begin{aligned} F(\eta) &= 2\eta - 2\eta^3 + \eta^4 \\ G(\eta) &= \frac{1}{6}(\eta - 3\eta^2 + 3\eta^3 - \eta^4) \end{aligned}\right\} \qquad (10.43)$$

Due to $\eta = y/\delta_p(x)$ the boundary layer thickness $\delta_p(x)$ is here the only unknown. If that is calculated, the parameter λ follows immediately from equation (10.41). From equation (10.42) one understands that the velocity profiles form with the form parameter $\lambda(x)$ a one-parameter family. The functions $F(\eta)$ and $G(\eta)$ indicated in figure 45 and table 4 have a universal character, that is, they do not depend on the special body shape. The velocity profiles for various values of λ are plotted in figure 46. The profile with $\lambda = 0$ is obtained for $dU/dx \equiv 0$, that is, for the boundary layer without pressure gradient (flat plate in longitidinal flow). The separation profile with $(\partial u/\partial y)_0 = 0$, that is, $a = 0$, has according to equation (10.40b) the parameter $\lambda = -12$. The profile at the stagnation point has, as will be shown below, $\lambda = 7.052$. For $\lambda > 12$ there result values of $u/U > 1$ in the boundary layer, which physically does not make sense. These values therefore have to be excluded. Since behind the separation point the boundary layer calculation loses its validity anyway, the form parameter λ is limited to the region

$$-12 \leq \lambda \leq +12 \tag{10.44}$$

The unknown boundary layer thickness $\delta_p(x)$ remains to be calculated. For this the momentum equation (10.36), so far not utilized, is at our disposal. Before performing this computation, a few preparatory calculations are required, namely the determination of the boundary layer characteristics, displacement thickness δ^*, momentum loss thickness ϑ, and surface shearing stress τ_0 on the basis of the approximation-expression equation (10.42): One obtains from equations (10.32) and (10.42):

$$\frac{\delta^*}{\delta_p} = \int_{\eta=0}^{1} \left[1 - F(\eta) - \lambda G(\eta)\right] d\eta$$

$$\frac{\vartheta}{\delta_p} = \int_{\eta=0}^{1} \left[F(\eta) + \lambda G(\eta)\right]\left[1 - F(\eta) - \lambda G(\eta)\right] d\eta$$

The calculation of the definite integrals, with the values of $F(\eta)$ and $G(\eta)$ according to equation (10.43), gives:

$$\frac{\delta^*}{\delta_p} = \frac{3}{10} - \frac{\lambda}{120} \tag{10.45}$$

$$\frac{\vartheta}{\delta_p} = \frac{37}{315} - \frac{\lambda}{945} - \frac{\lambda^2}{9072} \tag{10.46}$$

Further, there results for the surface shearing stress from $\tau_o = \mu\left(\frac{\partial u}{\partial y}\right)_o$ according to equations (10.42) and (10.43)

$$\frac{\tau_o}{\mu}\frac{\delta_p}{U} = \frac{12 + \lambda}{6} \tag{10.47}$$

Now the momentum equation (10.36) is to be used for calculation of $\delta_p(x)$. After multiplication by $\vartheta/\nu U$ it acquires the dimensionless form:

$$\frac{U\vartheta\vartheta'}{\nu} + \left(2 + \frac{\delta^*}{\vartheta}\right)\frac{U'\vartheta^2}{\nu} = \frac{\tau_o}{\mu}\frac{\vartheta}{U} \tag{10.48}$$

The boundary layer thickness δ_p does not even appear in this equation; however, this is not particularly astonishing, since δ_p is a rather arbitrary quantity of our approximate calculation and therefore without special physical significance. The physically important quantities, displacement thickness δ^* and momentum loss thickness ϑ, appear instead in equation (10.48). Hence it suggests itself to first calculate ϑ from the momentum equation (10.48) and then to pass on to δ_p by means of equation (10.46). For this purpose one introduces according to Holstein and Bohlen (reference 25) aside from the first form parameter λ according to equation (10.41) a second form parameter κ, formed analogously with the momentum thickness ϑ:

$$\kappa = \frac{\vartheta^2}{\nu} U' \tag{10.49}$$

Then one sets:

$$Z = \frac{\vartheta^2}{\nu} \tag{10.50}$$

Then

$$\kappa = Z\, U' \tag{10.51}$$

Between the second form parameter κ and the first form parameter λ exists, according to equations (10.40) and (10.41) the universal relation:

$$\kappa = \left(\frac{37}{315} - \frac{\lambda}{945} - \frac{\lambda^2}{9072}\right)^2 \lambda \tag{10.52}$$

Furthermore, for simplification, one substitutes:

$$\frac{\delta^*}{\vartheta} = \frac{\frac{3}{10} - \frac{\lambda}{120}}{\frac{37}{315} - \frac{\lambda}{945} - \frac{\lambda^2}{9072}} = f_1(\kappa) \tag{10.53}$$

$$\frac{\tau_o}{\mu}\frac{\vartheta}{U} = \frac{\tau_o}{\mu}\frac{\delta_p}{U}\frac{\vartheta}{\delta_p} = \left(\frac{12 + \lambda}{6}\right)\left(\frac{37}{315} - \frac{\lambda}{945} - \frac{\lambda^2}{9072}\right) = f_2(\kappa) \tag{10.54}$$

By introduction of κ and Z according to equations (10.49) and (10.50) and by substituting from equation (10.53) and (10.54) one now obtains from the momentum equation (10.48), because of $\vartheta\vartheta'/\nu = \frac{1}{2}\frac{dZ}{dx}$

$$\frac{1}{2} U \frac{dZ}{dx} + \left[2 + f_1(\kappa)\right]\kappa - f_2(\kappa) = 0 \tag{10.55}$$

Finally, one sets as further simplification

$$2f_2(\kappa) - 4\kappa - 2f_1(\kappa)\,\kappa = F(\kappa) \tag{10.56}$$

or written in detail:

$$F(\kappa) = 2\left(\frac{37}{315} - \frac{\lambda}{945} - \frac{\lambda^2}{9072}\right)\left\{2 - \frac{116}{315}\lambda + \left(\frac{2}{945} + \frac{1}{120}\right)\lambda^2 + \frac{2}{9072}\lambda^3\right\} \tag{10.57}$$

and thus obtains the following differential equation for the momentum thickness

$$\boxed{\frac{dZ}{dx} = \frac{F(\kappa)}{U} \qquad \kappa = Z\,U'} \tag{10.58}$$

This is a non-linear differential equation of the first order for $z = \vartheta^2/\nu$. The fact that the function $F(\kappa)$ is rather complicated does not constitute any appreciable drawback, since $F(\kappa)$ is universal, that is, independent of the shape of the body, and hence may be tabulated once and for all. The functions $F(\kappa)$, $f_1(\kappa)$, $f_2(\kappa)$ as also $\kappa = \kappa(\lambda)$ according to equation (10.52) are given in table 5.

As to the solution of equation (10.58) the following remains to be said: The calculation has to start at the stagnation point $x = 0$. There $U = 0$; and the initial slope $\frac{dZ}{dx}$ would be infinite if $F(\kappa)$ were not also equal to zero at the stagnation point. The function $F(\kappa)$ actually has a zero which yields a physically significant initial value. This zero of $F(\kappa)$ is given when the second bracket in equation (10.57) disappears. One finds:

$$F(\kappa) = 0 \text{ for } \kappa = \kappa_o = 0.0770; \quad \lambda = \lambda_o = 7.052 \tag{10.59}$$

The value $\lambda = 7.052$ therefore gives the value of the first form parameter at the stagnation point. Then the initial slope of the integral curve at the stagnation point now has the indeterminate value $\frac{0}{0}$. The latter may, however, be calculated and hence finally yields the initial value and the initial slope of the integral curve as:

$$\left.\begin{aligned} Z_o &= \frac{\kappa_o}{U'_o} = \frac{0.0770}{U'_o} \\ \left(\frac{dZ}{dx}\right)_o &= -0.0652\,\frac{U''_o}{U'^2_o} \end{aligned}\right\} \tag{10.60}$$

The index o denotes the values at the stagnation point. With these initial values one succeeds easily in performing the integration of equation (10.58), for instance, according to the isocline method. A calculation example is given in the appendix, figure 47, and table 6. The calculation is to be carried up to the separation point $\lambda = -12$: $\kappa = -0.1567$. Quantities entering the calculation that are given by the potential flow are the velocity $U(x)$ and its first derivative with respect to the arc length dU/dx.* (Only at the stagnation point is d^2U/dx^2 also required for the initial slope of the integration curve.)

* In Pohlhausen's treatment (reference 24) a differential equation is obtained instead of equation (10.58), for the quantity $z = \delta_p^2/\nu$, formed analogously to Z. Pohlhausen's differential equation also contains d^2U/dx^2 which often can be obtained from the given potential flow only by a double graphical differentiation. The representation of Holstein which completely avoids the quantity d^2U/dx^2 therefore means an essential improvement of the method.

The values of the form parameters for the three special cases: stagnation point, velocity maximum ($U' = 0$) (pressure gradient equals zero), and separation point are compiled in the table below.

Case	λ	κ
Stagnation point	7.052	0.0770
Velocity maximum	0	0
Separation point	−12	−0.1567

The entire process of calculation takes the following course:

1. The integration of equation (10.58) yields $Z(x)$, $\kappa(x)$ and according to equation (10.50), also $\vartheta(x)$; furthermore it yields the position of the separation point.

2. First form parameter $\lambda(x)$ from equation (10.52)

3. Displacement thickness δ^* from equation (10.53)

4. Surface shearing stress τ_o from equation (10.54)

5. Boundary layer thickness $\delta_p(x)$ from equation (10.45)

6. Velocity distribution u/U from equation (10.42)

Flat Plate in Longitudinal flow

The special case of the flat plate in longitudinal flow which was treated in chapter Xa with a different form for the approximation can also be obtained very simply from the present calculation. $U = U_o$; $U' \equiv 0$, and hence $\kappa = \lambda = 0$, and according to equation (10.58):

$$\frac{dZ}{dx} = \frac{F(0)}{U_o} = \frac{0.4698}{U_o}$$

With the initial value $\vartheta = 0$ for $x = 0$ there results

$$\vartheta^2 = 0.4698 \frac{\nu x}{U_o} \quad \text{or} \quad \vartheta = 0.685\sqrt{\frac{\nu x}{U_o}} \tag{10.61}$$

whereas the exact value according to Blasius' calculation, equation (9.21b), is $\vartheta = 0.664\sqrt{\nu x/U_o}$. Furthermore, it follows that the displacement thickness is with $\delta^*/\vartheta = f_1(0) = 2.54$

$$\delta^* = 1.75\sqrt{\frac{\nu x}{U_o}} \tag{10.62}$$

The shearing stress becomes, from equation (10.54) with $f_2(0) = 0.235$;

$$\tau_o = 0.343\ \mu U_o\sqrt{\frac{U_o}{\nu x}} \tag{10.63}$$

while the exact value τ_o is $\tau_o = 0.332\ \mu U_o\sqrt{U_o/\nu x}$ according to equation (9.17). The agreement with the exact values is rather satisfactory. In figure 50b the velocity distribution obtained by the approximate calculation also is compared with the exact calculation in the plot u/U against y/δ^*. This agreement also is rather good.

Stagnation Point Profile

A similar comparison can be performed for the stagnation point profile the exact solution of which was given in chapter VI. For this case $\lambda = \lambda_o = 7.052$, $\kappa = \kappa_o = 0.0770$. For the approximate calculation the momentum thickness is:

$$\vartheta\sqrt{\frac{U'}{\nu}} = \sqrt{\kappa_o} = 0.278 \tag{10.64}$$

whereas according to the exact calculation equation (6.34) it is $\vartheta\sqrt{U'/\nu} = 0.292$. The displacement thickness is, for the approximate calculation;

$$\delta^*\sqrt{\frac{U'}{\nu}} = f_1(\kappa_o)\sqrt{\kappa_o} = 0.641 \tag{10.65}$$

whereas according to the exact calculation, equation (6.33), it is $\delta^*\sqrt{U'/\nu} = 0.648$. Finally, according to the approximate calculation the shearing stress is:

$$\frac{\tau_o}{\mu U}\sqrt{\frac{\nu}{U'}} = \frac{f_2 \kappa_o}{\sqrt{\kappa_o}} = \frac{0.332}{0.278} = 1.19 \qquad (10.66)$$

compared with $\frac{\tau_o}{\mu U}\sqrt{\frac{\nu}{U'}} = \varphi''(0) = 1.234$ by the exact calculation. Thus the agreement with the exact values is here also satisfactory.

The velocity distribution of the approximate calculation is compared with the exact calculation in figure 50-a in the plot u/U against y/δ^*. Here also the agreement is good.

The following table contains a compilation of the comparisons just given, between the characteristics δ^*, ϑ, τ_o from exact and from approximate calculation.

	Blasius Profile				Stagnation point profile			
	$\delta^*\sqrt{\frac{U_o}{\nu x}}$	$\vartheta\sqrt{\frac{U_o}{\nu x}}$	$\frac{\tau_o}{\mu\sqrt{U_o^3/\nu x}}$	$\frac{\delta^*}{\vartheta}$	$\delta^*\sqrt{\frac{U'}{\nu}}$	$\vartheta\sqrt{\frac{U'}{\nu}}$	$\frac{\tau_o}{\mu U\sqrt{\nu/U'}}$	$\frac{\delta^x}{\vartheta}$
Pohlhausen Approximation	1.75	0.685	0.343	2.55	0.641	0.278	1.19	2.31
Exact solution	1.73	0.664	0.332	2.61	0.648	0.292	1.234	2.21

Of course, it can not yet be concluded from this good agreement of the approximate with the exact solution that similar good agreement would exist for all the boundary layer profiles along the body. Accurate comparisons are not easily performed since very few exact solutions reaching from the stagnation point to the separation point exist. However, one may conclude from occasionally made comparisons that in the region of pressure decrease the agreement is mostly rather good; in the region of pressure increase, particularly near the separation point, some deviation might occur.

Since no other serviceable methods for boundary layer calculation have so far become known, the Pohlhausen method is for the present to be regarded as the best. The time required for a boundary layer calculation for one side of the body immersed in a given potential flow amounts to about three hours.

The calculation described here for the plane flow was applied by Tomotika (reference 26) to the rotationally-symmetrical case.

d. Examples

A few examples of boundary layer calculations will be given, all of which were performed according to the approximation method described in the previous section.

The first example, taken from a treatise of H. Schlichting and A. Ulrich (reference 35) concerns a series of elliptical cylinders in a flow parallel to the major axis. The axis ratios are $a_1/b_1 = 1$ (circular cylinder), 2, 4, 8, ∞ (flat plate). The velocity distributions of the potential flow are given in figure 51. For slender cylinders they are characterized by the fact that the velocity has a very flat maximum and decreases steeply toward the front and rear. The result of the boundary layer calculation is illustrated in figure 52. Figure 52-a shows the dimensionless displacement thickness as a function of the arc length. It is noteworthy that for all elliptic cylinders the boundary layer on the front half is smaller than for the flat plate; this is caused by the pressure decrease. The laminar-separation point for the circular cylinder lies at $s/t = 0.604$ ($\varphi = 109.5^\circ$). With increasing fineness ratio it shifts further toward the rear; it is also plotted in figure 51. Figure 52-b shows the variation of the form parameter λ and figure 52-c the variation of the surface shearing stress. For every elliptic cylinder the latter has a maximum, the position of which shifts frontward with increasing fineness ratio. The variation of the shearing stress for the cylinder of axis ratio eight shows only an insignificant difference from the one for the flat plate in longitudinal flow. Figure 53 gives a survey of the variation of the boundary layer on the body and the velocity profiles at various points along the surface. Corresponding calculations for the rotationally-symmetrical case (that is, for ellipsoids of revolution with flow parallel to the axis) have been performed by Pretsch (reference 27).

The second example (reference 35) gives the boundary layer on a symmetrical Joukowski profile of fifteen percent thickness for lift coefficients in the region of $c_a = 0$ to 1. Figure 54 gives the velocity distribution according to the potential theory for the lift coefficients $c_a = 0$, 0.25, 0.50, 0.75, and 1.0. For the symmetrical approach flow ($c_a = 0$) the velocity maximum lies rather far toward the front at $s/t = 0.141$. With growing lift coefficient the velocity maximum increases on the suction side and decreases on the pressure side. Simultaneously the maximum shifts farther forward on the suction side and farther rearward on the pressure side. The magnitude of the velocity maximum and its position are of primary importance for the development of the boundary layer and in particular for the position of the separation point. The results of the boundary layer calculation are plotted separately for the suction and pressure sides in figure 55. Figure 55-a gives the variation of the displacement thickness, figure 55-b the form parameter λ_1, and figure 55-c the surface shearing stress. The position of the laminar separation point is plotted in figure 54. Figure 56 gives

a survey of the variation of the boundary layer along the surface and of the velocity distribution in the boundary layer for $c_a = 0$, figure 57 for $c_a = 1$.

Finally, the third example gives a survey of the influence of the most important profile parameters of a wing profile on the laminar boundary layer. K. Bussmann (reference 36) performed the boundary layer calculation for a family of Joukowsky profiles of relative thickness $d/t = 0$ to 0.25 and relative camber $f/t = 0$ to 0.08 for c_a- values from 0 to 1. Figure 58 shows the family of Joukowsky profiles. Of the very voluminous results, only the position of the separation point shall be shown here. Figure 59 shows the position of the separation point on the suction side as a function of thickness, camber, and lift coefficient; figure 60 shows the same result for the pressure side.

Herewith the discussion of the approximation method for calculation of the laminar boundary layer will be concluded.

Eighth Lecture (January 26, 1942)

CHAPTER XI. PREVENTION OF SEPARATION

For practical flow problems the flow with pressure increase (retarded flow) plays an important role. It is always desirable that no separation of the flow from the wall occur, because of the resulting large losses in energy. The wing presents a good example. A pressure increase exists on the suction side toward the trailing edge (fig. 61). If separation occurs, the wing will have an undesirably large drag and small lift. Another example is the flow in an expanding passage (diffuser) which transforms kinetic energy into pressure energy (as for instance in the wind tunnel or in the bucket grid of a turbine).

Calculations will presently show that the ability of a laminar flow to overcome a pressure increase without separation is exceedingly small. Thus the pressure increases present in practical flows would, for laminar flow, almost always lead to separation. The reason that, nevertheless, in many cases of practical flows considerable pressure increases are surmounted without separation is that the flow is turbulent. As we shall see more clearly later, the ability to overcome a pressure increase without separation is very much greater for turbulent than for laminar flow. Since, moreover, the pressure increase always gives rise to an early transition from laminar to turbulent*, one has to deal almost exclusively with turbulent flow in practical flows with pressure increase.

Nevertheless it is useful to clarify the fundamental relations regarding prevention of separation for laminar flow, particularly because its phenomena lend themselves more readily to numerical treatment than those of the turbulent flow.

---

*Details are given in chapter XXI "Transition from Laminar to Turbulent."

Various possibilities exist for prevention of separation. The simplest way is to make the pressure increase so small that separation is avoided. A numerical estimation in the next section will give information about this possibility. Another possibility consists in artificially influencing the boundary layer, for instance by blowing or suction of fluid, or else by application of an auxiliary wing that provides acceleration at the critical points of the boundary layer. Some details will be given in the following sections of this chapter.

a. Estimation of the Admissible Pressure Gradient

We are going to make, following Prandtl (reference 2), a generally valid estimation of the pressure increases in a laminar boundary layer that are possible without the occurrence of separation. We take as the basis the Kármán-Pohlhausen approximate calculation according to Chapter X and make the assumption that under the effect of the pressure gradient given by the potential flow the boundary layer has developed till near the separation point (Point 0 in fig. 62). From here on the pressure distribution is to be such that the form of the velocity profile does not change further downstream, that is, the form parameter λ is to remain constant. Since the value corresponding to the separation point is $\lambda = -12$, this constant λ-value shall be chosen at $\lambda = -10$*. A definite value of the second form parameter (according to table 5) corresponds to this choice:

$$\lambda = -10; \quad \kappa = -0.1369; \quad F(\kappa) = 1.523 \tag{11.1}$$

For the prevention of separation the following relation between the potential-flow velocity $U(x)$ and the momentum thickness $\vartheta(x)$ results according to equations (10.50) and (10.51):

$$\frac{\vartheta^2}{\nu} = Z = \frac{0.1369}{-U'} \tag{11.2}$$

or

$$\frac{dZ}{dx} = 0.1369 \cdot \frac{U''}{U'^2} \tag{11.3}$$

or

$$U \frac{dZ}{dx} = 0.1369 \frac{UU''}{U'^2} = 0.1369 \, \sigma \tag{11.4}$$

if one puts for simplification

*At any rate, this λ-value must be negative, since otherwise the flow in question is not retarded.

$$\sigma = \frac{UU''}{U'^2} \tag{11.5}$$

On the other hand, the momentum equation according to equation (10.58) holds for the further development of the boundary layer for $x > 0$:

$$U \frac{dZ}{dx} = F(\kappa) = F(-0.1369) = 1.523 \tag{11.6}$$

The numerical value must be substituted for $F(\kappa)$, if the form parameters are to remain constant at the values given by equation (11.1). From equations (11.6) and (11.4) follows therewith, for the constancy of the form parameter $\lambda = -10$, the conditional equation

$$0.1369 \frac{UU''}{U'^2} = 1.523$$

or

$$\sigma = \frac{UU''}{U'^2} = 11.13 \approx 11 \tag{11.7}$$

For $\sigma > 11$ the boundary layer can still bear the pressure increase; for $\sigma < 11$ separation occurs; for $\sigma = 11$ the boundary layer always remains with $\lambda = -10$, on the verge of separation. Qualitatively, the following can be immediately said about the distribution of the potential-flow velocity $U(x)$ which gives no separation. Because of equation (11.7) a necessary condition for avoiding separation in retarded flow is:

$$U'' > 0 \quad \text{for} \quad U' < 0 \tag{11.7a}$$

that is, a negative velocity gradient U' must exist, the magnitude of which decreases in the flow direction. If, therefore, the curve $U(x)$ in figure 63 is curved downward behind the maximum ($U'' < 0$), separation occurs in every case; if it is curved upward ($U'' > 0$), separation sometimes does not occur. The limiting case $U'' = 0$ for $U' < 0$ always leads to separation. The sufficient condition for avoiding separation is $UU''/U'^2 > 11$.

One now proceeds to calculate what potential flow and what boundary layer thickness variation correspond to $\sigma = +11$. From equation (11.7) follows:

$$\frac{U''}{U'} = 11 \frac{U'}{U}$$

and after integration: $\log U' = 11 \log U - \log C_1'$ or

$$\frac{U'}{U^{11}} = - C_1'$$

with C_1' as integration constant. Repeated integration gives:

$$\frac{1}{10} U^{-10} = C_1' x + C_2 \qquad (11.8)$$

For $x = 0$, $U(x)$ shall be $U(x) = U_o$, thus

$$C_2 = \frac{1}{10} U_o^{-10} \qquad (11.9)$$

Furthermore, one puts

$$C_1' U_o^{10} = C_1 \qquad (11.10)$$

and obtains from equation (11.8) for the potential flow

$$U = \frac{U_o}{(1 + 10 C_1 x)^{0.1}} \qquad (11.11)$$

Thereby is found the desired velocity distribution that just avoids separation. The constant C_1 can be determined from the boundary layer thickness δ_o at the initial point $x = 0$:

$$\lambda = \frac{U'\delta^2}{\nu} = -10$$

$$\delta = \sqrt{\frac{10\nu}{-U'}}$$

According to equation (11.11)

$$U' = - \frac{C_1 \, U_o}{(1 + 10 \, C_1 x)^{1.1}}$$

and thence

$$\delta = \sqrt{\frac{10 \, \nu}{C_1 U_o}} \, (1 + 10 \, C_1 x)^{0.55}$$

From $\delta = \delta_o$ for $x = 0$ follows

$$C_1 = \frac{10 \, \nu}{U_o \delta_o^2} \tag{11.12}$$

and thus, as the final solution for the potential flow and the boundary layer thickness variation,

$$U = U_o \left(1 + 100 \, \frac{\nu x}{U_o \delta_o^2} \right)^{-0.1} * \tag{11.13}$$

$$\delta = \delta_o \left(1 + 100 \, \frac{\nu x}{U_o \delta_o^2} \right)^{0.55} \tag{11.14}$$

The permissible retardation (velocity decrease) is therefore comparable to $1/\sqrt[10]{x}$ and is thus very small. The velocity is thus very close to the constant velocity of the flat plate in longitudinal flow. For the present case the growth of the boundary layer thickness δ must therefore be somewhat larger than for the flat plate, where $\delta \sim x^{1/2}$. Here $\delta \sim x^{0.55}$; thus the increase is only slightly larger.

The flow in a divergent channel with plane walls (two-dimensional problem) will be treated as another example. In figure 64 let x be the radial distance from the origin 0. The walls start at $x = a$, where the entrance velocity of the potential flow equals U_o. The potential flow is

---

*Compare Chapter IX e where it was found, as exact solution of the differential equation of the boundary layer, that in retarded flow separation occurs when $U(x) = u_1 \, x^{-0.091}$

$$\left.\begin{aligned} U(x) &= U_o \frac{a}{x} \\ U' &= -U_o \frac{a}{x^2} \\ U'' &= 2U_o \frac{a}{x^3} \end{aligned}\right\} \qquad (11.15)$$

Thus $U' < 0$ and $U'' > 0$ for all x so that the necessary condition equation (11.7a) for avoiding separation is satisfied. However, calculation of the dimensionless number σ according to equation (11.5) gives

$$\sigma = 2 \qquad (11.16)$$

The sufficient condition for avoiding separation, $\sigma > 11$ according to equation (11.7) is therefore violated. For the divergent channel with plane walls separation therefore occurs for any included angle. This example shows especially clearly the low ability of the laminar flow to overcome a pressure increase without separation. According to a calculation of Pohlhausen (reference 24) the separation point lies at $(x/a)_A = 1.213$ and thus is independent of the included angle α.

b. Various Technical Arrangements for Avoiding Separation

It is a favorable circumstance for technical applications that for higher Reynolds numbers the boundary layer does not remain laminar but becomes turbulent. The turbulence consists of an irregular mixing motion. By this mixing motion momentum is continuously transported into the layers near the wall, and the particles retarded at the wall are carried out into the free stream and thus re-accelerated.

Because of this mechanism the turbulent flow is able to withstand, without separation, considerably higher pressure increases than the laminar flow; thus the pressure increases existing in technical flows are made possible.

A few technical possibilities for avoiding separation will be discussed.

1. Blowing. For a wing profile the separation of the boundary layer for large angles of attack (fig. 65) can be prevented by blowing air in the flow direction from a slot directed toward the rear. The velocity for the layer near the surface is thus increased by the energy

supplied and the danger of separation is therefore eliminated. It is true that in the practical execution not much is gained, because of the large jet energy required for any considerable improvement of the flow. In order to make the energy output small, the width of the jet must be kept small. But then the jet, soon after its exit, breaks up into vortices.

2. Another possibility of avoiding separation is the arrangement of a slotted wing according to figure 66. The effect depends on the boundary layer formed on the slot AB being carried away into the free stream, before it separates, by the flow through the slot. A new boundary layer develops at C which is, however, at first very thin and reaches D without separation.

The same principle is used for the Townend ring and NACA cowling (fig. 67).

3. Suction. A further possibility for the prevention of separation is suction. For the wing, for instance, the retarded boundary-layer material is sucked off into the interior of the wing through one or several slots (fig. 68). The point of suction lies slightly ahead of or behind the separation point so that no reversal of the flow can occur. A new boundary layer which at first is very thin develops behind the suction point and permits the pressure to increase further. In this manner one can overcome considerably larger pressure increases and attain higher values of maximum lift for the wing. Many different suction arrangements for increasing maximum lift have been investigated by O. Schrenk (reference 28). Values for $c_{a\ max}$ of 3 to 4 were obtained.

c. Theory of the Boundary Layer with Suction

Suction is a very effective means for influencing the friction layer on a body immersed in a flow and particularly for avoiding separation. This was pointed out for the first time in 1904 by L. Prandtl in his fundamental work on the boundary layer.

Another possibility of application of suction, recognized only recently, is to keep the friction layer laminar. Here the boundary layer is, by suction, kept so thin that transition to the turbulent state of flow is avoided. The surface friction drag is thereby reduced. Experimental investigations of this effect were carried out by Ackeret (reference 39).

The laminar friction layer with suction can also be subjected to a numerical treatment which will be briefly discussed. The following assumptions are made for the calculation:

1. The suction is introduced into the calculation through the assumption that the normal velocity at the wall $v_o(x)$ is different from zero. The wall is therefore assumed to be permeable. A continuous distribution of the suction velocity $v_o(x)$ serves the purpose of numerical treatment best.

2. The suction quantities are so small that only the parts in the immediate neighborhood of the wall are sucked from the boundary layer. This leads to a very small ratio of suction velocity $v_o(x)$ to free stream velocity U_o: $v_o/U_o = 0.001$ to 0.01.

3. The no-slip condition at the wall $u = 0$ is retained with suction, likewise the expression for the wall shearing stress

$$\tau_o = \mu\left(\frac{\partial u}{\partial y}\right)_o$$

The equations of motion for the boundary layer with suction therefore read

$$\left.\begin{aligned} u\frac{\partial u}{\partial x} + v\frac{\partial u}{\partial y} &= U\frac{dU}{dx} + \nu\frac{\partial^2 u}{\partial y^2} \\ \frac{\partial u}{\partial x} + \frac{\partial v}{\partial y} &= 0 \end{aligned}\right\} \qquad (11.17)$$

with the boundary conditions

$$\left.\begin{aligned} y = 0 \quad u &= 0 \quad v = v_o(x) \\ y = \infty \quad u &= U \end{aligned}\right\} \qquad (11.18)$$

$v_o < 0$ signifies suction; $v_o > 0$ blowing.

As in chapter X b the momentum theorem is again applied to the boundary layer with suction. The momentum equation for the boundary layer with suction is obtained in exactly the same manner as in chapter X b (compare fig. 44) provided one takes into consideration, in addition, that the normal velocity at the wall is different from zero. In chapter X b the momentum equation was derived by integration of the equation of

motion for the x-direction over y between the limits $y = 0$ and $y = \infty$ (compare equation (10.28)). One imagines exactly the same calculation performed for the boundary layer with suction: then the expression for the normal velocity at the distance from the wall $y = h$ is different, compared with the calculation in chapter X b. The normal velocity now becomes

$$v_h = v_o - \int_{u_o}^{h} \frac{\partial u}{\partial x}\, dy \tag{11.19}$$

The remaining calculation is exactly the same as in chapter X b and finally yields as the momentum equation for the boundary layer with suction.

$$\boxed{\frac{\tau_o}{\rho} = U^2 \frac{d\vartheta}{dx} + (2\vartheta + \delta^*)\, U \frac{dU}{dx} - v_o\, U} \tag{11.20}$$

The newly added term $-v_o U$ (compared with equation (10.36)) gives the loss of momentum due to the suction at the wall.

We shall now treat the special case of the flat plate with suction in longitudinal flow (fig. 69) (reference 29). The free-stream velocity is U_o. Equation (11.20) then becomes

$$U_o^2 \frac{d\vartheta}{dx} - v_o U = \frac{\tau_o}{\rho} = \nu \left(\frac{\partial u}{\partial y}\right)_{y=o} \tag{11.21}$$

if one takes the law for the laminar wall shearing stress into consideration. Furthermore, the assumption is made that the suction velocity (or blowing velocity) $-v_o$ along the plate is constant. In this case one can obtain from the momentum equation (11.21), by the following simple calculation, an estimate of the variation of the momentum thickness along the plate. One puts

$$\left(\frac{\partial u}{\partial y}\right)_o = \beta \frac{U_o}{\vartheta} \tag{11.22}$$

$\beta \geq 0$ signifying a dimensionless form parameter of the velocity profile. It may be assumed, to a first approximation, that β varies only little

with the length of run x; accordingly, β will be considered constant. Then equation (11.21) may be written

$$\frac{1}{2}\frac{d\vartheta^2}{dx} = \beta\frac{\nu}{U_o} + \frac{v_o}{U_o}\vartheta \tag{11.23}$$

with the initial condition $\vartheta = 0$ for $x = 0$. For suction $(v_o < 0)$ one obtains $d\vartheta/dx = 0$ for

$$\vartheta_\infty = \beta\frac{\nu}{-v_o} \text{ (suction)} \tag{11.24}$$

(that is, therefore, the momentum thickness reaches, after a certain approach length, a constant asymptotic value given by equation (11.24)). Simultaneously, displacement thickness, velocity distribution, and all other boundary layer coefficients also become asymptotically independent of x.

For blowing $(v_o > 0)$ the value $d\vartheta/dx$ is, according to equation (11.23), larger than zero along the entire plate; that is, $\vartheta(x)$ increases with the length of run x without limit so that for large values of x, one can neglect in equation (11.23) the first term on the right side as compared with the second. One obtains therefore, as asymptotic law,

$$\vartheta_\infty = \frac{v_o}{U_o}x \text{ (blowing)} \tag{11.25}$$

On the whole, one obtains the remarkable result that for the flat plate in longitudinal flow with constant suction or blowing velocity, the boundary layer thickness for suction becomes constant after a certain approach length, whereas for blowing, it increases proportionally to the length of run x. In between lies the case of the impermeable wall where the boundary layer thickness increases with $\sqrt{x}$.

For the case of the laminar boundary layer with the asymptotically constant boundary layer thickness it is also possible to give immediately an exact solution of the differential equations of the boundary layer in a surprisingly simple form. In this case $\partial u/\partial x \equiv 0$, hence also, according to equation (11.17), $\partial v/\partial y \equiv 0$ and therefore

$$v(x,y) = v_o = \text{constant} \tag{11.26}$$

Hence there follows from equation (11.17)

$$v_o \frac{\partial u}{\partial y} = \nu \frac{\partial^2 u}{\partial y^2} \tag{11.27}$$

and from it the solution which satisfies the boundary conditions equation (11.18)

$$u(y) = U_o \left\{ 1 - e^{\frac{v_o y}{\nu}} \right\} \tag{11.28}$$

From this equation results the displacement thickness of the asymptotic boundary layer

$$\delta^*_\infty = \frac{\nu}{-v_o} \tag{11.29}$$

the momentum thickness

$$\vartheta_\infty = \frac{1}{2} \frac{\nu}{-v_o} \tag{11.30}$$

and the form parameter $\frac{\delta^*_\infty}{\vartheta_\infty} = 2$. By comparing equation (11.29) with equation (11.24) one finds the factor $\beta = 1$. The velocity distribution of the asymptotic boundary layer profile according to equation (11.28) is plotted in figure 70 together with the Blasius solution for the impermeable wall.

Herewith the considerations of boundary layer with suction will be concluded.

CHAPTER XII. APPENDIX TO PART I

a. Examples of the Boundary Layer Calculation According to the Pohlhausen–Holstein Method

For the integration of the differential equation (10.58) it is best to use the isocline method. It is expedient to calculate with dimensionless quantities. The arc length s is made dimensionless by

dividing by a characteristic length of the body immersed in the flow, for instance, for the wing, by the wing chord t. The variable $Z = \vartheta^2/\nu$ is made dimensionless by multiplying by $\frac{U_o}{t}$. Thus one puts:

$$\left.\begin{aligned} Z^* &= \frac{\vartheta^2 U_o}{\nu\, t} = \left(\frac{\vartheta}{t}\right)^2 \frac{U_o t}{\nu} \\ x^* &= \frac{s}{t} \end{aligned}\right\} \qquad (12.1)$$

Hence the differential equation reads:

$$\frac{dZ^*}{dx^*} = F(\kappa);\quad \kappa = \frac{t}{U_o}\frac{dU}{ds} Z^* \qquad (12.2)$$

The calculated example concerns a symmetrical wing profile (J 015) in symmetrical approach flow ($c_a = 0$). The prescribed potential-flow velocity and its first derivative with respect to the arc length is given in table 6. The initial values for the integration are calculated, according to equation (10.60), to be, for the present case:

$$Z_o^* = 0.00\ 149$$

$$\left(\frac{dZ^*}{dx^*}\right)_o = 0$$

since at the stagnation point $d^2U/ds^2 = 0$. The auxiliary function $F(\kappa)$ required for the integration is given in figure 47-a and table 5. The calculation according to the isocline method is shown in figure 48. Here the curve $\kappa = -0.1567$ which gives the separation point can be calculated according to the relation:

$$Z^* = -\kappa_A \Big/ \frac{t}{U_o}\frac{dU}{ds} = -0.1567 \Big/ \frac{t}{U_o}\frac{dU}{ds}$$

The intersection of the integral curve with this curve gives the separation point. As a result of the integration one obtains at first the variation of the momentum thickness. By means of the function $\delta^*/\vartheta = f(\kappa)$ and $\frac{\vartheta}{U}\frac{\tau_o}{\mu} = f_2(\kappa)$ given in table 5 one can also calculate the displacement

thickness and the shearing stress. The result of the calculation is compiled in table 6 and given in figure 49. Moreover, the velocity distribution in the boundary layer can be seen from figure 56.

Translated by Mary L. Mahler
National Advisory Committee
for Aeronautics

BIBLIOGRAPHY*

Part A. – Laminar Flows

1. Textbooks and Encyclopedias:

1. Prandtl-Tietjens: Hydro- und Aeromechanik. Bd. I and II. Berlin, 1929 and 1931.

2. Prandtl, L.: The Mechanics of Viscous Fluids. In F. W. Durand, Aerodynamic Theory, Bd. III, 1935.

3. Tollmien, W.: Laminare Grenzschichten. Handbuch der Experimentalphysik, Bd. IV, Teil I, Leipzig, 1931.

4. Goldstein, S.: Modern Developments in Fluid Dynamics. Vols. I and II. Oxford, 1938.

5. Müller, W.: Einführung in die Theorie der zähen Flüssigkeiten. Liepzig, 1932.

6. Lamb, H.: Lehrbuch der Hydrodynamik. Teubner, Leipzig, 1907.

2. Articles:

7. Prandtl, L.: Ueber Flüssigkeitsbewegung bei sehr kleiner Reibung. Verhandlung III. Intern. Math. Kongress, Heidelberg, 1904, represented in "Vier Abhdnlg. zur Hydrodynamik", Göttingen, 1927

8. Blasius, H.: Grenzschichten in Flüssigkeiten mit kleiner Reibung. Zs. Math. u. Phys. Bd. 56, p. 1 (1908).

9. Boltze, E.: Grenzschichten an Rotationskörpern in Flüssigkeiten mit kleiner Reibung. Diss. Göttingen 1908.

10. Hiemenz, K.: Die Grenzschicht an einem in den gleichförmigen Flüssigkeitsstrom eingetauchten geraden Kreiszylinder. (Diss. Göttingen, 1911). Dingl. Polytechn. Journ. Bd. 326, p. 321, 1911.

11. Hamel, G.: Spiralförmige Bewegungen zäher Flüssigkeiten. Jahresber. Mathem. Vereinigung 1916, p. 34.

12. Szymanski: Quelques solutions exactes des équations de l'hydrodynamique du fluide visqueux dans le cas d'un tube cylindrique. Journ. de math. pures et appliquées. Reihe 9, Bd. 11, 1932, p. 67. See also: Intern. Congr. of Mechanics Stockholm, 1930.

---

* On the whole, only the more recent publications, since about 1932, are given here. The older literature can be found for instance, in Prandtl's contribution to Durand: Aerodynamic Theory, vol. III.

13. Schlichting, H.: Berechnung ebener periodischer Grenzschichtströmungen. Physik. Zeitschrift, 1932, p. 327.

14. Schlichting, H.: Laminare Kanaleinlaufströmung. Zs. f. angew. Math. u. Mech. Bd. 14, p. 368, 1934.

15. Howarth, L.: On the Calculation of Steady Flow in the Boundary Layer Near the Surface of a Cylinder in a Stream. ARC Rep. 1632, 1935.

16. Frössling, Nils: Verdunstung, Wärmeübergang und Geschwindigkeitsverteilung bei zweidimensionaler und rotationssymmetrischer laminarer Grenzschichtströmung. Lunds. Univ. Arsskr. N. F. Avd. 2, Bd. 35, Nr. 4, 1940.

17. Homann, F.: Der Einfluss grosser Zähigkeit bei der Strömung um den Zylinder und um die Kugel. Zs. f. angew. Math. u. Mech. Bd. 16, p. 153 (1936).

18. Howarth, L.: On the Solution of the Laminar Boundary Layer Equations. Proc. Roy. Soc. Lond. A No. 919, vol.164, 1938, p. 547.

19. v. d. Hegge-Zynen: Thesis Delft 1924, Burgers Proc. I. Intern. Congress appl. Mech. Delft 1924.

20. Hansen, M.: Die Geschwindigkeitsverteilung in der Grenzschicht an einer eingetauchten Platte. Zs. f. angew. Math. u. Mech. Bd. 8, p. 185, 1928.

21. Goldstein, S.: Concerning Some Solutions of the Boundary Layer Equations in Hydrodynamics. Proc. Phil. Soc. Vol. 26, I, 1936.

22. Schlichting, H.: Laminare Strahlausbreitung. Zs. f. angew. Math. u. Mech. Bd. 13, p. 260 (1933).

23. v. Kármán, Th.: Laminare und turbulente Reibung. Zs. f. angew. Math. u. Mech. Bd. 1, p. 235, 1921.

24. Pohlhausen, K.: Zur näherungsweisen Integration der Differentialgleichungen der laminaren Reibungsschicht. Zs. f. angew. Math. u. Mech. Bd. 1, p. 252, 1921.

25. Holstein-Bohlen: Ein vereinfachtes Verfahren zur Berechnung laminarer Reibungsschichten, die dem Näherungsansatz von K. Pohlhausen genügen. (Not yet published.)

26. Tomotika, S.: The laminar boundary Layer on the Surface of a Sphere in a uniform stream. ARC Rep. 1678, 1936.

27. Pretsch, J.: Die laminare Reibungsschicht an elliptischen Zylindern und Rotationsellipsoiden bei symmetrischer Umströmung. Luftfahrtforschung Bd. 18, p. 397, 1941.

28. Schrenk, O.: Versuche mit Absaugeflügeln. Luftfahrtforschung 1935, p. 16.

29. Schlichting, H.: Die Grenzschicht mit Absaugung und Ausblasen. Luftfahrtforschung Bd. 19, p. 179, 1942.

30. Bickley, W.: The Plane Jet. Phil. Mag., ser. 7, vol 23, No. 156, p. 727, Apr. 1937.

31. Prandtl, L.: Anschauliche und nutzliche Mathematik. Vorlesung W. S. 1931/32.

32. Schiller, L.: Forschungsarbeiten auf dem Gebiet des Ingenieurwesens. Heft 248, 1922.

33. Results of the Aerodynamics Test Institute at Gottingen. Aerodynamischen Versuchsanstalt zu Göttingen. 2. Lieferung, p. 29.

34. Gruschwitz: Turbulente Reibungsschicht in ebener Strömung bei Druckabfall und Druckanstieg. Ing.-Arch. Bd. 2 (1931).

35. Schlichting, H., and Ulrich, A.: Zur Berechnung des Umschlages laminar – turbulent. (not yet published).

36. Bussmann, K.: Die laminare Reibungsschicht an Joukowsky-Profilen. (not yet published).

37. Falkner, V. M., and Skan, S. W.: Some Approximate Solutions of the Boundary Layer Equations. R. & M. No. 1314, British A.R.C., 1930.

38. Hartree, D. R.: On an Equation Occurring in Falkner and Skan's Approximate treatment of the Equations of the Boundary Layer. Cambridge Phil. Soc., Bd. 33 (1937).

39. Ackeret, J., Pfenninger, W., Kas, M.: Verhinderung des Turbulentwerdens einer Reibungsschicht durch Absaugung. Naturw. 1941, p. 622.

TABLE I. — THE FUNCTION φ OF THE PLANE STAGNATION POINT FLOW (ACCORDING TO HIEMENZ (REFERENCE 10)); TO FIGURE 16

$$\xi = \sqrt{\frac{a}{\nu}}\, y; \quad \frac{u}{U} = \varphi'(\xi)$$

ξ	φ	φ'	φ''
0	0	0	1.23264
0.1	0.0060	0.1183	1.1328
0.2	0.0233	0.2266	1.0345
0.3	0.0510	0.3252	0.9386
0.4	0.0881	0.4144	0.8463
0.5	0.1336	0.4946	0.7583
0.6	0.1867	0.5662	0.6751
0.7	0.2466	0.6298	0.5973
0.8	0.3124	0.6859	0.5251
0.9	0.3835	0.7350	0.4586
1.0	0.4592	0.7778	0.3980
1.1	0.5389	0.8149	0.3431
1.2	0.6220	0.8467	0.2937
1.3	0.7081	0.8739	0.2498
1.4	0.7966	0.8968	0.2109
1.5	0.8873	0.9161	0.1769
1.6	0.9798	0.9324	0.1473
1.7	1.0738	0.9457	0.1218
1.8	1.1688	0.9569	0.0999
1.9	1.2650	0.9659	0.0814
2.0	1.3619	0.9732	0.0658
2.1	1.4596	0.9792	0.0528
2.2	1.5577	0.9841	0.0420
2.3	1.6563	0.9876	0.0332
2.4	1.7552	0.9905	0.0260
2.5	1.8543	0.9928	0.0202
2.6	1.9537	0.9946	0.0156
2.7	2.0533	0.9960	0.0119
2.8	2.1529	0.9971	0.0091
2.9	2.2528	0.9979	0.0068
3.0	2.3525	0.9985	0.0051
3.1	2.4523	0.9988	0.0036
3.2	2.5522	0.9992	0.0027
3.3	2.6521	0.9994	0.0023
3.4	2,7521	0.9996	0.0019
3.5	2.8520	0.9997	0.0014
3.6	2.9520	0.9998	0.0010
3.7	3.0519	0.9999	0.0008
3.8	3.1518	0.9999	0.0004
3.9	3.2518	0.9999	0.0003
4.0	3.3518	1.0000	0.0002
4.1	3.4518	1,0000	0.0001
4.2	3.5518	1.0000	0.0001
4.3	3.6518	1.0000	0

TABLE II. — THE FUNCTION f OF THE BOUNDARY LAYER ON THE FLAT PLATE IN LONGITUDINAL FLOW (ACCORDING TO BLASIUS (REFERENCE 8)); TO FIGURE 30 $\eta = y\sqrt{\frac{U_o}{\nu x}}$; $\frac{u}{U_o} = f'(\eta)$

η	f	f'	f''
0	0	0	0.33206
0.2	0.00664	0.06641	0.33199
0.4	0.02656	0.13277	0.33147
0.6	0.05974	0.19894	0.33008
0.8	0.10611	0.26471	0.32739
1.0	0.16557	0.32979	0.32301
1.2	0.23795	0.39378	0.31659
1.4	0.32298	0.45627	0.30787
1.6	0.42032	0.51676	0.29917
1.8	0.52952	0.57477	0.28293
2.0	0.65003	0.62977	0.26675
2.2	0.78120	0.68132	0.24835
2.4	0.92230	0.72899	0.22809
2.6	1.07252	0.77246	0.20646
2.8	1.23099	0.81152	0.18401
3.0	1.39682	0.84605	0.16136
3.2	1.56911	0.87609	0.13913
3.4	1.74696	0.90177	0.11788
3.6	1.92954	0.92333	0.09809
3.8	2.11605	0.94112	0.08013
4.0	2.30576	0.95552	0.06424
4.2	2.49806	0.96696	0.05052
4.4	2.69238	0.97587	0.03897
4.6	2.88826	0.98269	0.02948
4.8	3.08534	0.98779	0.02187
5.0	3.28329	0.99155	0.01591
5.2	3.48189	0.99425	0.01134
5.4	3.68094	0.99616	0.00793
5.6	3.88031	0.99748	0.00543
5.8	4.07990	0.99838	0.00365
6.0	4.27964	0.99898	0.00240
6.2	4.47948	0.99937	0.00155
6.4	4.67938	0.99961	0.00098
6.6	4.87931	0.99977	0.00061
6.8	5.07928	0.99987	0.00037
7.0	5.27926	0.99992	0.00022
7.2	5.47925	0.99996	0.00013
7.4	5.67924	0.99998	0.00007
7.6	5.87924	0.99999	0.00004
7.8	6.07923	1.00000	0.00002
8.0	6.27923	1.00000	0.00001
8.2	6.47923	1.00000	0.00001
8.4	6.67923	1.00000	0
8.6	6.87923	1.00000	0
8.8	7.07923	1.00000	0

TABLE III. – THE FUNCTIONS f_3, g_5 AND h_5 OF THE BOUNDARY LAYER ON THE CYLINDER (SYMMETRICAL CASE) ACCORDING TO HOWARTH (REFERENCE 15) AND FRÖSSLING (REFERENCE 16). $\eta = y\sqrt{\frac{u_1}{\nu}}$

η	f_3	f_3'	f_3''
0	0	0	0.7244
0.1	0.0035	0.0675	0.6249
0.2	0.0132	0.1251	0.5286
0.3	0.0282	0.1734	0.4375
0.4	0.0476	0.2129	0.3539
0.5	0.0705	0.2444	0.2780
0.6	0.0962	0.2688	0.2112
0.7	0.1240	0.2869	0.1530
0.8	0.1534	0.2997	0.1037
0.9	0.1838	0.3080	0.0626
1.0	0.2149	0.3125	0.0292
1.1	0.2462	0.3140	0.0028
1.2	0.2776	0.3132	−0.0173
1.3	0.3088	0.3107	−0.0320
1.4	0.3397	0.3070	−0.0420
1.5	0.3702	0.3025	−0.0482
1.6	0.4002	0.2947	−0.0513
1.7	0.4297	0.2923	−0.0518
1.8	0.4587	0.2871	−0.0506
1.9	0.4871	0.2822	−0.0480
2.0	0.5151	0.2775	−0.0444
2.1	0.5426	0.2733	−0.0402
2.2	0.5698	0.2695	−0.0358
2.3	0.5966	0.2662	−0.0314
2.4	0.6230	0.2632	−0.0271
2.5	0.6492	0.2607	−0.0230
2.6	0.6752	0.2586	−0.0194
2.7	0.7010	0.2568	−0.0160
2.8	0.7266	0.2554	−0.0131
2.9	0.7520	0.2542	−0.0106
3.0	0.7774	0.2533	−0.0085
3.1	0.8027	0.2525	−0.0067
3.2	0.8279	0.2519	−0.0052
3.3	0.8531	0.2515	−0.0041
3.4	0.8782	0.2511	−0.0032
3.5	0.9033	0.2508	−0.0024
3.6	0.9284	0.2506	−0.0019
3.7	0.9534	0.2504	−0.0014
3.8	0.9785	0.2503	−0.0011
3.9	1.0035	0.2502	−0.0008
4.0	1.0285	0.2502	−0.0006
4.1	1.0535	0.2501	−0.0004
4.2	1.0785	0.2501	−0.0003
4.3	1.1035	0.2500	−0.0002
4.4	1.1285	0.2500	−0.0001

η	g_5	g_5'	g_5''
0	0	0	0.6348
0.2	0.0114	0.1072	0.4402
0.4	0.0405	0.1778	0.2717
0.6	0.0806	0.2184	0.1408
0.8	0.1264	0.2367	0.0483
1.0	0.1742	0.2399	−0.0106
1.2	0.2218	0.2342	−0.0431
1.4	0.2676	0.2239	−0.0567
1.6	0.3112	0.2123	−0.0580
1.8	0.3526	0.2012	−0.0522
2.0	0.3918	0.1916	−0.0432
2.2	0.4293	0.1839	−0.0335
2.4	0.4655	0.1781	−0.0245
2.6	0.5007	0.1740	−0.0171
2.8	0.5352	0.1712	−0.0114
3.0	0.5692	0.1694	−0.0072
3.2	0.6030	0.1682	−0.0043
3.4	0.6365	0.1676	−0.0026
3.6	0.6700	0.1672	−0.0015
3.8	0.7034	0.1669	−0.0010
4.0	0.7368	0.1668	−0.0004
4.2	0.7701	0.1667	−0.0001
4.4	0.8035	0.1667	−0.0001

η	h_5	h_5'	h_5''
0	0	0	0.1192
0.2	0.0017	0.0141	0.0249
0.4	0.0045	0.0117	−0.0436
0.6	0.0057	−0.0010	−0.0783
0.8	0.0039	−0.0176	−0.0833
1.0	−0.0012	−0.0330	−0.0680
1.2	−0.0090	−0.0441	−0.0423
1.4	−0.0185	−0.0498	−0.0149
1.6	−0.0286	−0.0503	+0.0088
1.8	−0.0384	−0.0468	0.0256
2.0	−0.0472	−0.0406	0.0351
2.2	−0.0546	−0.0331	0.0380
2.4	−0.0604	−0.0257	0.0361
2.6	−0.0649	−0.0189	0.0312
2.8	−0.0681	−0.0133	0.0249
3.0	−0.0703	−0.0089	0.0187
3.2	−0.0717	−0.0058	0.0132
3.4	−0.0726	−0.0036	0.0089
3.6	−0.0732	−0.0021	0.0057
3.8	−0.0735	−0.0012	0.0036
4.0	−0.0737	−0.0006	0.0022
4.2	−0.0738	−0.0003	0.0012
4.4	−0.0738	−0.0001	0.0007

TABLE IV. – THE FUNCTIONS $F(y/\delta_p)$ and $G(y/\delta_p)$ FOR THE VELOCITY DISTRIBUTION IN THE BOUNDARY LAYER ACCORDING TO POHLHAUSEN (REFERENCE 24) AND HOWARTH (REFERENCE 15)

$\frac{y}{\delta_p}$	F	G
0	0	0
0.1	0.1981	0.01215
0.2	0.3856	0.01725
0.3	0.5541	0.01715
0.4	0.6976	0.0144
0.5	0.8125	0.0104
0.6	0.8976	0.0064
0.7	0.9541	0.00315
0.8	0.9856	0.00105
0.9	0.9981	0.00015
1.0	1	0

TABLE V. – AUXILIARY FUNCTIONS FOR THE BOUNDARY LAYER CALCULATION

ACCORDING TO HOLSTEIN (REFERENCE 25)

λ	κ	$F(\kappa)$	$f_1(\kappa) = \frac{\delta^*}{\vartheta}$	$f_2(\kappa) = \frac{\vartheta}{U}\frac{\tau_0}{\mu}$
15	0.0885	-0.0657	2.279	0.345
14	0.0920	-0.0814	2.262	0.351
13	0.0941	-0.0913	2.253	0.354
12	0.0948	-0.0946	2.250	0.356
11	0.0941	-0.0911	2.253	0.354
10	0.0920	-0.0806	2.260	0.351
9	0.0882	-0.0608	2.273	0.346
8	0.0831	-0.0332	2.289	0.340
7.8	0.0820	-0.0271	2.293	0.338
7.6	0.0807	-0.0203	2.297	0.337
7.4	0.0794	-0.0132	2.301	0.335
7.2	0.0780	-0.0051	2.305	0.333
7.052	0.0770	0	2.308	0.332
7	0.0767	0.0021	2.309	0.331
6.9	0.0760	0.0061	2.312	0.330
6.8	0.0752	0.0102	2.314	0.330
6.7	0.0744	0.0144	2.316	0.329
6.6	0.0737	0.0186	2.318	0.328
6.5	0.0729	0.0230	2.321	0.327
6.4	0.0721	0.0274	2.323	0.326
6.3	0.0713	0.0319	2.326	0.325
6.2	0.0706	0.0365	2.328	0.324
6.1	0.0697	0.0412	2.331	0.322
6	0.0689	0.0459	2.333	0.321
5	0.0599	0.0978	2.361	0.310
4	0.0497	0.1579	2.392	0.297
3	0.0385	0.2255	2.427	0.283
2	0.0264	0.3000	2.466	0.268
1	0.0135	0.3820	2.508	0.252
0	0	0.4698	2.554	0.235
-1	-0.0140	0.5633	2.604	0.217
-2	-0.0284	0.6616	2.658	0.199
-3	-0.0429	0.7640	2.716	0.179
-4	-0.0575	0.8698	2.779	0.160
-5	-0.0720	0.9780	2.847	0.140
-6	-0.0862	1.0853	2.921	0.119
-7	-0.0999	1.1981	2.999	0.100
-8	-0.1130	1.3078	3.084	0.079
-9	-0.1255	1.4173	3.177	0.059
-10	-0.1369	1.5231	3.276	0.039
-11	-0.1474	1.6251	3.383	0.019
-12	-0.1567	1.7237	3.500	0
-13	-0.1648	1.8159	3.627	-0.019
-14	-0.1715	1.9020	3.765	-0.037
-15	-0.1767	1.9821	3.920	-0.054

TABLE VI. — EXAMPLE FOR THE BOUNDARY LAYER CALCULATION ACCORDING TO HOLSTEIN (REFERENCE 25). (PROFILE J 015; $c_a = 0$)

φ (deg)	$\frac{s}{t}$	$\frac{U}{U_o}$	$\frac{t}{U_o}\frac{dU_m}{ds}$	κ	$Z^* = \frac{\vartheta^2 U_o}{\nu t}$	λ	$\frac{\delta^*}{t}\sqrt{\frac{U_o t}{\nu}}$	$\frac{2\tau_o}{\rho U_o^2}\sqrt{\frac{U_o t}{\nu}}$
180	0	0	51.7	0.0770	0.00149	7.052	0.089	0
177.5	0.0049	0.231	49.0	0.0745	0.00152	6.70	0.0895	3.90
175	0.0099	0.445	42.2	0.0708	0.00168	6.24	0.0957	7.05
172.5	0.0148	0.632	32.6	0.0662	0.00203	5.64	0.1057	8.95
170	0.0197	0.782	24.75	0.0631	0.00255	5.32	0.119	9.74
165	0.0308	0.993	12.70	0.0513	0.00404	4.15	0.152	9.36
160	0.0443	1.111	6.16	0.0389	0.00632	3.03	0.193	7.94
150	0.0787	1.233	1.573	0.0209	0.01325	1.57	0.287	5.57
140	0.123	1.270	0.215	0.0057	0.0267	0.41	0.410	3.81
136	0.145	1.271	0	0	0.0340	0	0.460	3.43
130	0.178	1.267	−0.209	−0.0101	0.0485	−0.71	0.564	2.58
120	0.241	1.245	−0.387	−0.0317	0.0820	−2.23	0.765	1.69
110	0.313	1.212	−0.468	−0.0616	0.1315	−4.27	1.005	1.05
100	0.390	1.178	−0.485	−0.1024	0.211	−7.18	1.385	0.49
90	0.473	1.136	−0.487	−0.1510	0.310	−11.37	1.910	0.049
A 89.5	0.483	1.130	−0.487	−0.1567	0.324	−12	1.990	0
80	0.561	1.095	−0.487					
70	0.648	1.053	−0.474					
60	0.733	1.014	−0.458					
50	0.812	0.997	−0.442					
40	0.885	0.945	−0.420					
30	0.944	0.917	−0.416					
20	0.990	0.899	−0.414					
10	1.018	0.889	−0.409					
5	1.025	0.886	−0.409					
0	1.028	0.884	−0.409					

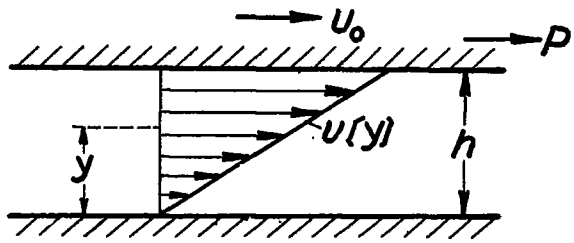

Figure 1.- Simple shear flow.

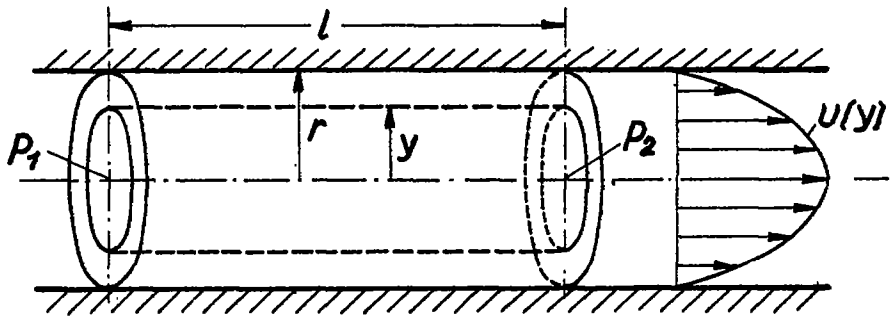

Figure 2.- Hagen-Poiseuille's pipe flow.

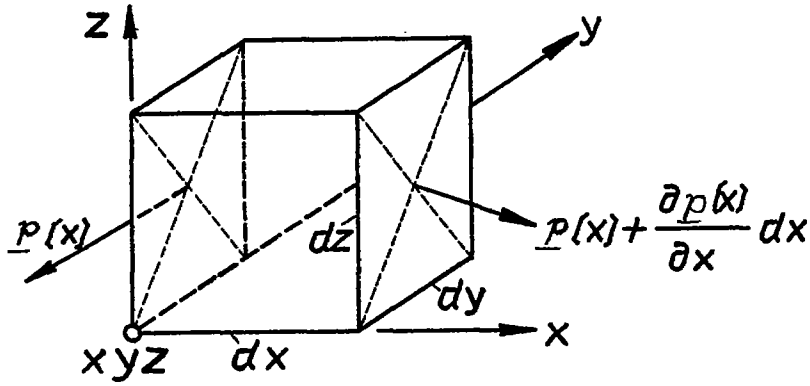

Figure 3.- The general stress tensor.

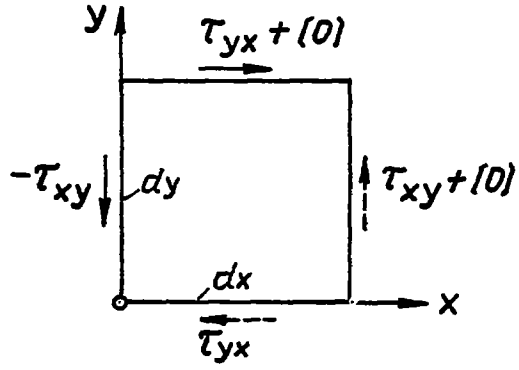

Figure 4.- The shearing stress (to fig. 3).

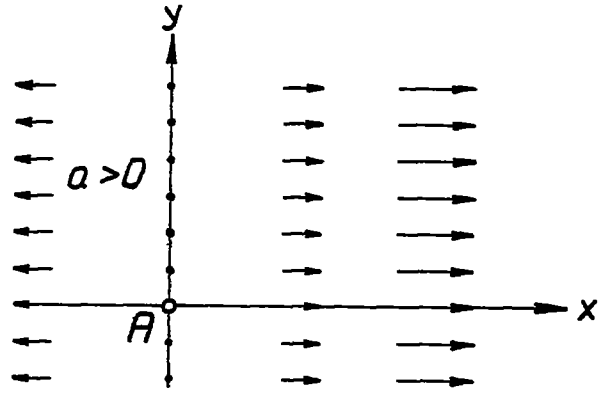

Figure 5.- The deformation of a pure elongation.

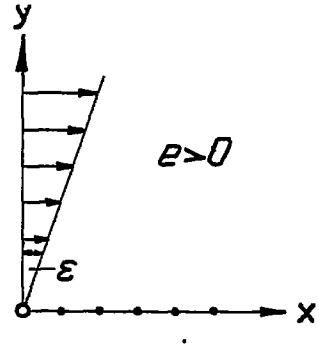

Figure 6.- Pure angular deformation (e > 0).

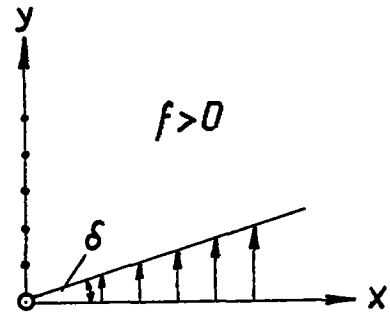

Figure 7.- Pure angular deformation (f -> 0).

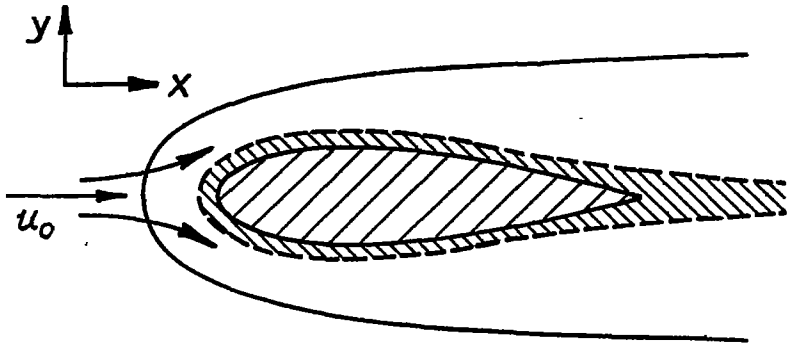

Figure 8.- Analogy between heat boundary layer and flow boundary layer.

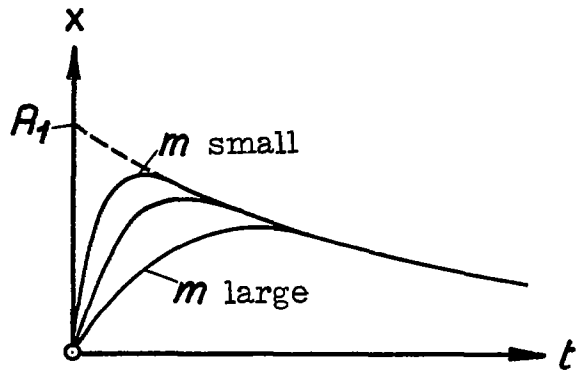

Figure 9.- Types of solutions of the Navier-Stokes differential equations.

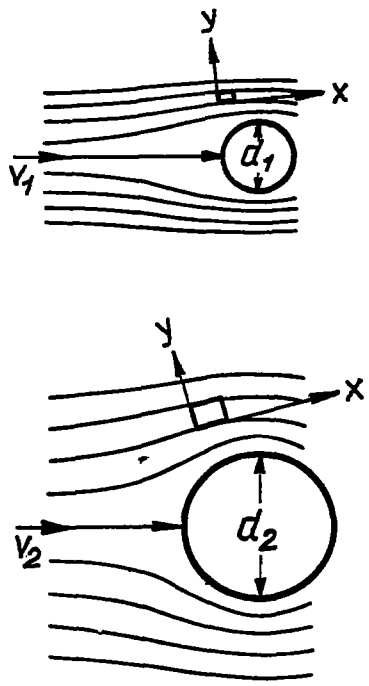

Figure 10.- Reynolds' law of similarity.

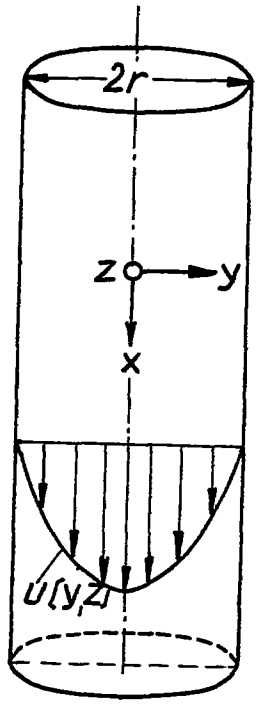

Figure 11.- Laminar pipe flow.

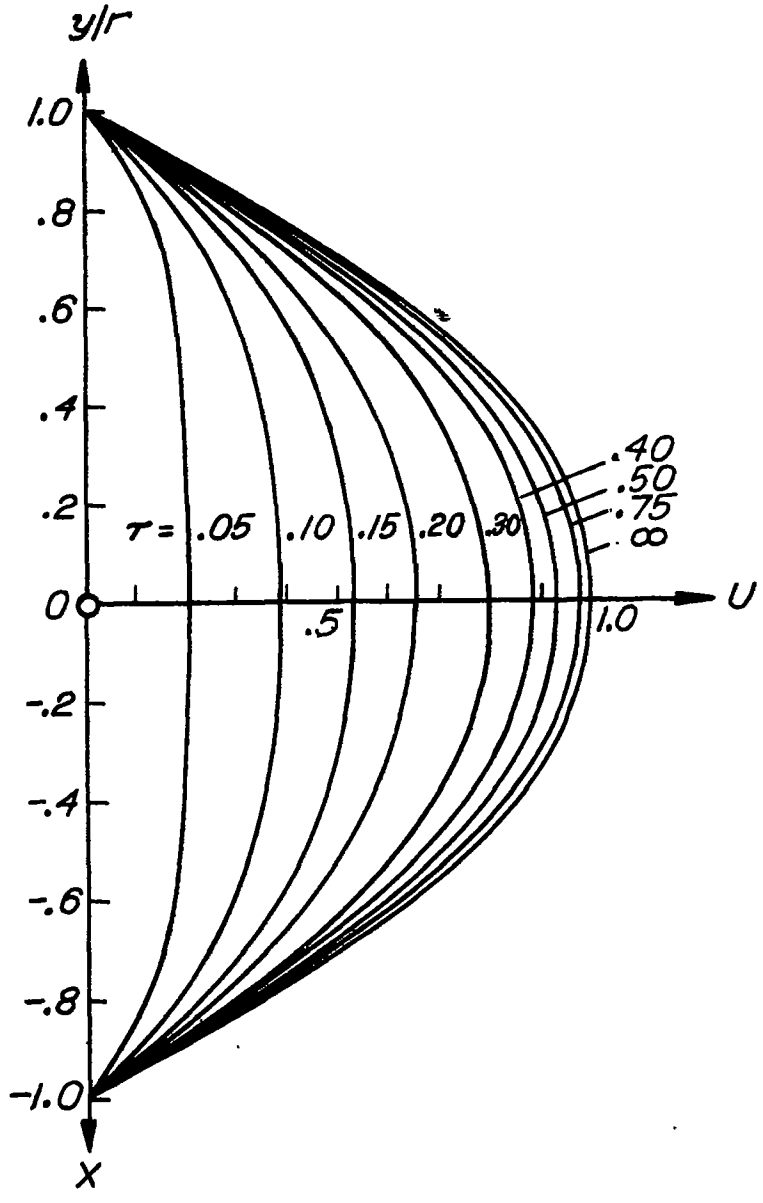

Figure 12.- Velocity profiles of the starting pipe flow $\left(\tau = \frac{vt}{r^2}\right)$.

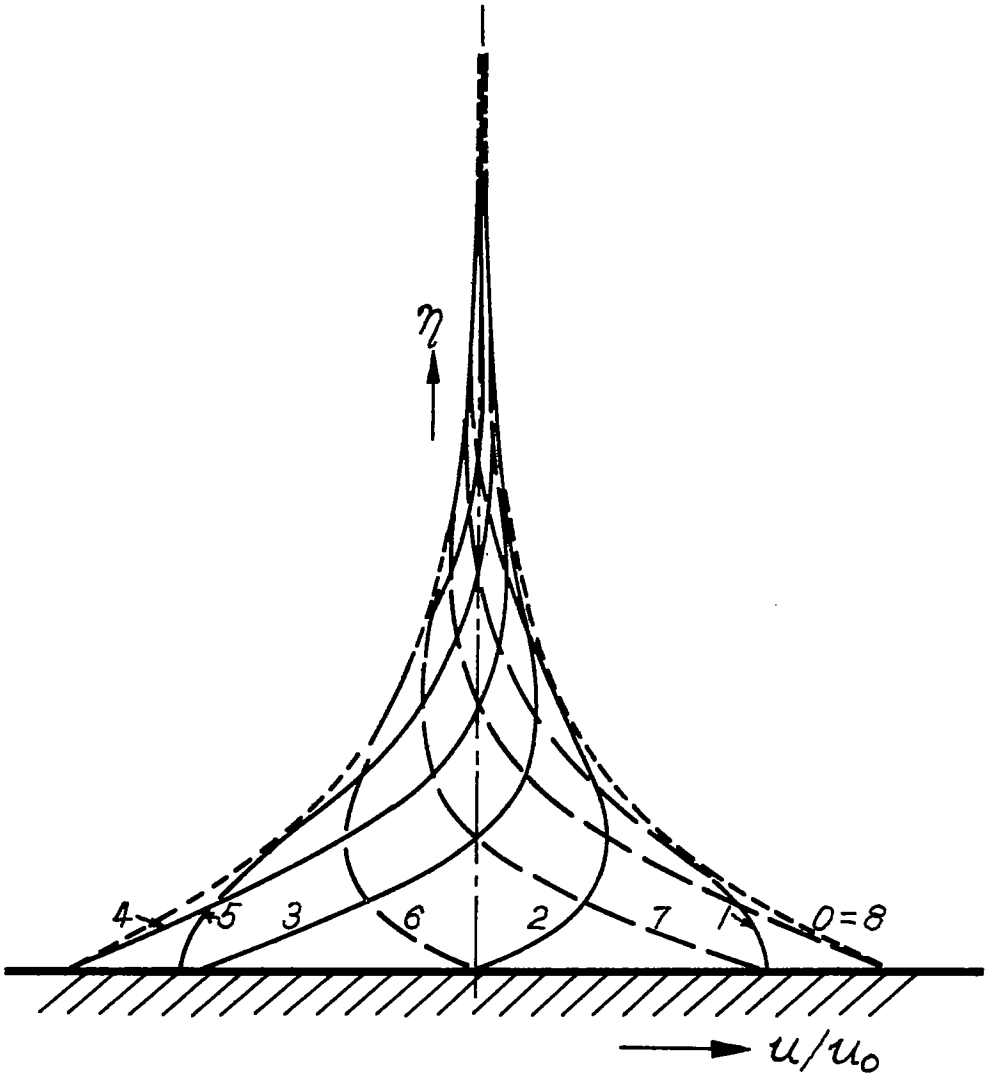

Figure 13.- Velocity distribution on an oscillating surface.

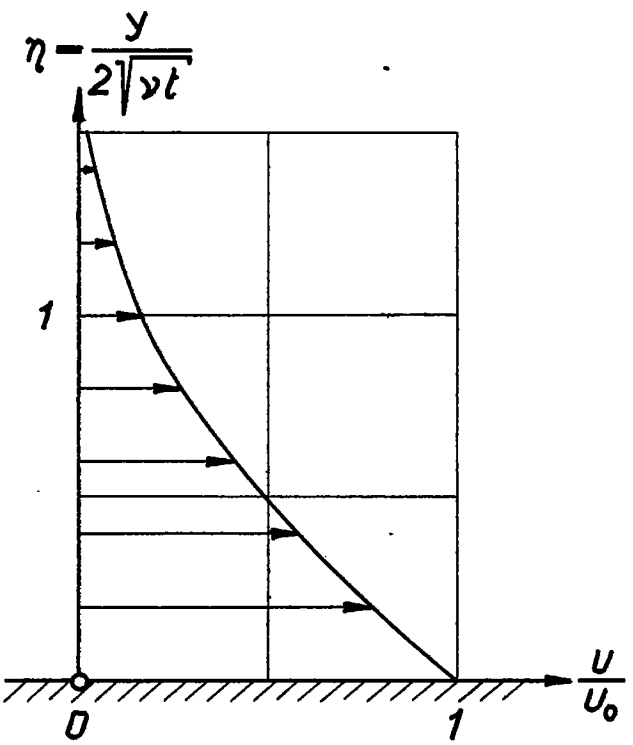

Figure 14.- Velocity distribution on a surface set suddenly in motion.

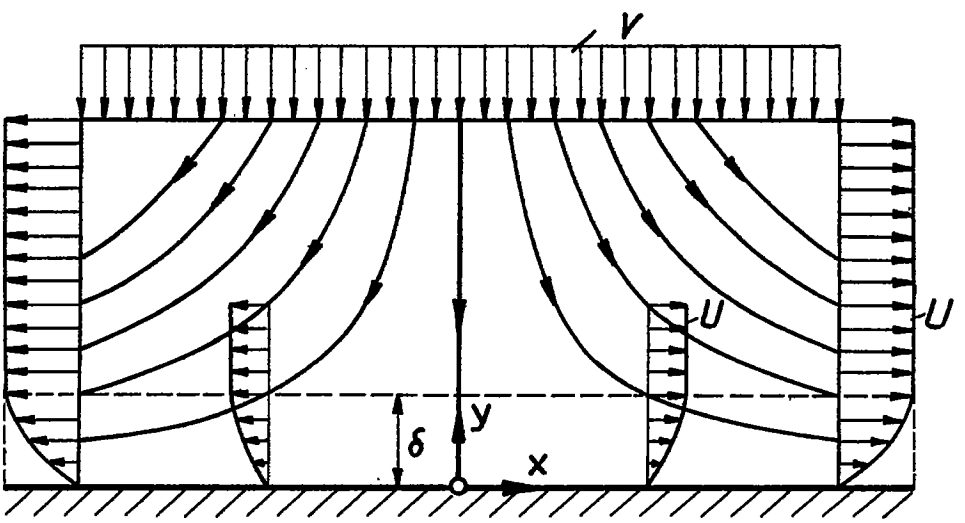

Figure 15.- The plane stagnation point flow.

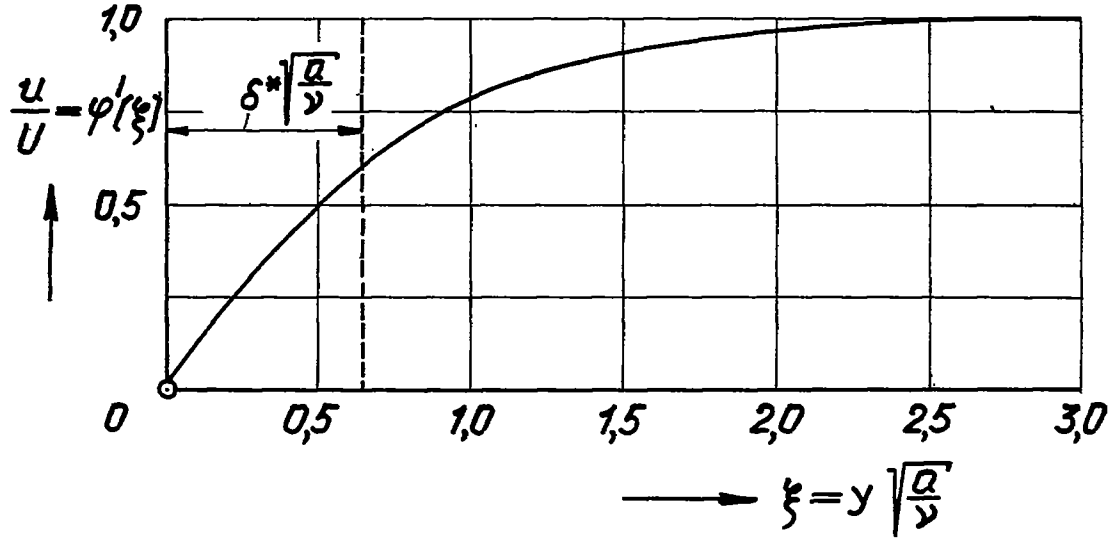

Figure 16.- The velocity profile of the plane stagnation point flow.

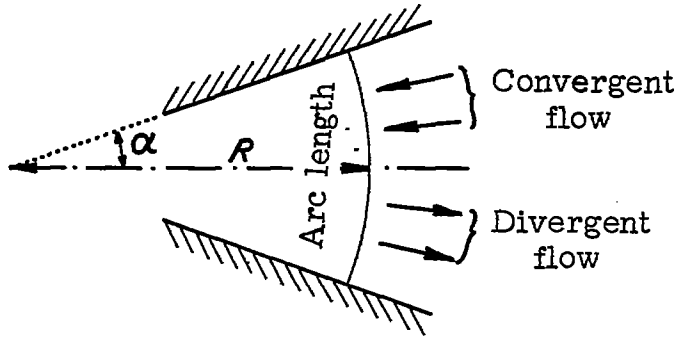

Figure 17.- The convergent and divergent channel.

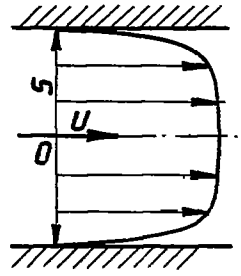

Figure 18.- Velocity distribution in the convergent channel.

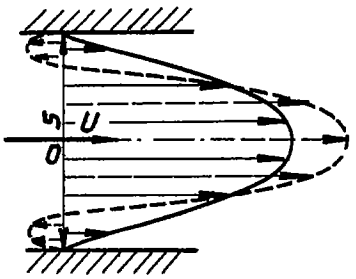

Figure 19.- Velocity distribution in the divergent channel.

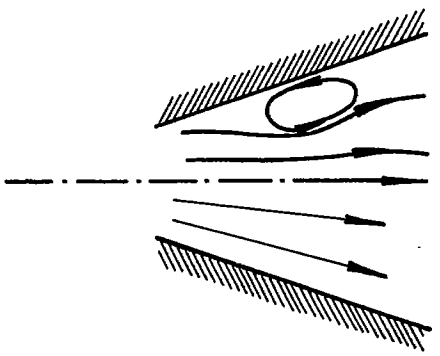

Figure 20.- Separation in the divergent channel.

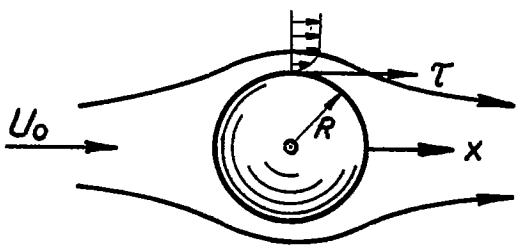

Figure 21.- Viscous flow around a sphere.

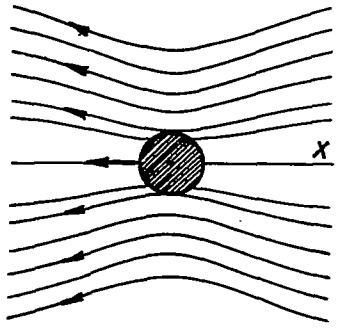

Figure 22.- Streamline pattern of the viscous flow around a sphere (according to Stokes).

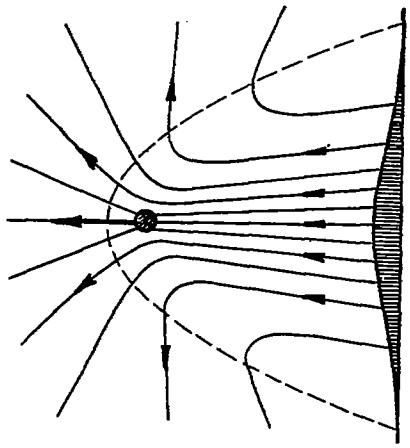

Figure 23.- Streamline pattern of the viscous flow around a sphere (according to Oseen).

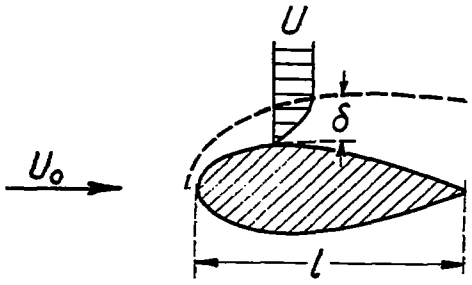

Figure 24.- Concerning Prandtl's boundary-layer equation. (Boundary-layer thickness δ magnified.)

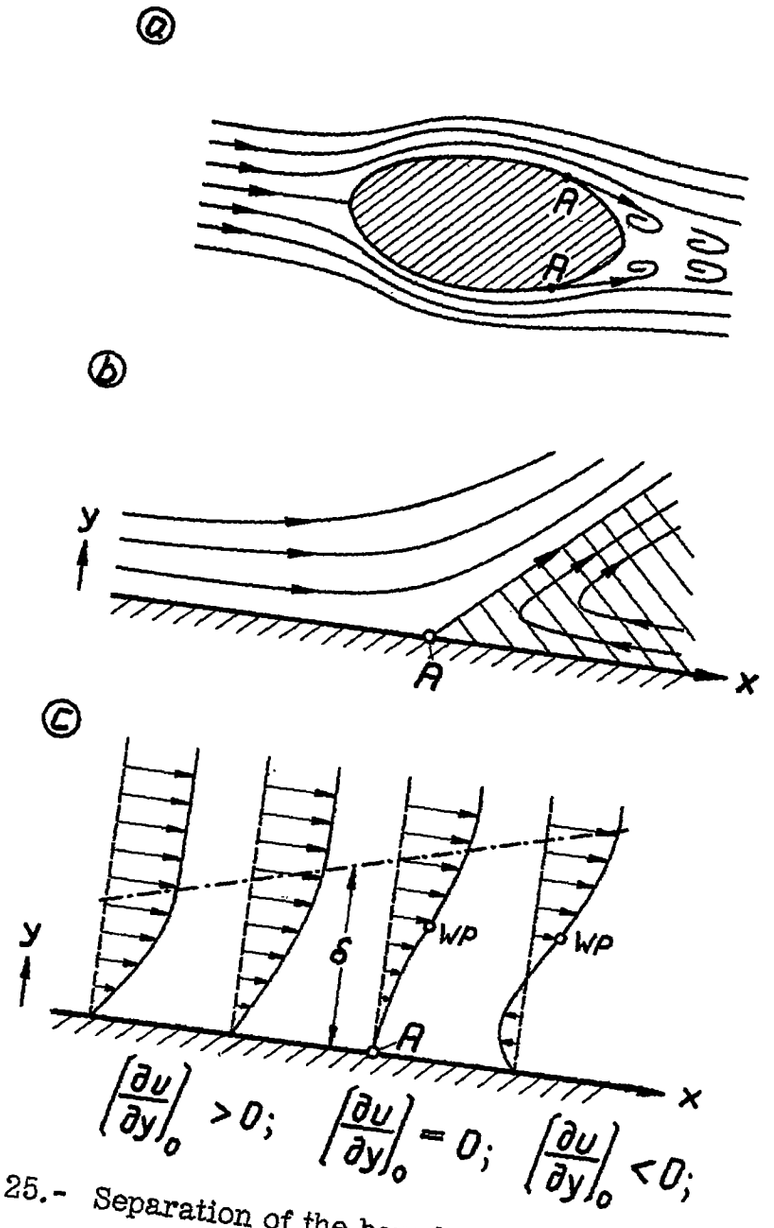

Figure 25.- Separation of the boundary layer. (A = point of separation.)

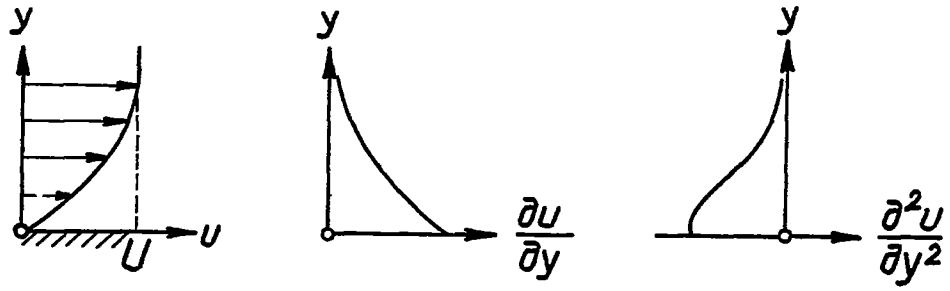

Figure 26.- Velocity distribution in the boundary layer for pressure decrease $\left(\frac{dp}{dx} < 0\right)$.

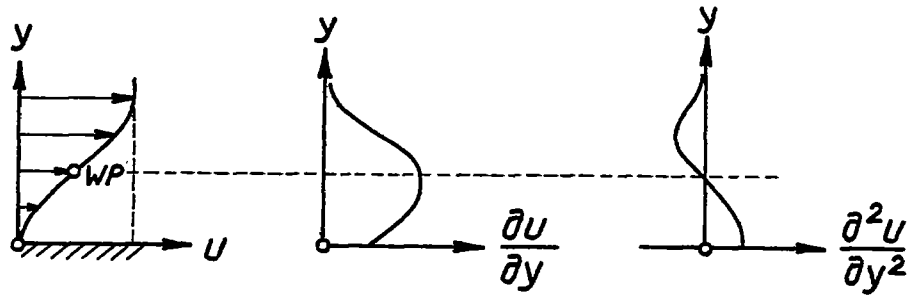

Figure 27.- Velocity distribution in the boundary layer for pressure increase $\left(\frac{dp}{dx} > 0\right)$.

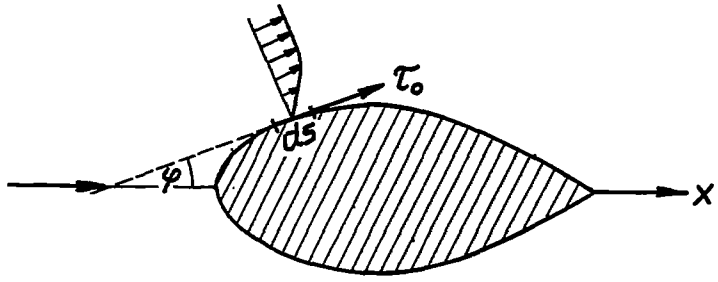

Figure 28.- Concerning the calculation of the friction drag.

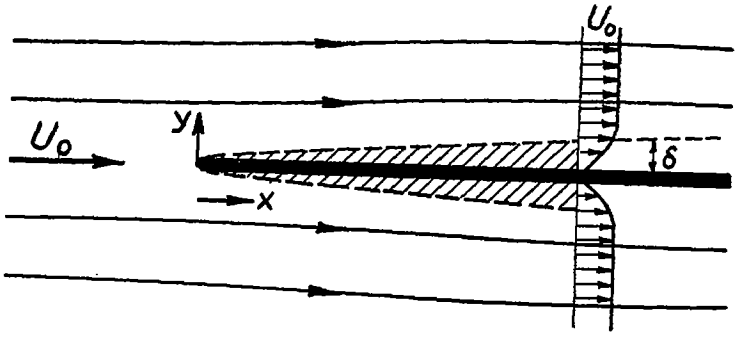

Figure 29.- The boundary layer on the flat plate in longitudinal flow.

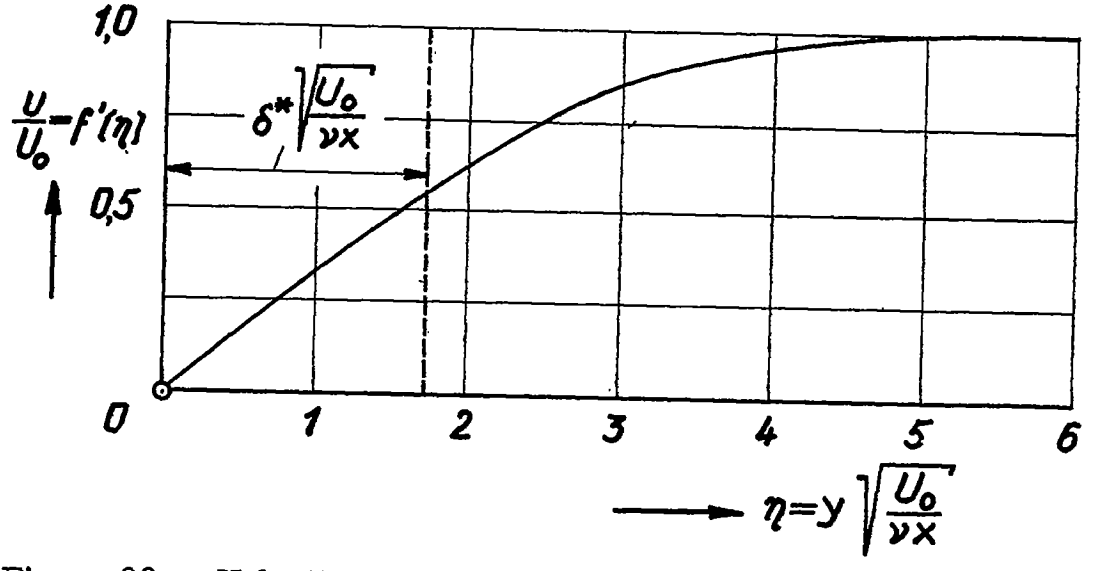

Figure 30.- Velocity distribution u(x,y) in the boundary layer on the flat plate (according to Blasius).

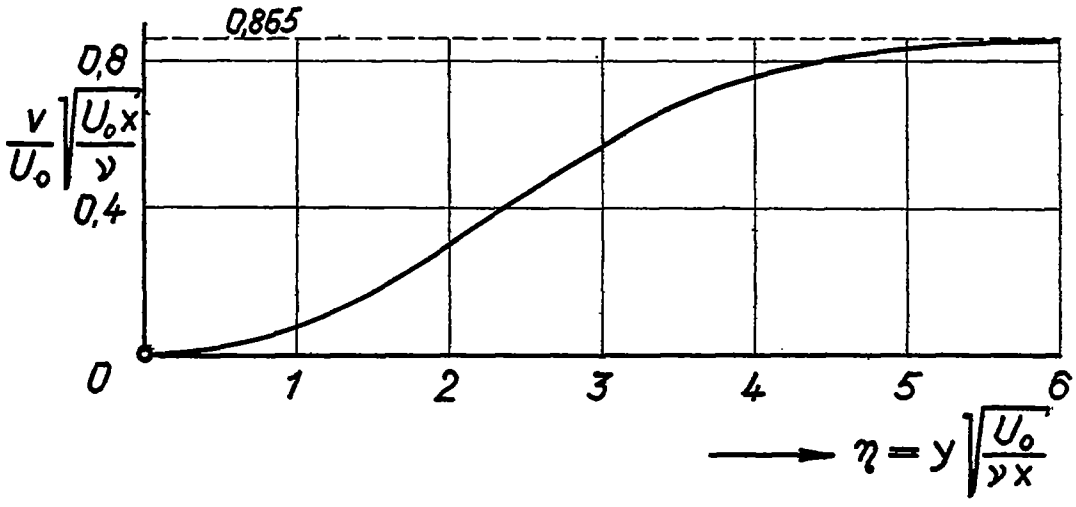

Figure 31.- The transverse velocity v(x,y) in the boundary layer on the flat plate.

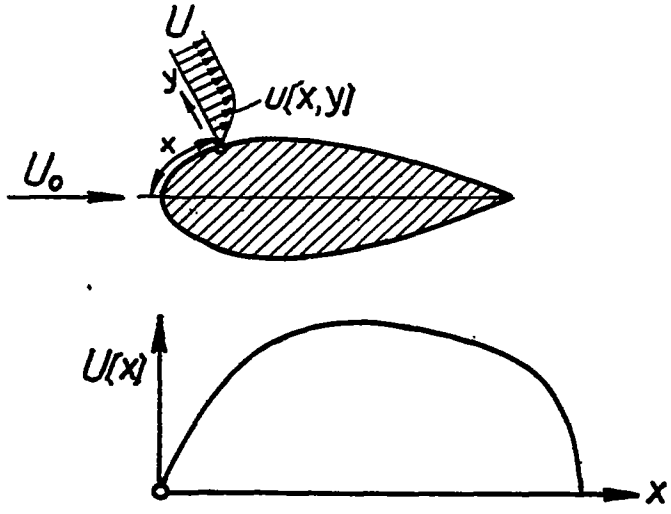

Figure 32.- The boundary layer on a cylindrical body of arbitrary cross section (symmetrical case).

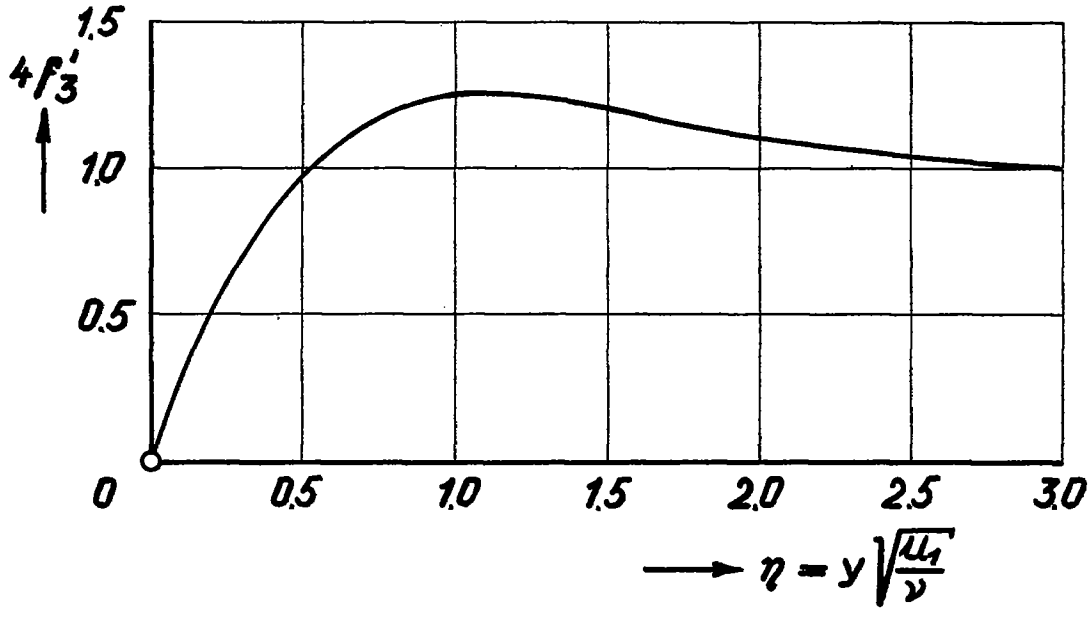

Figure 33.- The function f_3' of the velocity distribution in the boundary layer.

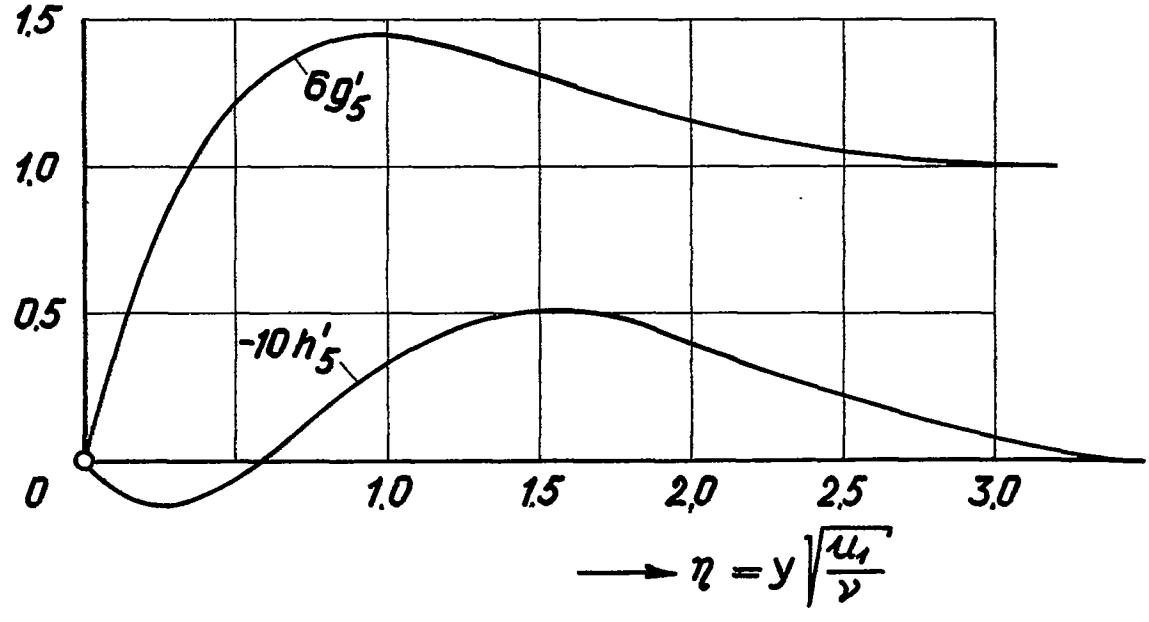

Figure 34.- The functions g_5' and h_5' of the velocity distribution in the boundary layer.

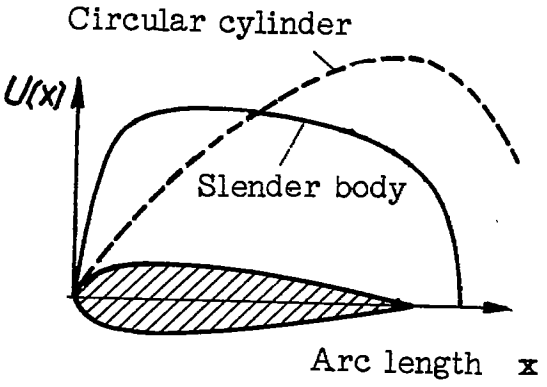

Figure 35.- Velocity distribution of the potential flow for a wing profile.

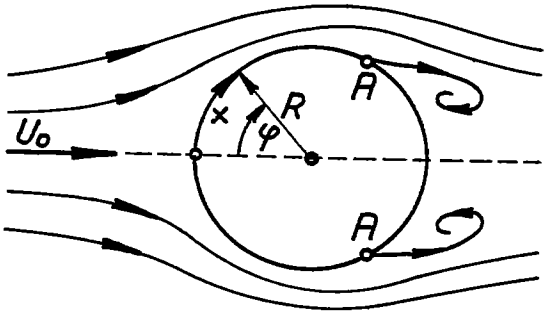

Figure 36.- Concerning the calculation of the friction layer on the circular cylinder.

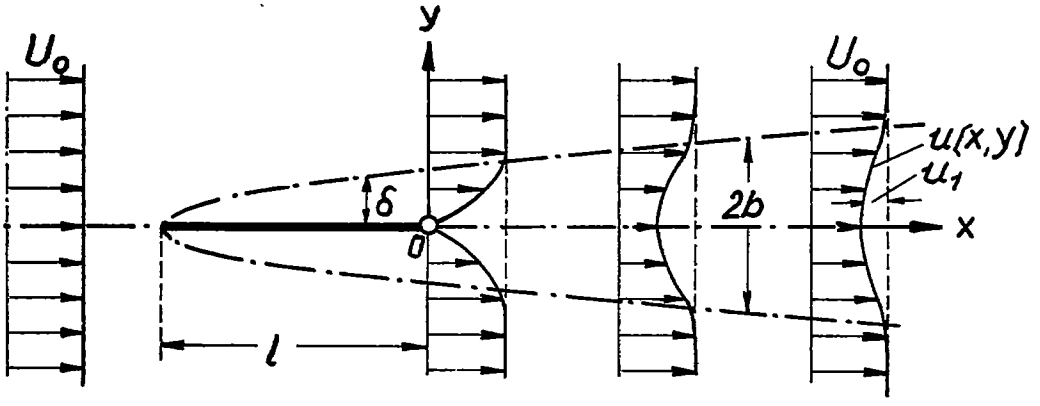

Figure 37.- Wake flow behind the flat plate in longitudinal flow.

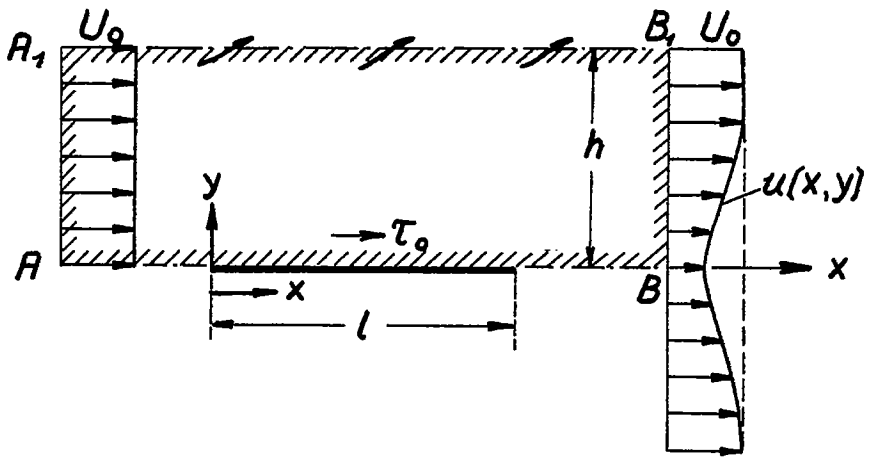

Figure 38.- Concerning application of the momentum theorem for the flat plate in longitudinal flow.

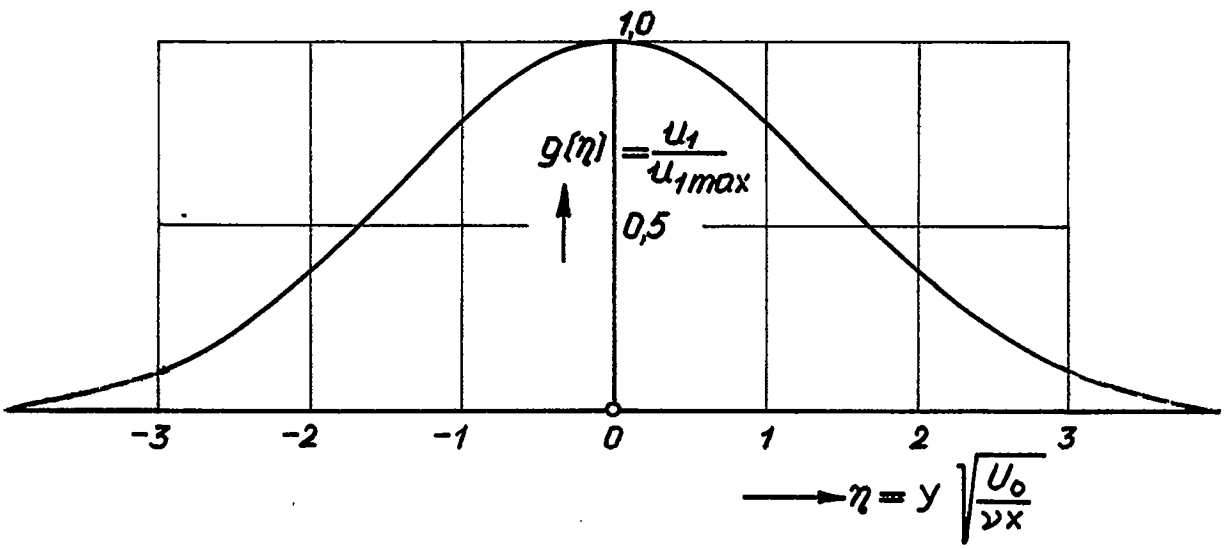

Figure 39.- Asymptotic velocity distribution in the wake behind the flat plate in longitudinal flow.

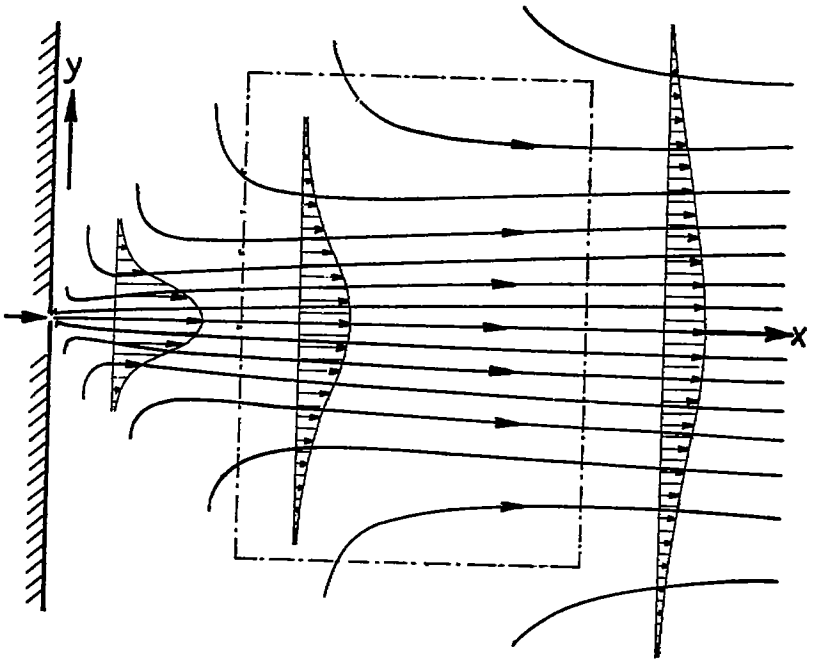

Figure 40.- Streamline pattern and velocity distribution of the plane jet.

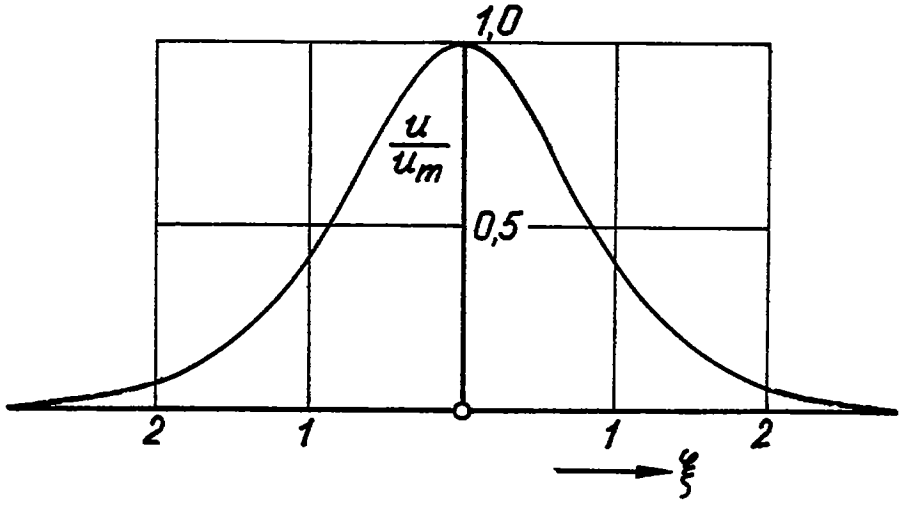

Figure 41.- The velocity profile of the plane jet.

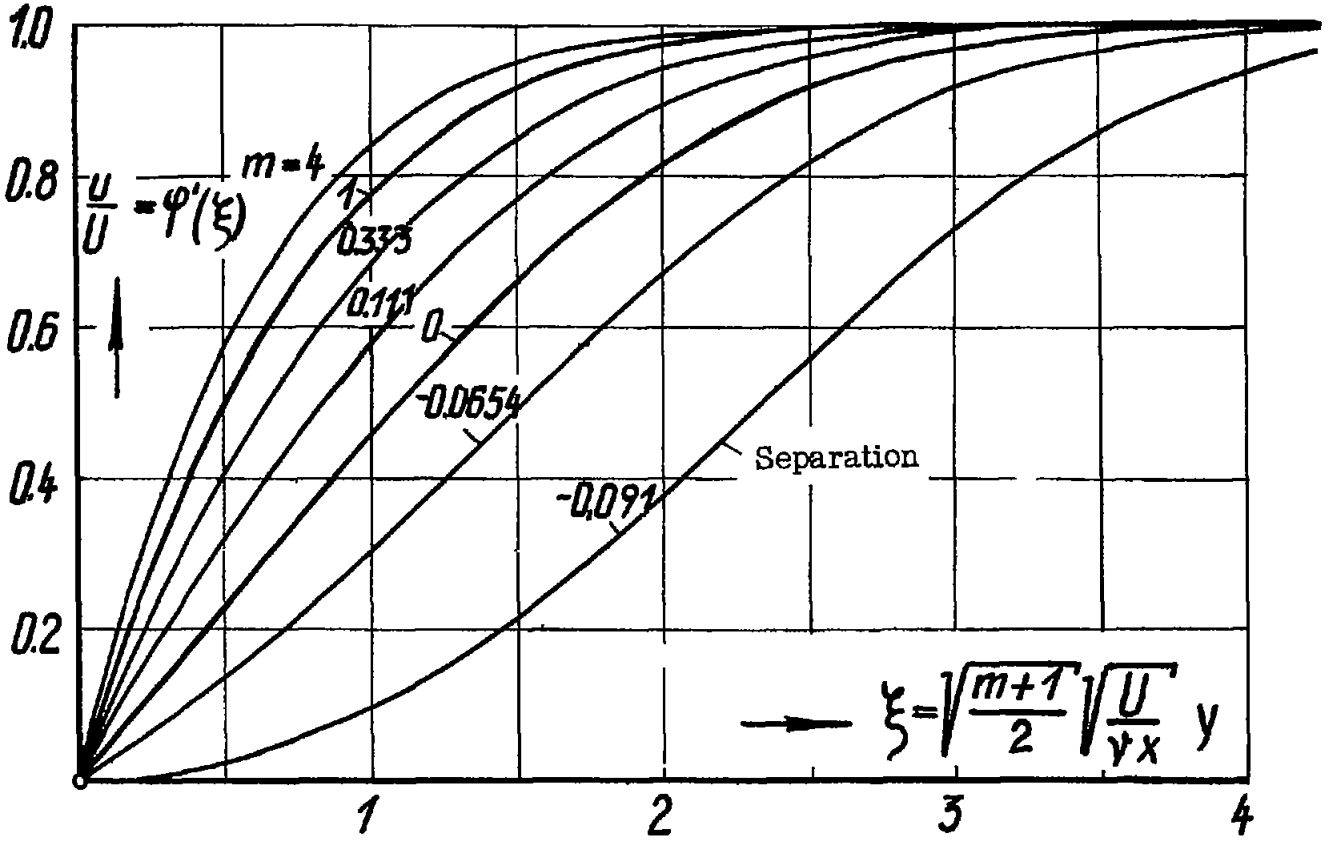

Figure 41(a).- Boundary-layer profiles for the potential flow $U(x) = u_1 x^m$.

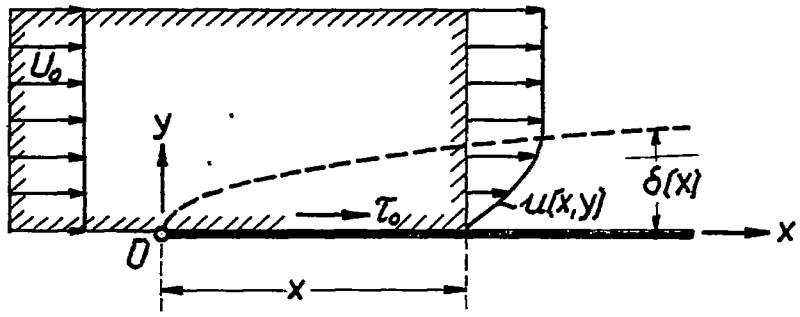

Figure 42.- Application of the momentum theorem for the flat plate in longitudinal flow.

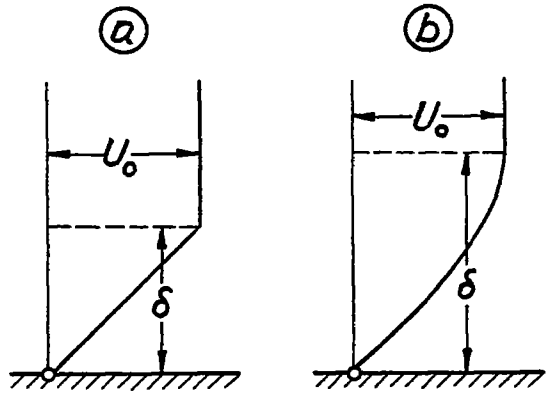

Figure 43.- Velocity distribution in the boundary layer on the flat plate in longitudinal flow.

(a) Linear approximation.

(b) Cubic approximation for the velocity profile.

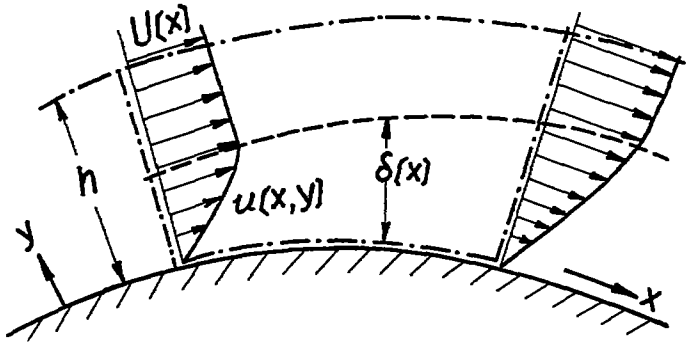

Figure 44.- Application of the momentum theorem to the boundary layer with pressure gradient.

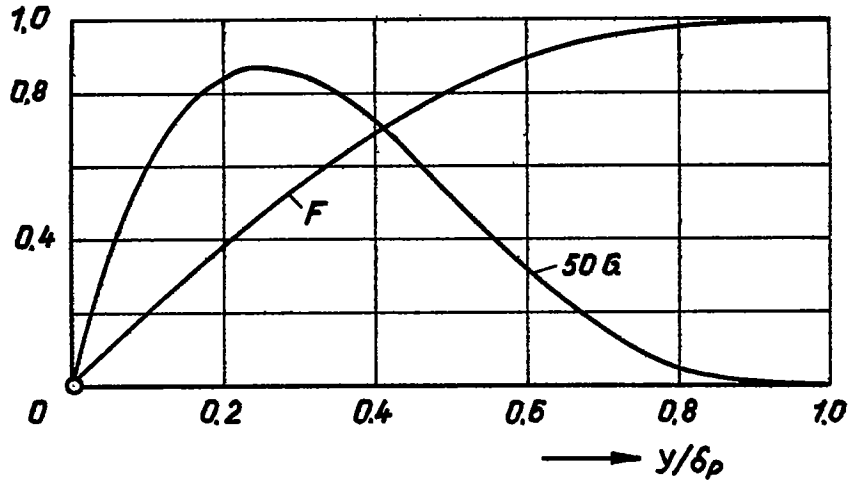

Figure 45.- The universal functions $F(y/\delta_p)$ and $G(y/\delta_p)$ for the velocity distribution in the boundary layer according to Pohlhausen.

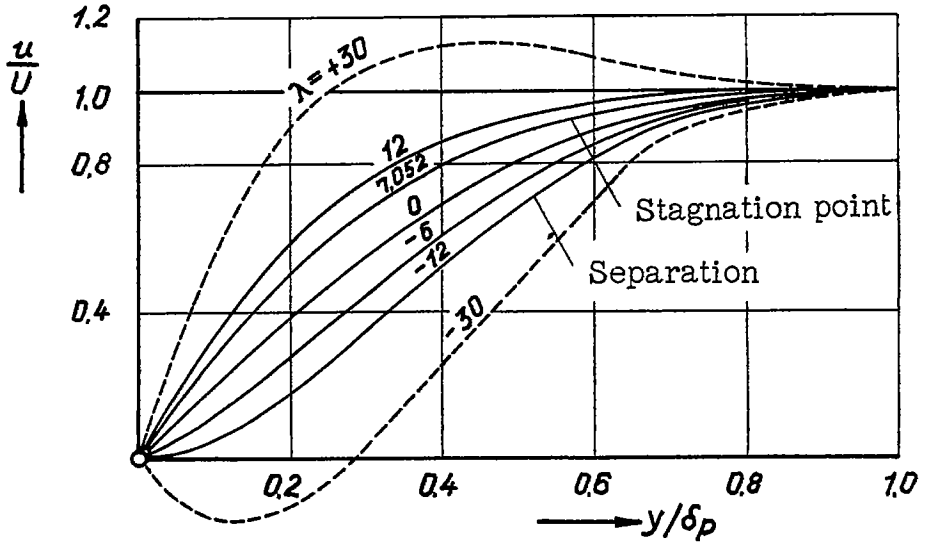

Figure 46.- The one-parameter family of velocity profiles according to Pohlhausen.

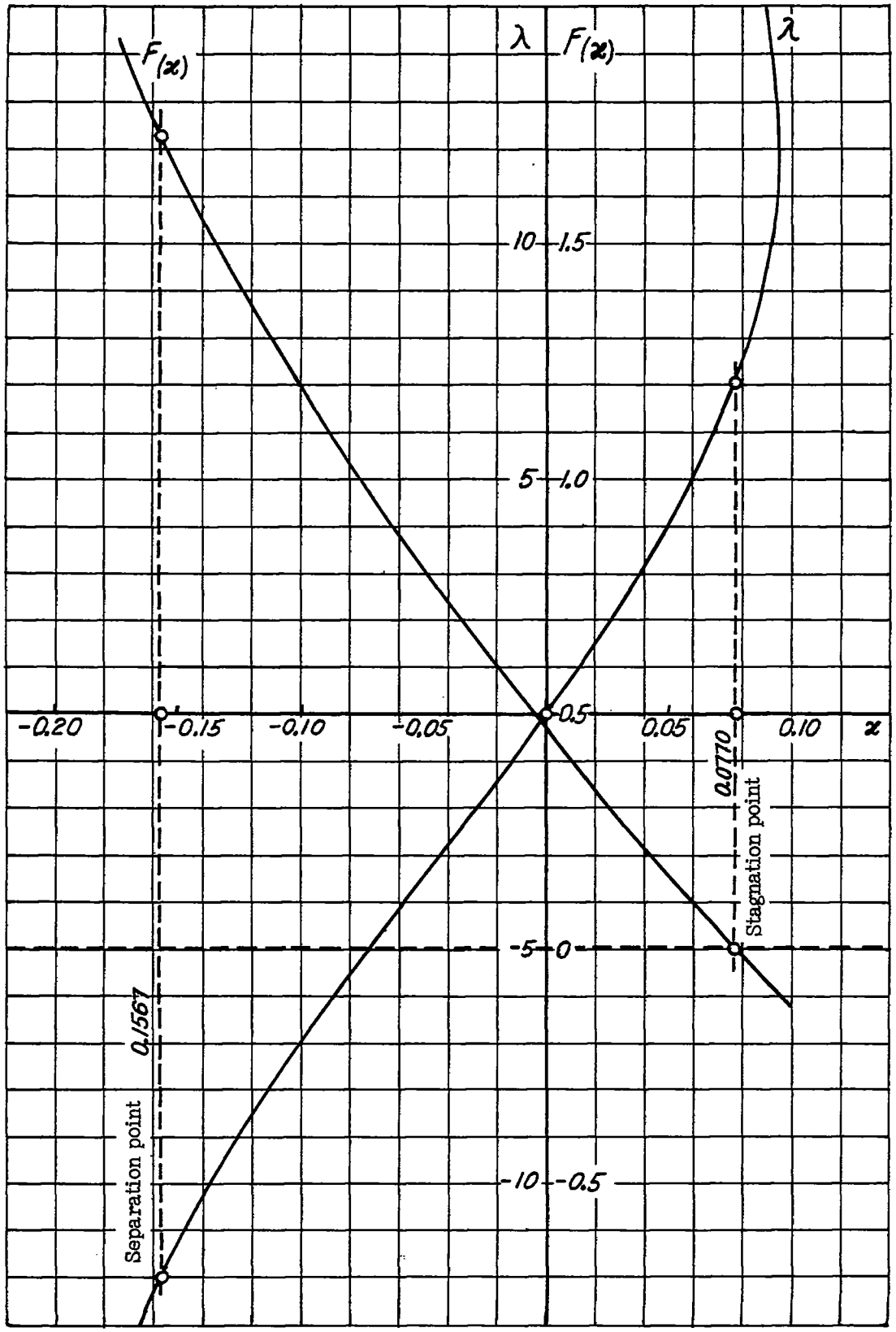

Figure 47(a).- Auxiliary functions of the boundary layer calculation according to Holstein (cf. table 5); λ and $F(\kappa)$ against κ.

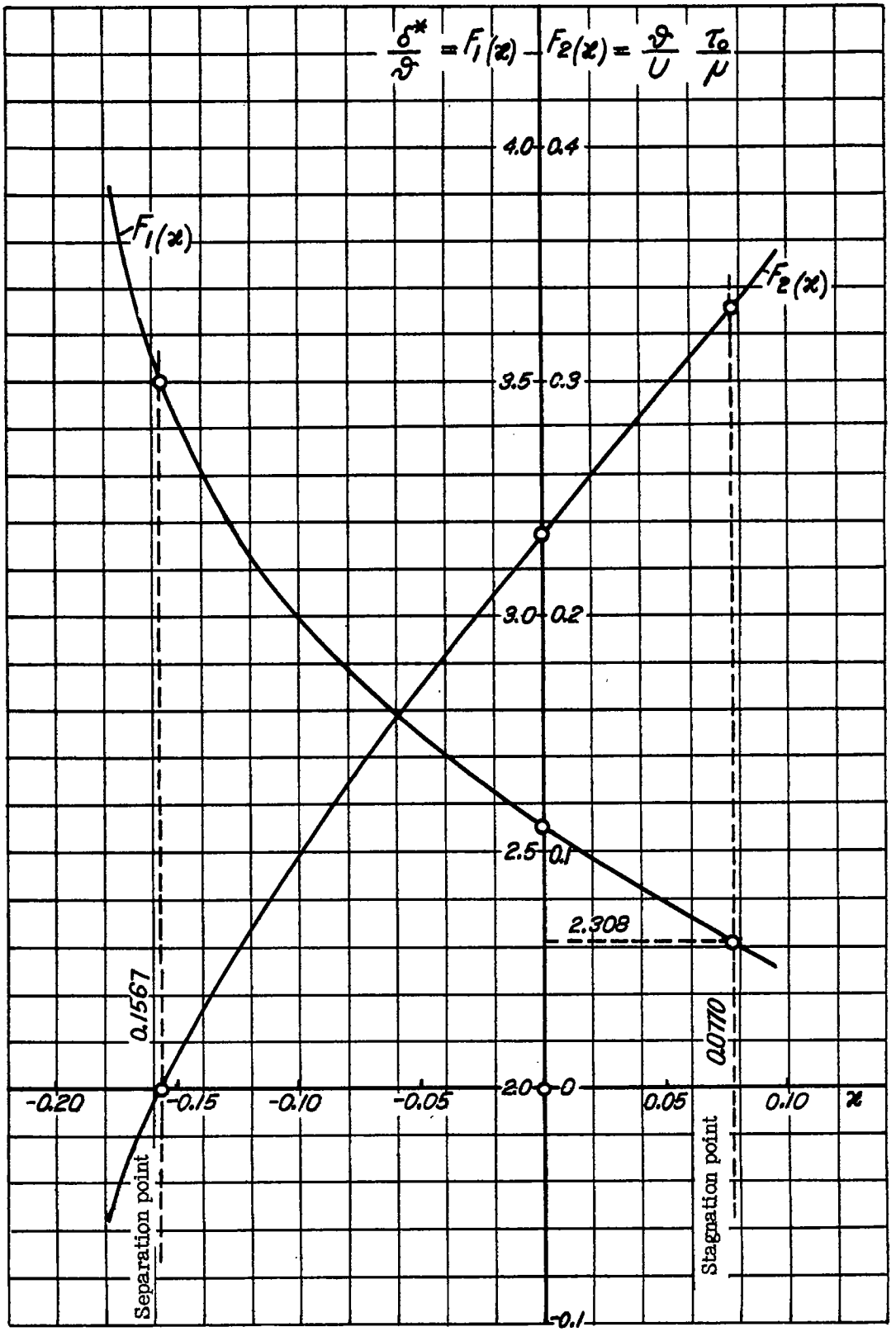

Figure 47(b).- Auxiliary functions for the boundary layer calculation according to Holstein (cf. table 5); $f_1(\kappa)$ and $f_2(\kappa)$ against κ.

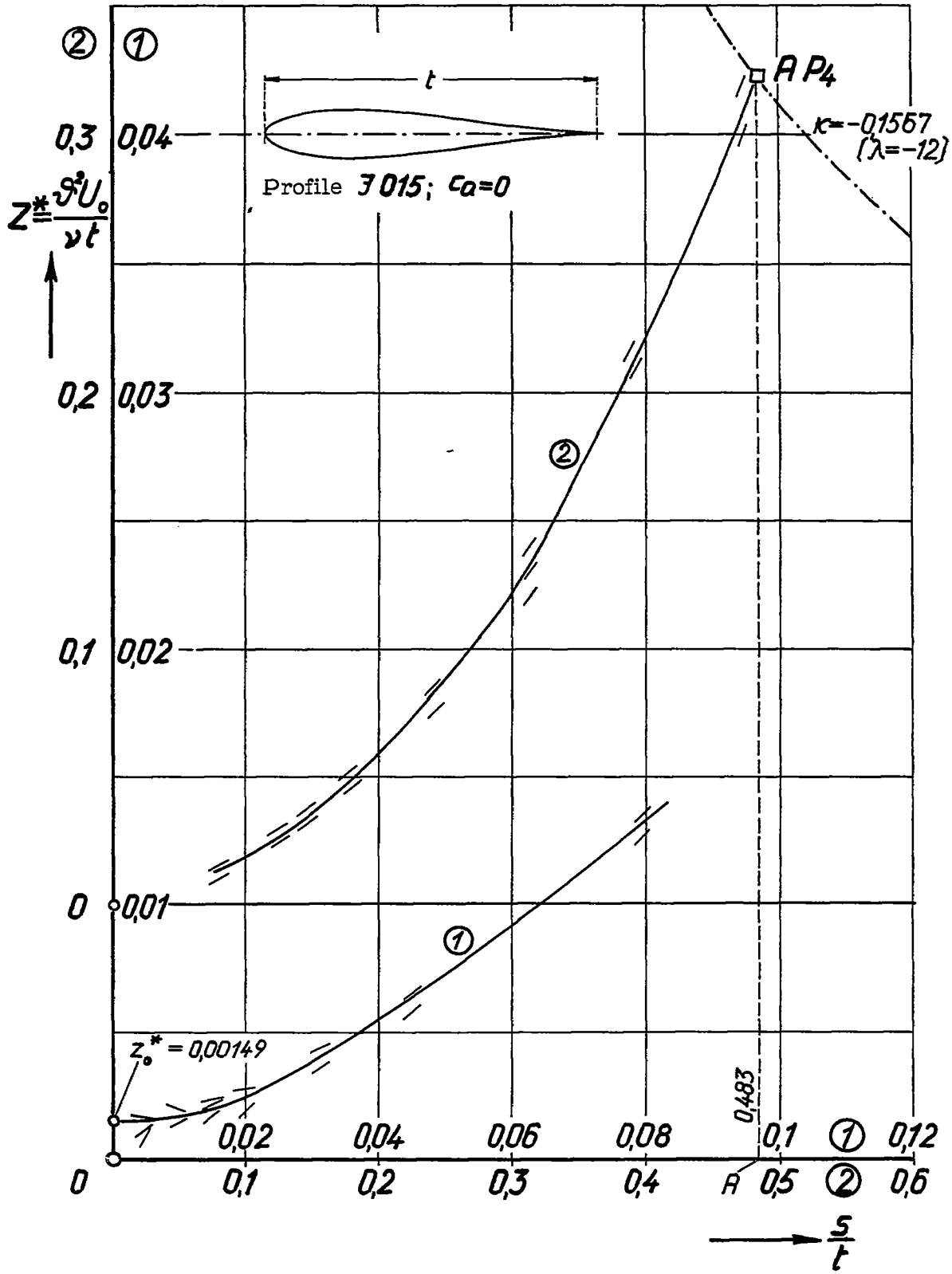

Figure 48.- Integration of the differential equation of the boundary layer according to Pohlhausen and Holstein (profile J 015; $c_a = 0$).

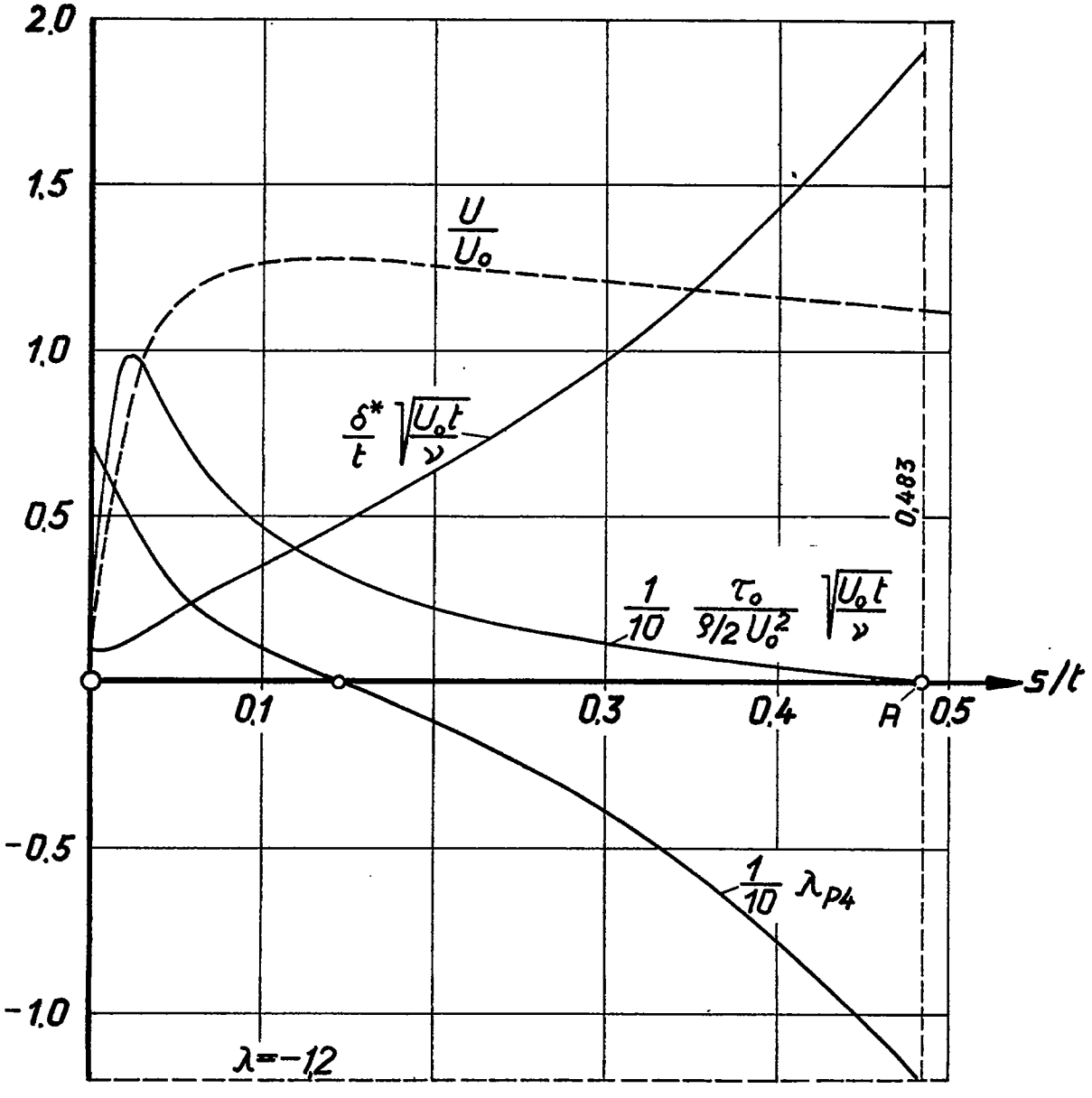

Joukowsky profile d/t = 0.15

Figure 49.- Result of the boundary-layer calculation for the example according to figure 48 (profile J 015; $c_a = 0$).

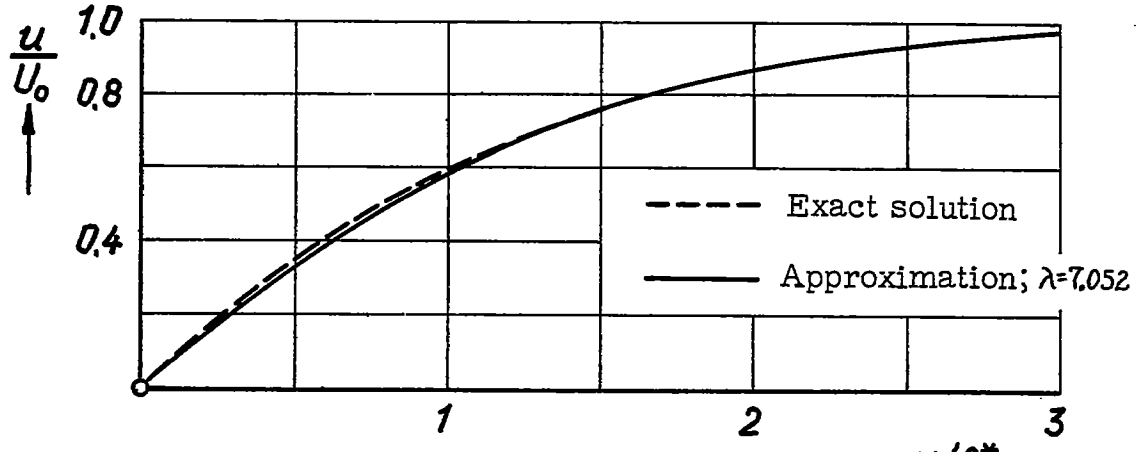

a) Stagnation point profile

$U = u_1 x$

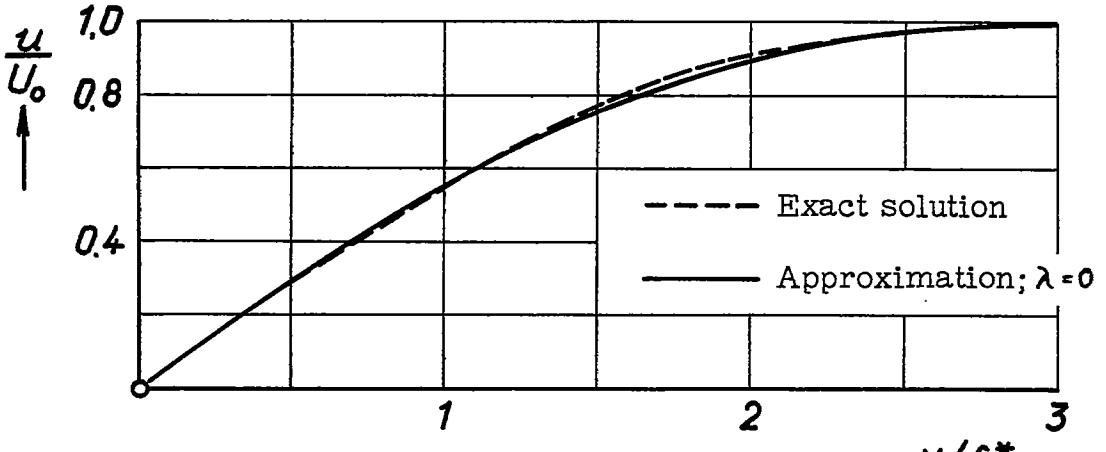

b) Plate profile

$U = U_0$

Figure 50.- Comparison of the approximate calculation according to Pohlhausen with the exact solution.

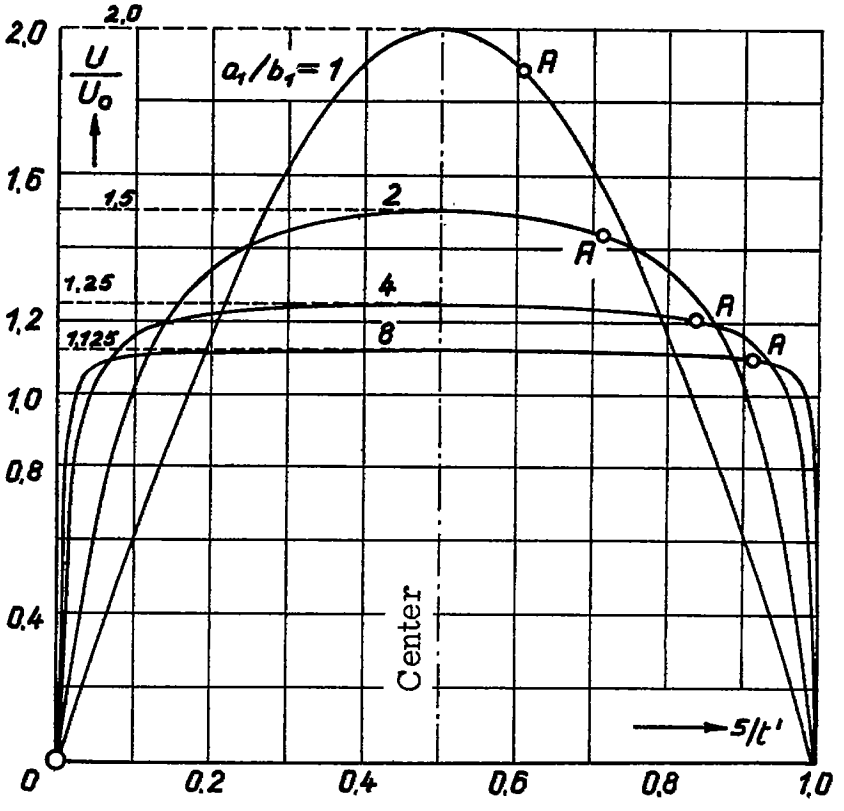

Figure 51.- Potential-theoretical velocity distribution on the elliptic cylinders with axis ratio a_1/b_1 = 1, 2, 4, 8 for flow parallel to the major axis (A = laminar separation point), t′ = half the circumference.

P R E F A C E

I gave the lecture series "Boundary-Layer Theory" in the winter semester 1941/42 for the members of my Institute and for a considerable number of collaborators from the Hermann Göring Institute for Aviation Research. The series embraced a total of sixteen two-hour lectures.

The aim of the lecture series was to give a survey of the more recent results of the theory of viscous fluids as far as they are of importance for actual applications. Naturally the theory of the boundary of frictional layer takes up the greatest part. In view of the great volume of material, a complete treatment was out of the question. However, I took pains to make concepts everywhere stand out clearly. Moreover, several important typical examples were treated in detail.

Dr. H. Hahnemann (LFA, Institute for Motor Research) went to considerable trouble in order to perfect an elaboration of this lecture series which I examimed and supplemented in a few places. Miss Hildegard Münz participated in the illustration. To both I owe my most sincere thanks for this collaboration.

Schlichting

Aerodynamisches Institut
der Technischen Hochschule, Braunschweig
October 1942.

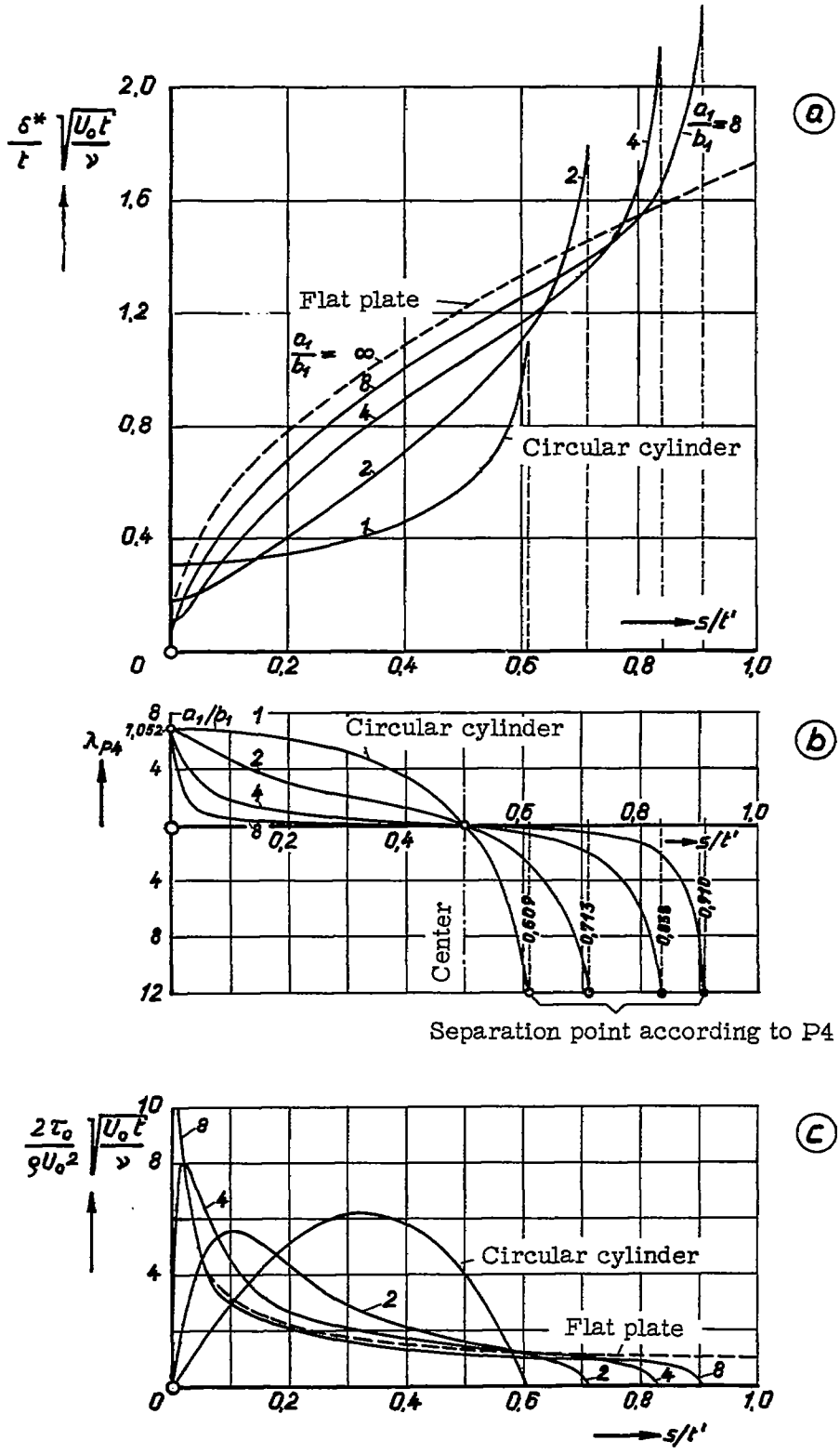

Figure 52.- Result of the boundary-layer calculation for the elliptic cylinders of axis ratio $a_1/b_1 = 1, 2, 4, 8$.

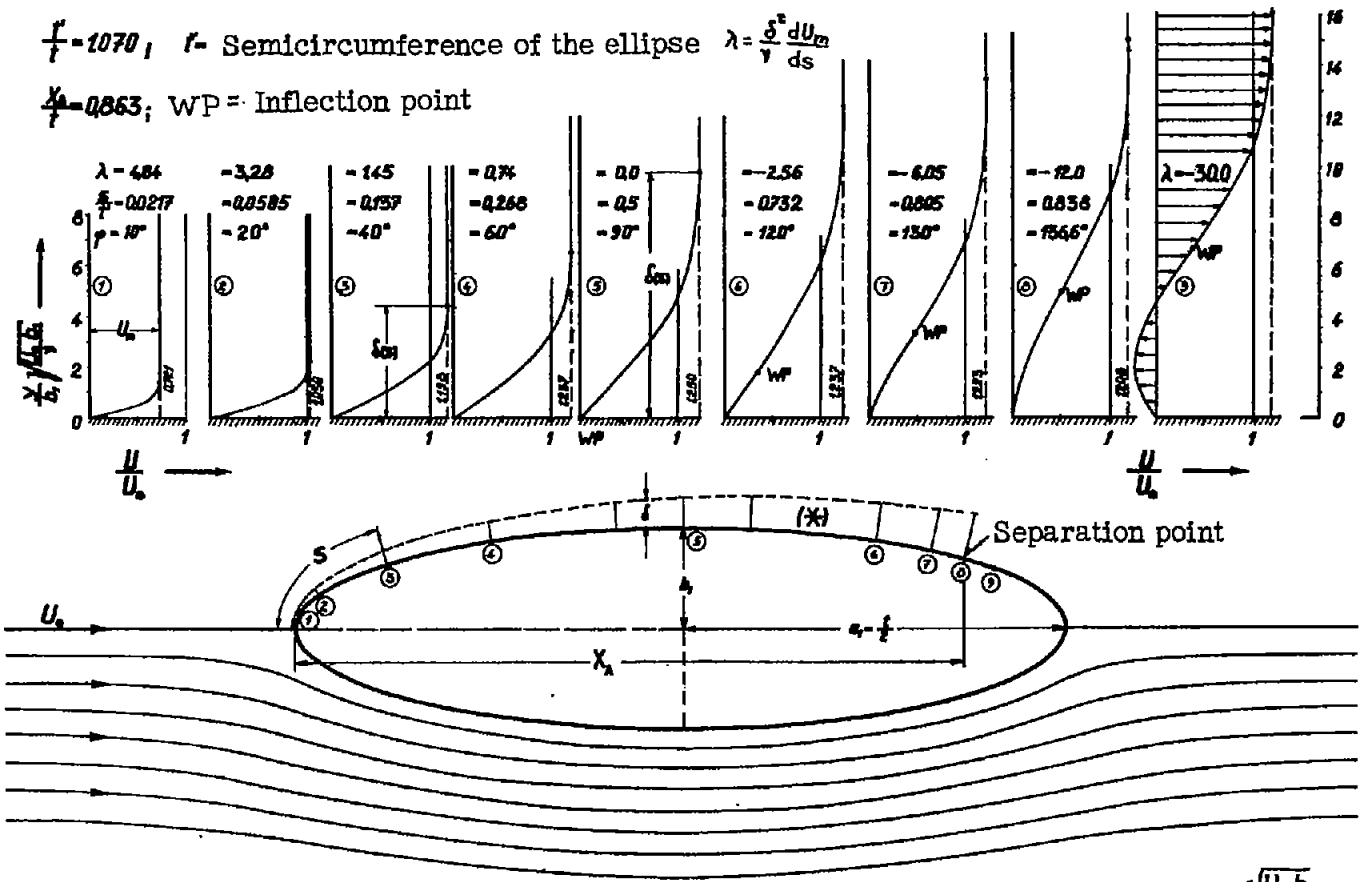

Friction layer calculated according to Pohlhausen P_4, ZAMM 1921 (*) Boundary layer is $\frac{1}{35}\sqrt{\frac{U_0 b_1}{\nu}}$ fold increased

Figure 53.- Potential flow and laminar friction layer on the elliptic cylinder of axis ratio $a_1/b_1 = 4$.

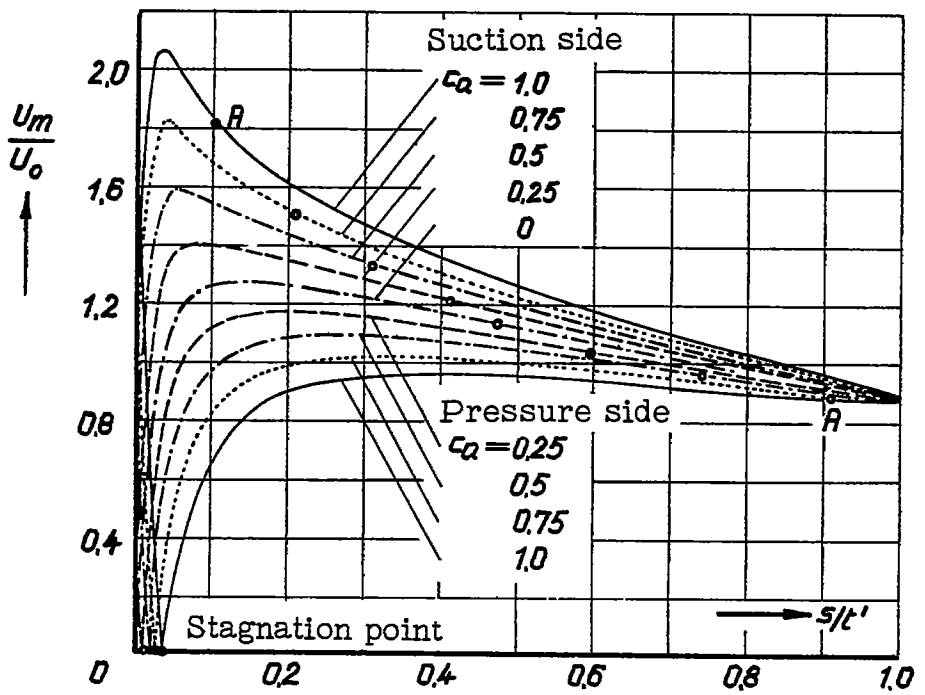

Figure 54.- Potential-theoretical velocity distribution for the Joukowsky profile J 015 for c_a = 0; 0.25; 0.50; 1.0.

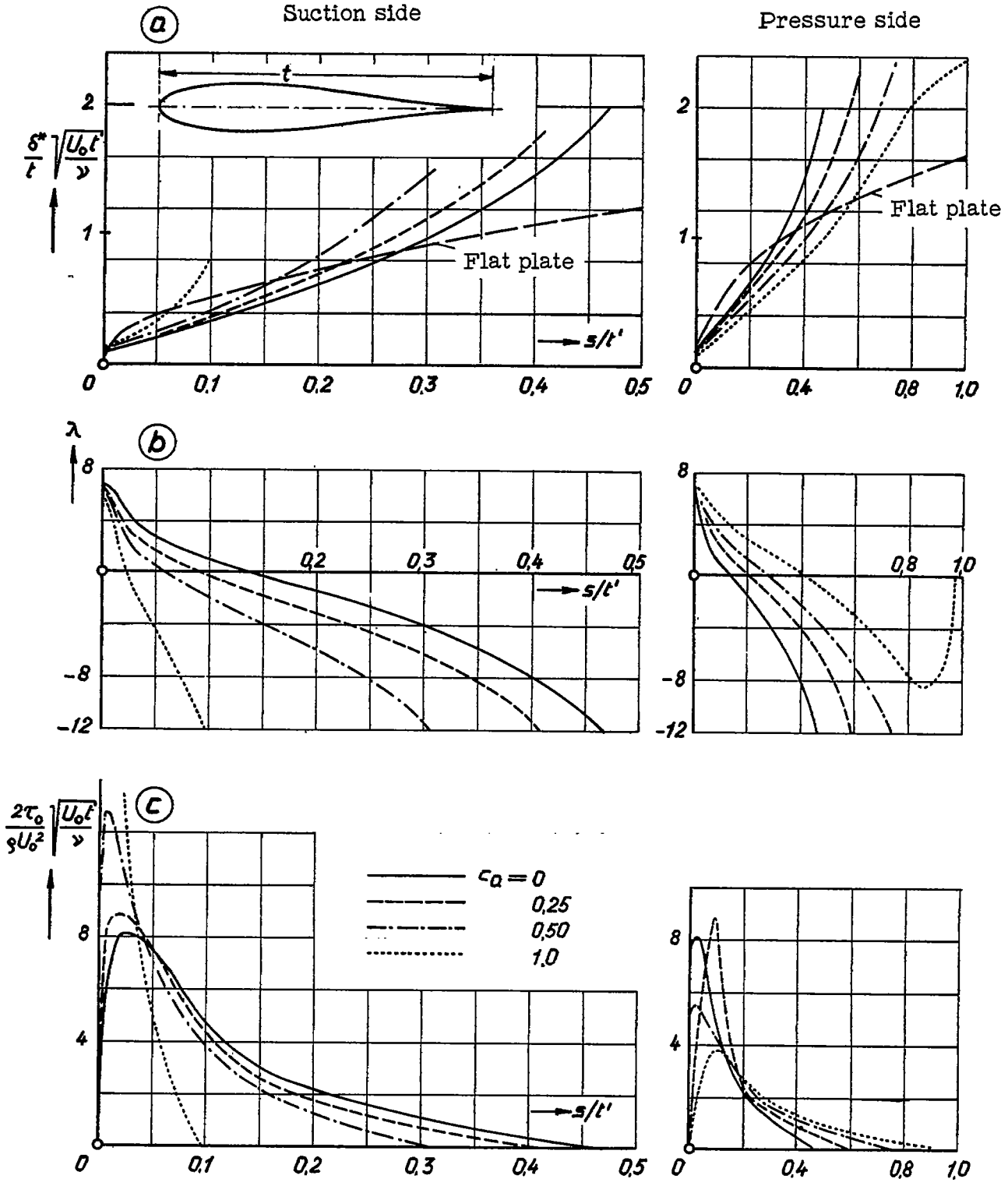

Figure 55.- Result of the boundary-layer calculation for the Joukowsky profile J 015 (t' = half the profile perimeter).

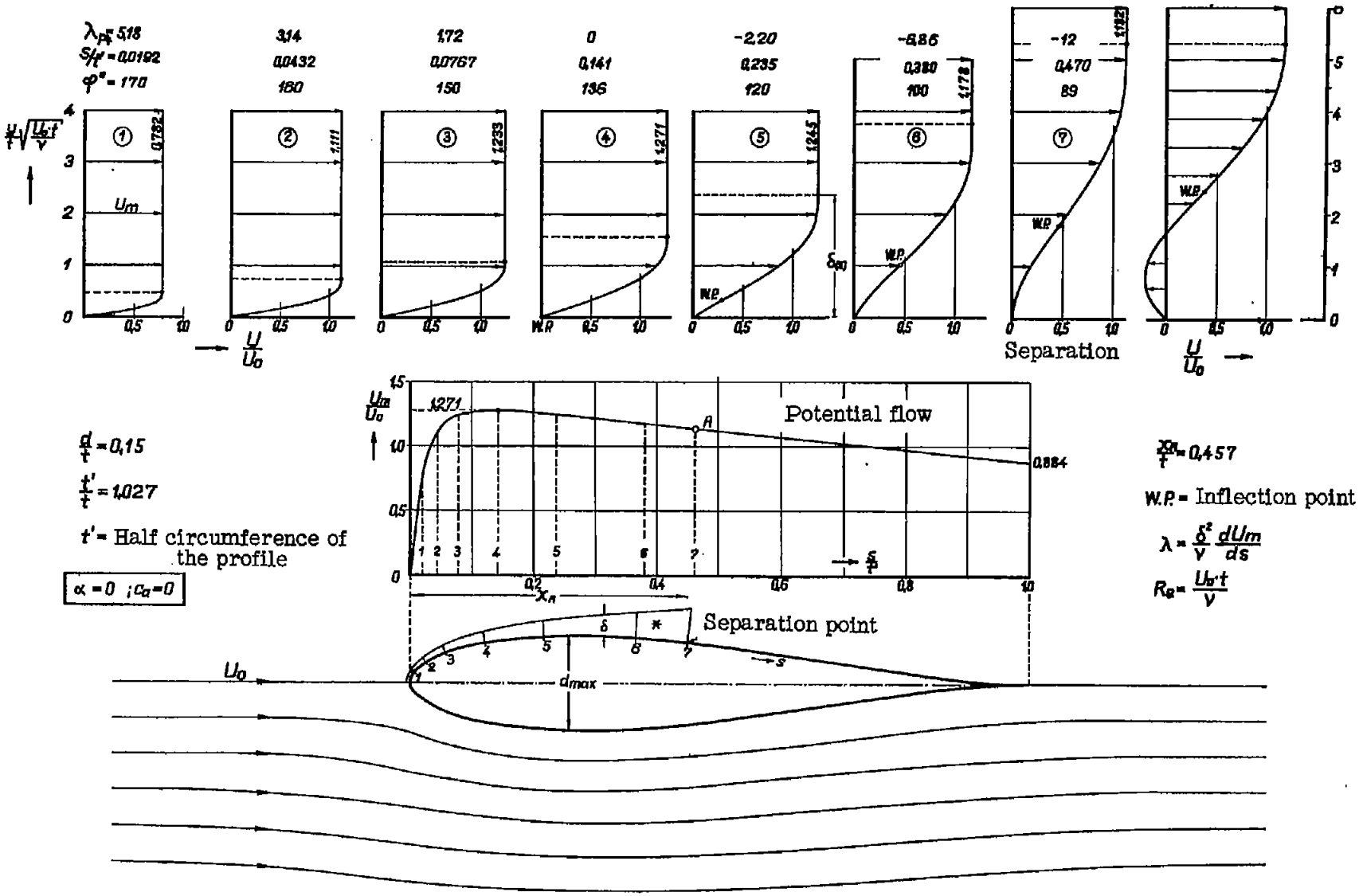

Figure 56.- Potential flow and laminar friction layer for the Joukowsky profile J 015 at $c_a = 0$.

*) The boundary-layer thickness is $\frac{1}{100}\sqrt{R_e}$ fold increased

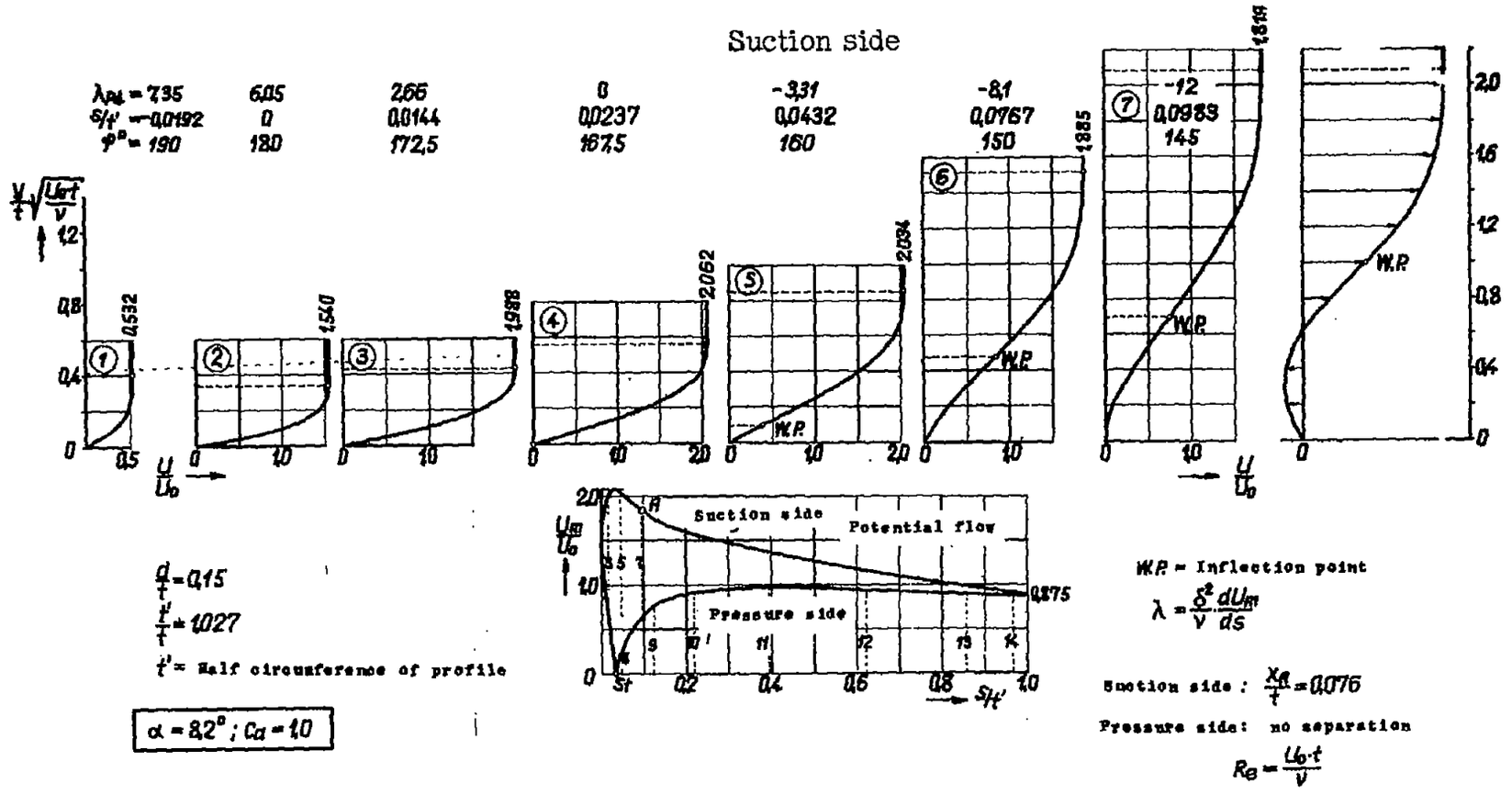

Figure 57.- Potential flow and laminar friction layer for the Joukowsky profile J 015 at $c_a = 1$.

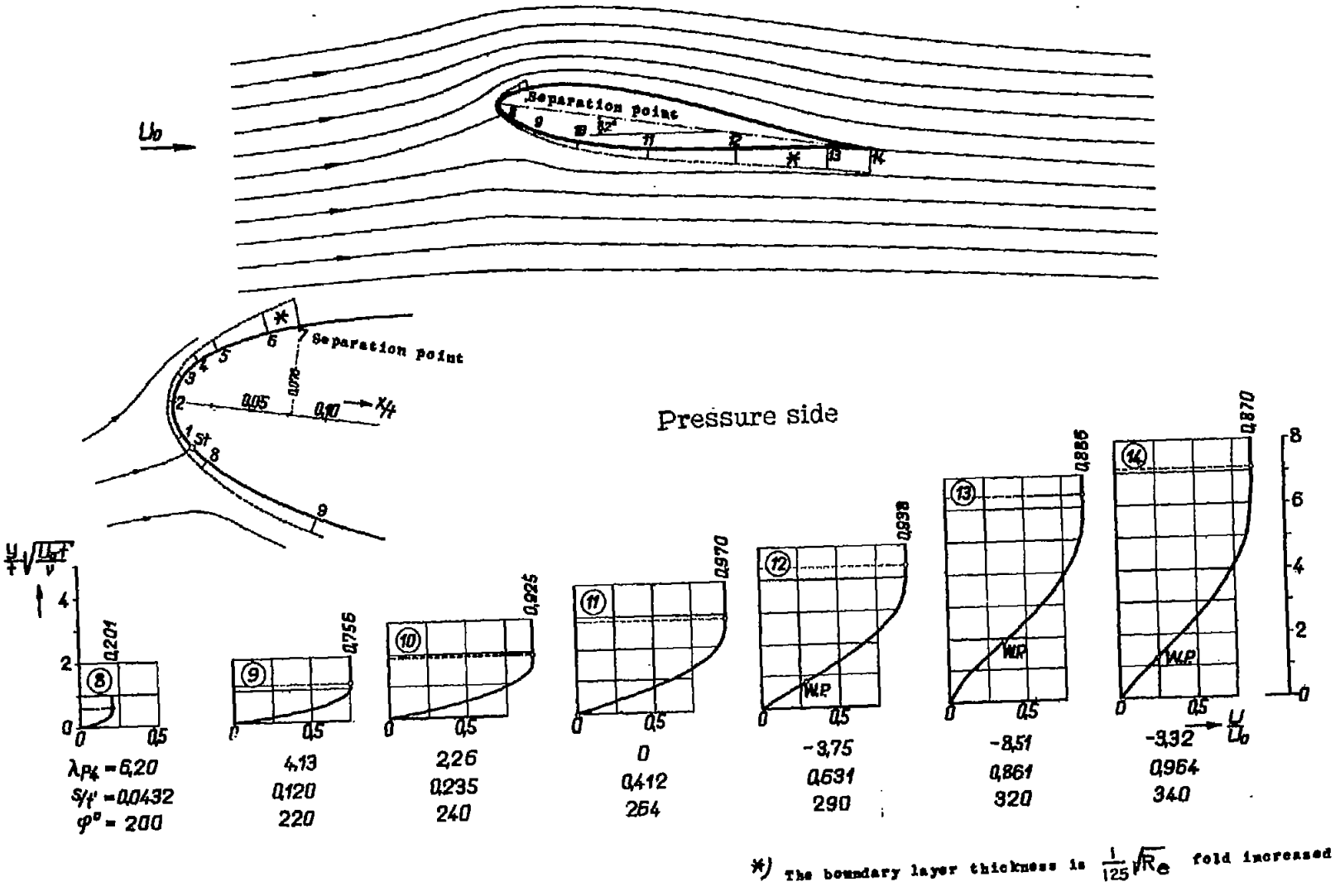

*) The boundary layer thickness is $\frac{1}{125}\sqrt{Re}$ fold increased

Figure 57.- Concluded.

Joukowsky profile

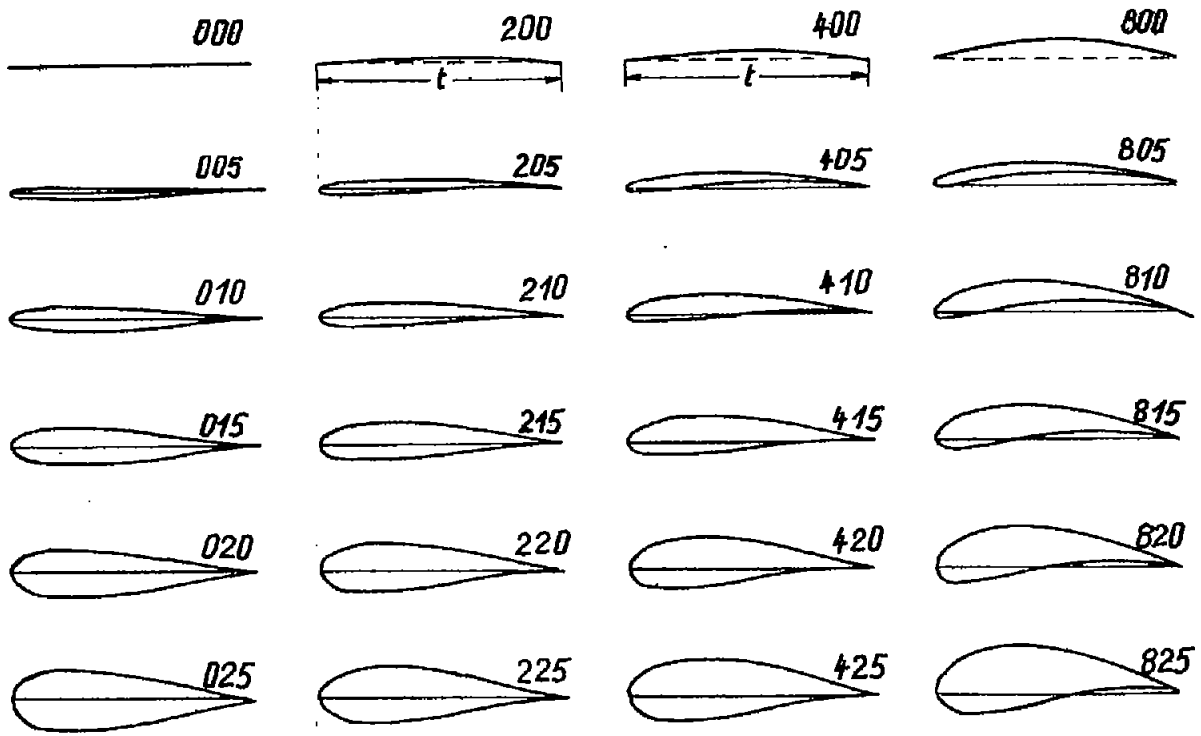

Figure 58.- Joukowsky profiles; thickness d/t = 0 to 0.25; camber f/t = 0 to 0.08.

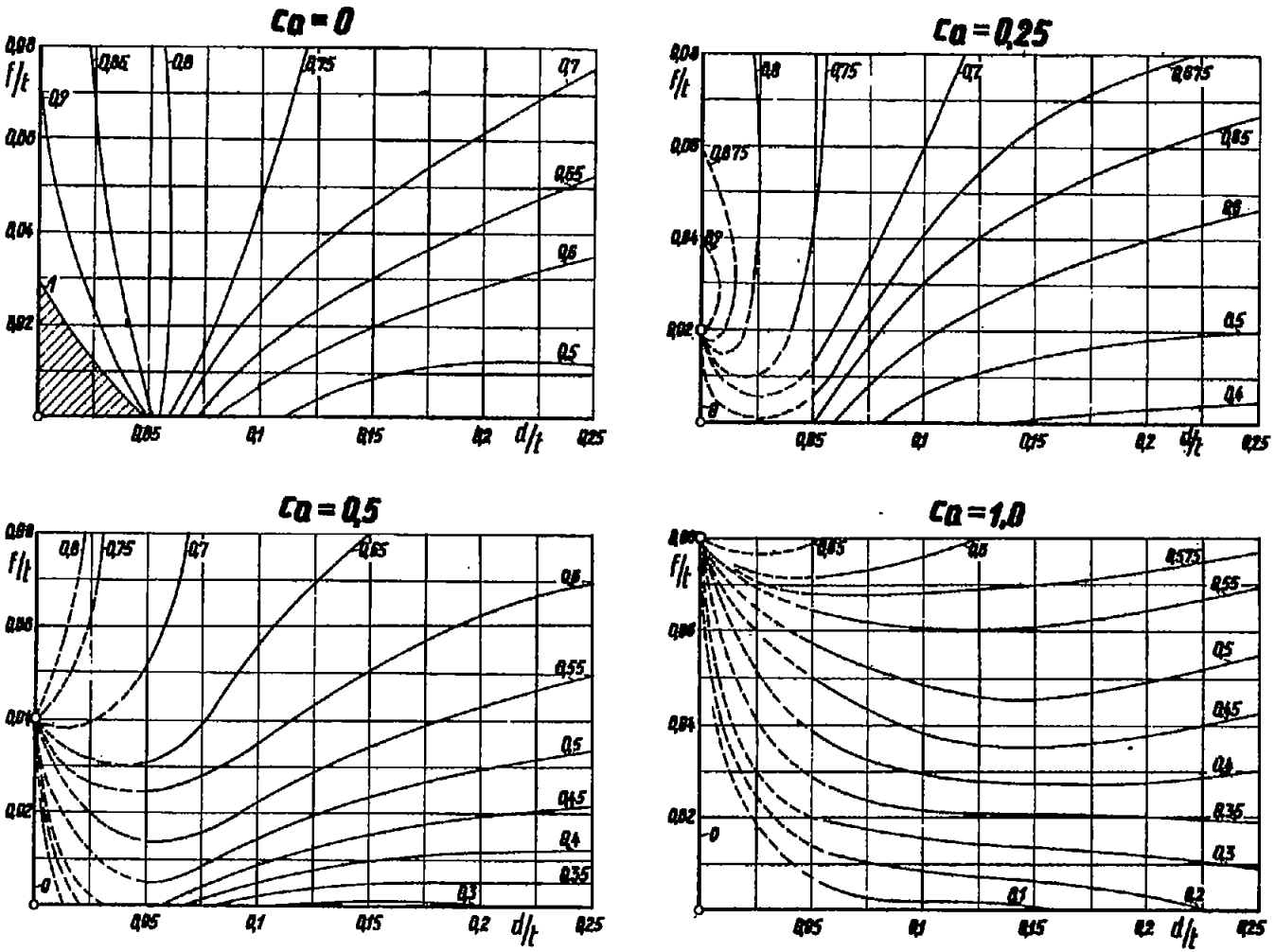

Figure 59.- Position of the laminar separation point for the Joukowsky profiles of figure 58; suction side.

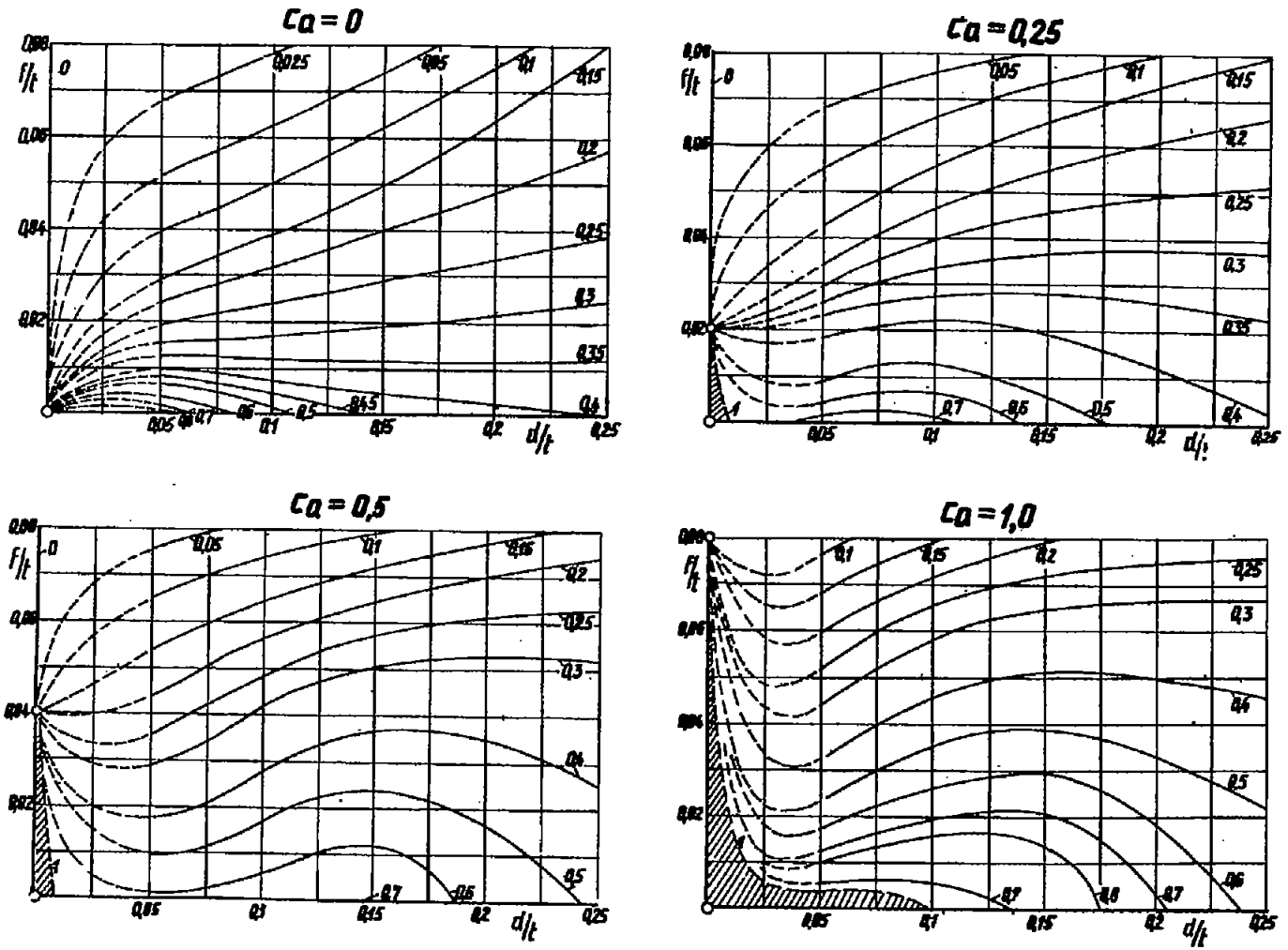

Figure 60.- Position of the laminar separation point for the Joukowsky profiles of figure 58; pressure side.

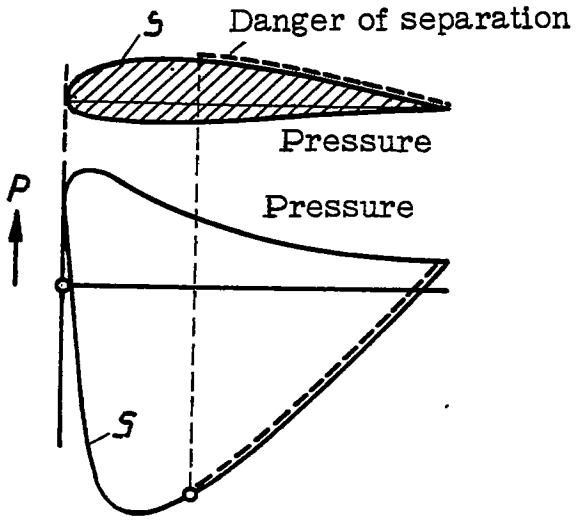

Figure 61.- Pressure distribution and separation on a wing.

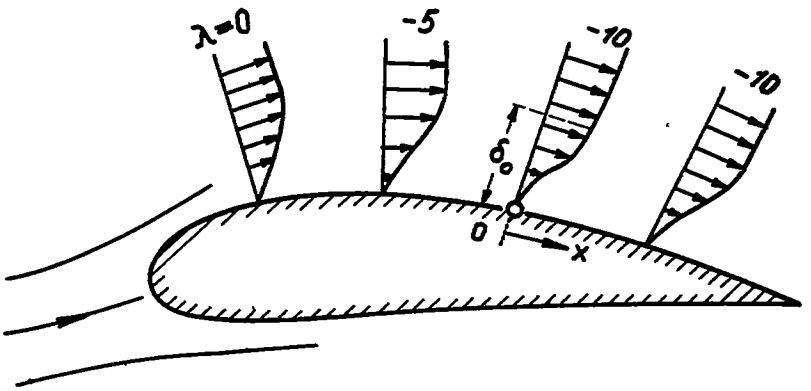

Figure 62.- Boundary layer with laminar separation avoided.

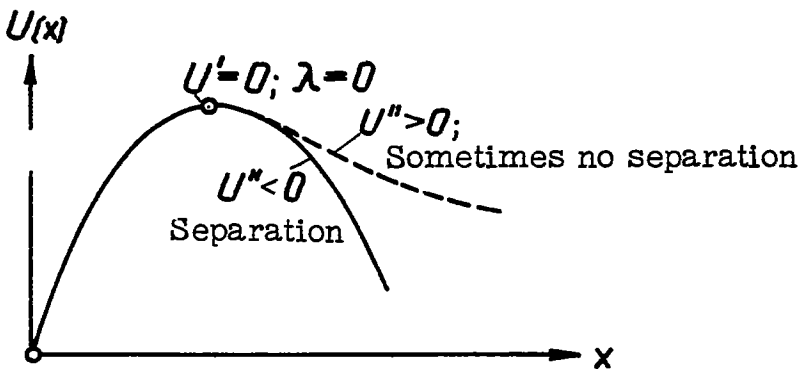

Figure 63.- Potential flow with separation: $U' < 0$; $U'' < 0$; sometimes without separation: $U' < 0$; $U'' > 0$.

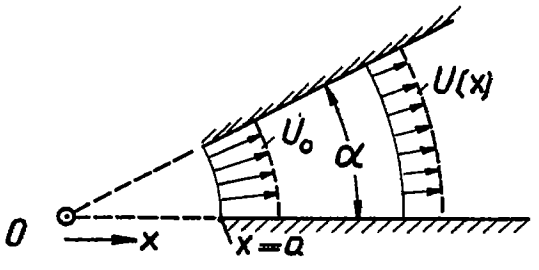

Figure 64.- Divergent channel.

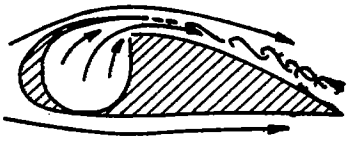

Figure 65.- Prevention of separation on wing by blowing.

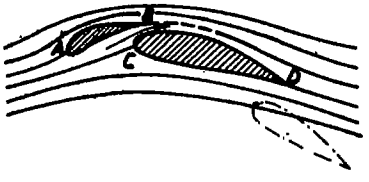

Figure 66.- Prevention of separation by a slotted wing.

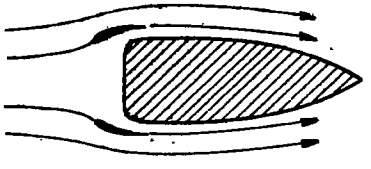

Figure 67.- NACA cowling for prevention of separation.

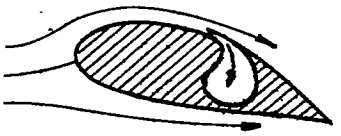

Figure 68.- Prevention of separation on wing by suction.

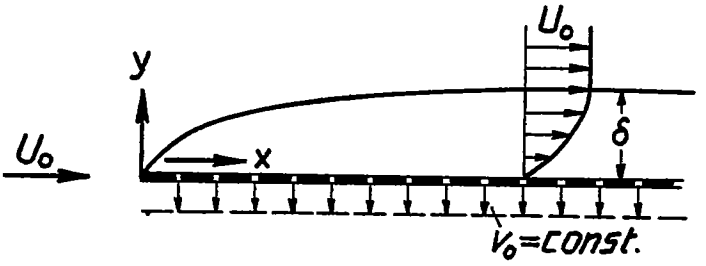

Figure 69.- Flat plate in longitudinal flow with suction.

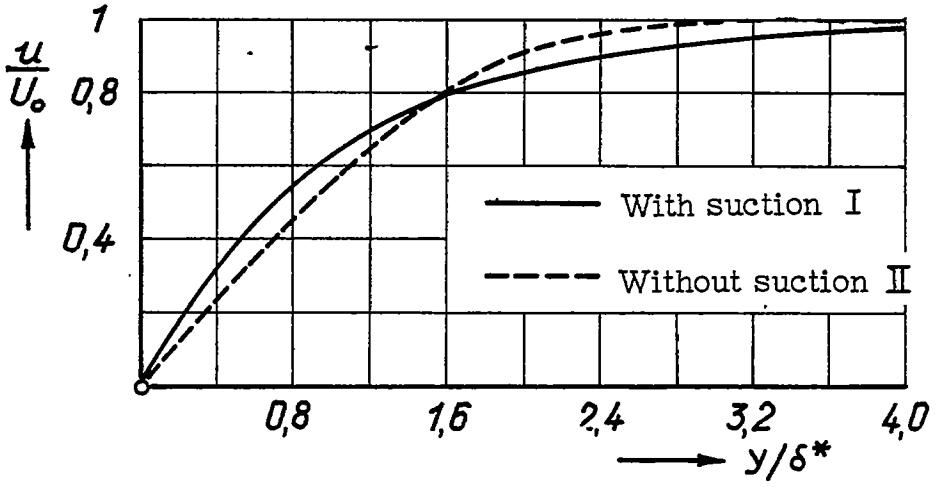

Figure 70.- Asymptotic velocity profile on flat plate in longitudinal flow with suction (I) $\delta^* = \nu/-v_o$ (II) $\delta^* = 1.73\sqrt{\frac{\nu x}{U_o}}$.